Processing of apurinic/apyrimidinic (AP) sites in mammalian cells

Prosessering av apurinske/apyrimidinske (AP) seter i mammalske celler

Meh Sameen Nawaz

Norwegian University of Life Sciences
Department of Chemistry, Biotechnology and Food Science
Master Thesis 60 credits 2012

Acknowledgements

This study presented in this master thesis was carried out between August 2011 to May 2012 at Oslo University Hospital, Rikshospitalet, Department of Microbiology, Centre for Molecular Biology and Neuroscience (CMBN) and the Norwegian University of Life Sciences, Department of Chemistry, Biotechnology and Food Sciences.

First and foremost I would like to express my gratitude to my supervisor at Department of Microbiology, Dr. Ingrun Alseth, for the guidance, enthusiasm, support and feedback provided throughout this study and while writing this thesis. Her interest was invaluable for the progress of this project.

I would also like to thank professor Professor Magnar Bjørås for accepting me into his research group and for positive encouragement. My stay has been very inspiring and educational. I am grateful to Professor Lars Eide, Dr. Catherine Fladeby and to other members of the staff for guidance and help in the laboratory, which was highly appreciated.

I also wish to express my gratitude to my supervisor at Norwegian University of Life Sciences, Professor Dzung Bao Diep for always being available for questions and for his support throughout this study.

Last, but not least, a big thanks to my parents and my family for their support and for always believing in me. I am forever grateful for your love, patience and understanding.

Oslo, May 2012

Meh Sameen Nawaz

Contents

Abstract

The integrity of deoxyribonucleic acid (DNA) is continuously challenged by endogenous and exogenous DNA damaging agents. Mutagenic and cytotoxic apurinic/apyrimidinic (AP) sites are amongst the most frequently formed lesions in cellular DNA and their repair is essential for genomic stability. AP sites in humans are processed and repaired mainly through base excision repair (BER), which is known to be initiated either by an AP endonuclease 1 (APE1) that incises 5' to the AP site or by bifunctional DNA that incise 3' to the AP site.

In this study, the processing of AP sites in mammals was investigated by knockout mice models of endonuclease eight-like DNA glycosylases (Neil1,Neil2), as well as down-regulation of the bifuctional endonuclease three (NTH1) and tyrosyl-DNA phosphodiesterase 1 (TDP1) in human epithelial cervical carcinoma (HeLa) S3 cells. The roles of bifunctional DNA glycosylases NEIL1, NEIL2 and NTH1 in AP site processing, using mouse and human whole-cell extracts, were examined by biochemical activity assays. Another aim of this study was to investigate whether an APE1-independent repair pathway involving NTH1 and TDP1 exist in mammals, since a recent study demonstrated such a mechanism in *Schizosaccharomyces pombe* where Tdp1 were shown to work downstream of Nth1.

The results obtained in this study show that APE1 is responsible for the main incision activity, whereas the roles of NEIL1 and NEIL2 in AP site processing were demonstrated to be non-essential. The product of NTH1 incision was observed in both mice and HeLa S3 extracts, indicating that NTH1 is also involved in AP site processing, although to a lesser extent than APE1. Biochemical analysis using recombinant NTH1, also demonstrated poor ability to process an APE1-nicked DNA substrate compared to an intact AP site, indicating that NTH1 most likely work upstream of APE1, and do not compete with polymerase β downstream of APE1.

The product of NTH1 was shown to be further processed by not only APE1, but also by TDP1 in both HeLa S3 cells and mice extracts, indicating that TDP1 is capable of working downstream of NTH1 in an APE1-independent manner and thus may serve as a back-up for APE1 in the repair of AP site.

Sammendrag

Integriteten av deoksyribonukleinsyre (DNA) utfordres kontinuerlig av endogene og eksogene forbindelser. Mutagene og cytotoksiske apurinske/apyrimidinske (AP)-seter er blant de mest forekommende DNA-skadene og deres reparasjon er essensiell for genomisk stabilitet. AP-seter i humane celler blir prosessert og reparert hovedsakelig gjennom baseeksisjonsreparasjon (BER), som antas å bli initiert av enten AP-endonuklease 1 (APE1) som kutter 5' til AP setet, eller av en bifunksjonell DNA-glykosylase som kutter 3' til AP setet.

I dette studiet ble prosesseringen av AP seter i mammalske celler undersøkt ved bruk knockout musemodeller av endonuklease VIII-lik DNA-glykosylaser (Neil1,Neil2), samt ved nedregulering av den bifunksjonell DNA-glykosylasen endonuclease three (NTH1) og tyrosyl-DNA fosfodiesterase 1 (TDP1) i human kreftcellelinje (HeLa S3). Rollen av NEIL1, NEIL2 og NTH1 i prosesseringen av AP-seter ble undersøkt ved hjelp av biokjemiske aktivitetsanalyser. En annen hensikt med dette studiet var å undersøke om en APE1-uavhengig reparasjonsmekanisme som involverer NTH1 og TDP1 finnes i mammalske celler. Bakgrunnen for dette var en studie som nylig demonstrerte en tilsvarende reparasjonsmekanisme i *Schizosaccharomyces pombe* som tyder på at Tdp1 fungerer nedstrøms for Nth1.

Resultatene fra dette studiet indikerer at APE1 er ansvarlig for mesteparten av kutteaktiviteten av AP seter, mens bidraget av NEIL1 og NEIL2 i AP-sete reparasjon, har mest sannsynlig ingen essensiell betydning i mammalske celler. Produktet av NTH1 aktiviteten ble også observert i både muse og HeLa S3 ekstrakter, noe som tyder på at NTH1 er involvert i AP-sete reparasjon, men i noe mindre grad enn APE1. Rekombinant NTH1 demonstrerte dårligere evne til å prosessere et APE1-kuttet DNA substrat enn et intakt AP-sete. Dette tyder på at NTH1 mest sannsynlig virker oppstrøms for APE1, og konkurrerer ikke med polymerase β nedstrøms for APE1.

Produktet generert av NTH1, ble videre prosessert av ikke bare APE1, men også av TDP1 i både muse og HeLa S3 ekstrakter. Dette kan tyde på at TDP1 er i stand til å fungere nedstrøms for NTH1 på en APE1-uavhengig måte og kan derfor muligens fungere som en reserve for APE1 under AP-sete reparasjon.

Abbreviations

3'dRP	3'-phospho-α,β-unsaturated aldehyde
3'OH	3´-hydroxyl
5'dRP	5´-deoxyribose-phosphate
5-OHC	5-hydroxycytosine
5-OHU	5-hydroxyuracil
(5')P	(5'-)phosphate
8-oxoG	7,8-dihydro-8-oxoguanine
A	adenine
AP	apurinic/apyrimidinic
APE	AP endonucleases
Asp	aspartic residue
ATCC	American type culture collection
BER	base excision repair"
BSA	bovine serum albumin
C	cytosine
cDNA	complementary DNA
CPT	camptothecin
(d)ATP	(deoxy)adenosine triphosphate
DMEM	Dulbeccos's Modified Eagle medium
DMSO	dimetylsulfoxide
D-KO	Double-knockout
DNA	deoxyribonucleic acid
Ds	double-stranded
DTT	dithiothreitol
EDTA	ethylenediaminetetraacetic acid
E. coli	*Escherichia coli*
e.g.	exempli gratia
FBS	fetal bovine serum
FEN1	flap endonuclease 1
Fpg	formamidopyrimidine DNA glycosylase
FT	flow-through
G	guanine
GFP	green fluorescent protein
HaCaT	Human keratinocytes
HCl	hydrogen chloride
HeLa	Human epithelial cervical carcinoma
His	histidine
HR	homologous recombination
HRP	horseradish peroxidase
IPTG	isopropyl β-D-1-thiogalactopyranoside
KD	knockdown
KO	knockout
LB	Luria-Bertani
LIG	ligase
LP	long-patch
Lys	lysine
$MgCl_2$	magnesium chloride
MMS	methyl methanesulfonate
MOPS	3-(N-morpholino) propanesulfonic acid
mRNA	messenger RNA

MQ	milli-Q water
NaOH	sodium hydroxide
Nei	endonuclease eight
NEIL	endonuclease eight-like
NER	nucleotide excision repair
Nfo	endonuclease four
NHEJ	non-homologous end-joining
Ni-NTA	nickel-nitrilotriacetic
NIR	nucleotide incision repair
Nth	endonuclease three
NTH1	endonuclease three- like 1
OGG1	8-oxoguanine DNA glycosylase
ON	over night
p	probability
PAGE	polyacrylamide gel electrophoresis
PARP1	poly (Adenosine diphosphate(ADP)-ribose) polymerase 1
PBS	phosphate buffered saline
PCNA	proliferating cell nuclear antigen
PNKP	polynucleotide kinase phosphatase
POL	polymerase
pTyr	phosphotyrosine
PTM	post-translational modification
PVDF	polyvinylidene difluoride
RISC	RNA-induced silencing complex
RNA	ribonucleic acid
ROS	reactive oxygen species
RT	room temperature
RT-PCR	real time-polymerase chain reaction
SCAN1	spinocerebellar ataxia with axonal neuropathy
SDS	sodium dodecyl sulphate
S-KO	single knockout
siRNA	small interfering RNA
SP	short-patch
S. pombe	*Schizosaccharomyces pombe*
ss	single-stranded
SSB	Single-strand break(s)
SSBR	Single strand break repair
T	thymine
Tdp1	tyrosyl-DNA phosphodiesterase 1
Tg	thymine glycol
Tm	melting temperature
Top1	topoisomerase 1
tRNA	transfer RNA
U	uracil
Udg	uracil DNA glycosylase
WT	Wild-type
XRRC1	X-ray cross complementation group 1
Xth	Exonuclease three

Abbreviations of measurements units	
˚C	Celsius
fmol	femtomole (10^{-15} mol)
g	gram(s)
h	hours
kDa	kilo dalton (10^{3} dalton)
l	liter
M	molar
mg	milligram(s) (10-3 g)
min	minutes
ml	milliliter (10^{-3} l)
mM	millimolar (10^{-3} M)
ng	nanogram(s) (10^{-9} g)
pmol	picomole (10^{-12} mole)
rpm	revolutions per minute
µg	microgram(s) (10^{-6} g)
µl	microliter (10^{-6} l)
U	unit
V	volt
W	watt

1 Introduction

The preservation of the genetic material through generations is essential for the survival of a species. Deoxyribonucleic acid (DNA), a stable molecule in all cells, is the carrier of the genetic information. However, all cells are constantly exposed to DNA damaging agents that threaten the integrity of the DNA (Klungland, 2001). Without DNA repair, damages can result in genetic instability, mutations, chromosome alterations and eventually cell death (Barnes *et al.*, 1993).

DNA undergoes damage from reactive metabolites that are present in the cell and from environmental agents such as UV or ionizing radiation and chemicals (Lindahl, 1993).

Different DNA repair pathways have been identified and these pathways are often remarkably conserved in several species. This underscores the critical role of DNA repair enzymes in the cells, as well as the importance of maintaining the functional properties of DNA. There are an increasing number of recent studies that illustrate the importance of DNA repair in context with neurodegenerative diseases or cancer. A detailed understanding of the different repair mechanisms is thus important in order to gain insight in different diseases (David and Williams, 1998).

1.1 DNA damage

One of the most frequently formed lesions in DNA are apurinic/apyrimidinic (AP) sites, which have been calculated to arise at a rate of about 10,000 times in a mammalian cell per day (Loeb and Preston, 1986). Thus, efficient DNA repair mechanisms have evolved to ensure repair and to protect the cells from the damaging effects caused by cellular metabolites and environmental agents. These different repair processes work together in a complex manner coordinated by a large number of proteins and cofactors. Their proper functioning at different levels is therefore critical for survival and prevention of mutagenesis (Barnes *et al.*, 1992).

The replication and transcription machinery uses proofreading mechanisms to ensure high degree of accuracy in DNA replication and transcription. Because an AP site lacks a base, it will during replication and transcription, present a block to continued synthesis by the DNA polymerases or ribonucleic acid (RNA) polymerases, respectively. However, replication through an AP site can still occur by the action of translesion polymerases that

provide a certain level of tolerance towards replication blocking lesions, by incorporating random bases resulting in base substitutions (Lange *et al.*, 2011;Pages *et al.*, 2008).

Thus, AP sites are harmful cellular DNA lesions that give rise to an increase in genetic mutations (Almeida and Sobol, 2007). The formation of AP sites in DNA are caused by spontaneous base loss and by the action of specific DNA glycosylases that hydrolyze the N-glycosylic bond between the 2'-deoxyribose and the damaged or incorrect base (Berdal *et al.*, 1998). AP sites occur regardless of base type, although more frequently for purines (David and Williams, 1998). In addition, AP sites are also induced directly by radiation, reactive oxygen species (ROS) and to some extent by alkylation as well. ROS, arisen from normal aeorobic metabolism, can also generate oxidized DNA bases, deamination products, oxidized sugar fragments and DNA single strand breaks (SSB).

Base residues of DNA can also undergo hydrolytic deamination, such as the deamination of cytosine (C) to uracil (U) (Figure 1.1) (Lindahl, 1993). It is one of the most common base lesions found in DNA, and occurs about 200 times in a mammalian cell per day. Since uracil pairs with adenine (A) during replication, this deamination will lead to guanine (G): C →A: thymine (T) transition mutation (Kavli *et al.*, 2007).

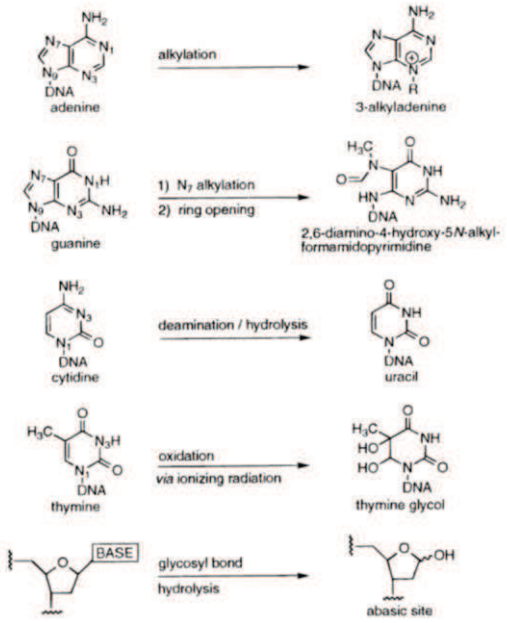

Figure 1.1. Examples of common base lesions of all four DNA bases. The AP site, generated by hydrolysis of the glycosylic bond, occurs regardless of base. "BASE" refers therefore to any of the four bases (David and Williams, 1998).

Oxidized DNA bases are considered to be major contributors in causing cell death and mutation in the genome. They have for a number of years attracted much attention in order to gain insight into the repair mechanisms. One of the most studied oxidized base lesion is the guanine oxidation product 7,8-dihydro-8-oxoguanine (8-oxoG). Oxidations of guanine residues tend to occur more often relative to the other DNA bases due to its low oxidation potential (Bjelland and Seeberg, 2003;Krishnamurthy *et al.*, 2008;Neeley and Essigmann, 2006).

Thus, AP sites and oxidized base residues can pose mutagenic and cytotoxic threats to the cells if the damages are not properly repaired. The sheer quantity of these lesions suggests that a tightly controlled system is necessary for accurate repair. Efficient and overlapping repair mechanisms are therefore required for maintaining the structural integrity of the genomic DNA (Loeb and Preston, 1986).

1.2 DNA repair

The different repair pathways are conserved defence mechanisms with overlapping substrate specificities that function as back-up systems for each other. Thus, various lesions may be repaired by different repair pathways and enzymes that may substitute for each other (Nilsen and Krokan, 2001).

Six major groups of DNA repair mechanisms have been broadly defined. One group of repair mechanisms, usually referred to as “direct reversal”, eliminates DNA lesions in a single step process and is the simplest type of DNA repair. All the other repair processes involve degradation of at least the damaged base followed by DNA resynthesis. Only a limited number of DNA lesions can be repaired by “direct reversal” mechanisms. These mechanisms include for instance photoreactivation repair, direct ligation of SSB with unmodified termini and dealkylation by specific alkyltransferases or AlkB (Falnes *et al.*, 2002;Zharkov, 2008). “Nucleotide excision repair” (NER) is another repair mechanism which removes primarily bulky helix-distorting lesions. “Mismatch repair” corrects errors made by DNA polymerases during replication by removing mismatched bases, as well as small insertion and deletion loops from the daughter DNA strand. “Non-homologous end-joining” (NHEJ) mechanism seals double strand breaks, whereas “homologous recombination” (HR) repair is involved in both repairing strand breaks and lesions that cannot be repaired in other ways.

Here focus will particularly be on the sixth type of DNA repair known as the "base excision repair" (BER) which deals mainly with a broad spectrum of DNA lesions generated in cells every day (Almeida and Sobol, 2007;Zharkov, 2008).

1.2.1 The BER pathway

The BER pathway is evolutionarily conserved and repairs non-bulky DNA base damages by removing simple base lesions derived from oxidation, alkylation and SSB. Removal of AP sites, arisen from a variety of exogenous and endogenous DNA damaging agents, is also the responsibility of BER. Importantly, AP sites function as mutagenic intermediates generated during the BER pathway as well. This DNA repair pathway is normally initiated by lesion-specific DNA glycosylases which can be divided in to three subtypes: a monofunctional DNA glycosylase, a bifunctional with associated β-elimination activity, a bifunctional with an associated β,δ-elimination activity, described in detail later.

As most DNA repair processes, BER functions through a series of repair complexes that assemble at the site of the DNA lesion. The lesion is then processed by recruiting and exchanging additional proteins throughout the repair in a coordinated way that involves protein-protein interactions. These proteins complexes may vary depending on the initiating lesion or on the post-translational modifications (PTMs) of the BER proteins involved. But more importantly, these BER complexes also vary by the chemistry of the repair intermediates created during the repair. Regardless of the initiating lesion, that is ultimately repaired, many similarities are found among the different assembled complexes of BER proteins (Almeida & Sobol, 2007;Demple and Harrison, 1994;Svilar *et al.*, 2011).

Although there are different variants of the BER model, there are five common steps that always occur during BER: lesion recognition and base removal, strand scission, gap tailoring, DNA synthesis and ligation. BER is initiated with the recognition and excision of the damaged base by one of the three subtypes of DNA glycosylases, resulting in an AP site. The AP site, which is a substrate primarily for AP endonuclease (APE), is either cleaved by the activity of an APE or by the AP lyase activity of bifunctional DNA glycosylases that generate SSB (Figure 1.2). Removal of the AP site by either of the two enzymes yields different chemical intermediates and hence different BER complexes during the repair. This difference defines a branching point for the BER pathway, depending on what subtype of DNA glycosylase initiate the pathway.

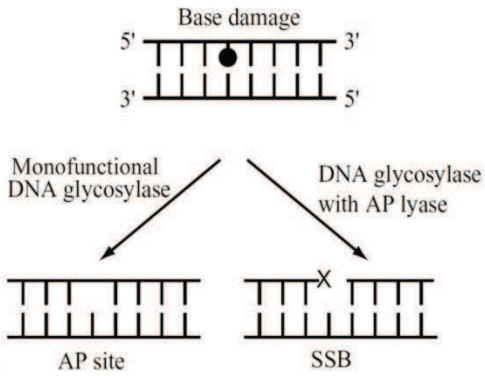

Figure 1.2. DNA glycosylases removes damages bases and generates either AP site or a SSB. X represents different 3'-terminus yielded by a bifunctional DNA glycosylase with β- or β,δ-elimination activity. Modified from (Izumi *et al.*, 2003).

The transient complexes formed after strand scission is mediated by scaffold proteins such as X-ray cross complementation group 1 (XRRC1) and poly (ADP-ribose) polymerase 1 (PARP1) (Mitra *et al.*, 2001;Svilar *et al.*, 2011). The precise steps of repair in each branch of the BER model in mammals are further described in more detail below (Figure 1.3). Even though each model goes through the five basic steps essential for BER, they still have common and unique transient protein complexes and protein-protein interactions that mediate the repair.

Repair intiated by a monofunctional DNA glycosylase

When BER pathway is initiated by a monofunctional DNA glycosylase in for example humans, it involves hydrolysis of the N-glycosylic bond to remove the damaged base. The resulting AP site is then removed by the enzymatic activity of the main human APE (APE1) that catalyzes the incision of the damaged strand 5' to the AP site. That leaves a single nick containing a 3′-hydroxyl (3'OH) and a 5′-deoxyribose-phosphate (5'dRP) terminus at the margins. The 5'dRP lyase activity of the DNA polymerase β (POL β) hydrolyzes the 5'dRP terminus to produce a ligatable 5'-phosphate (5'P) terminus. POL β also fills the single nucleotide gap, preparing the strand for ligation by DNA ligase I (LIGI) or by a complex of DNA ligase III (LIGIII) and XRCC1, and thereby completes the repair. Notably, two of the five steps require POL β (Figure 1.3(II)).

Repair initiated by a bifuntional DNA glycosylase with associated β-elimination activity

When a base lesion, usually an oxidative damaged base, is recognized by a bifunctional DNA glycosylase, the damaged base is excised from the DNA strand in a manner similar to monofunctional glycosylase as described above. However, bifunctional glycosylase add an additional level of complexity due to their 3'-AP lyase activity by incising 3' to the AP site through a β-elimination step. That yields a SSB with a replication-blocking 3'-phospho-α,β-unsaturated aldehyde (3' dRP) and a 5'P terminus at the margins (Figure 1.3(I)). The 3'-AP lyase activity is further referred also as β-elimination activity. The resulting nick is then tailored by the 3'-phosphodiesterase activity of APE1 which removes 3'dRP, thereby generating a 3'OH terminus and a single nucleotide gap. POL β and LIGIII/XRCC1 complex can then complete the further process by inserting the nucleotide and resealing the strand, respectively (Almeida and Sobol, 2007;Svilar *et al.*, 2011).

Repair initiated by bifuntional DNA glycosylase with associated β,δ-elimination activity

The third branch of the BER model has recently been characterized and is initiated by human DNA glycosylases named endonuclease eight-like (NEIL), discussed in detail in section 1.3.1. NEIL1 and NEIL2 are bifunctional DNA glycosylases with associated β,δ-elimination activity that initiate APE1-independent repair. Actions of NEIL1 and NEIL2 causes hydrolysis of the glycosylic bond to remove the damaged base followed by a β,δ-elimination step that yields a 3'P terminus and releases the *trans*-4-hydroxy-2,4-pentadienal. This results in a single nucleotide gap containing 5'P and 3'P at the margins (Figure 1.3(III)).

In mammalian cells the DNA 3'-phosphatase activity of APE1 seems to be very weak compared to for example it's homologues in *Escherichia coli* (*E. coli)*, which can remove all 3'-blocking termini including 3'P (Xu *et al.*, 2003). Since the β,δ-elimination product in mammals is not processed by APE1, polynucleotide kinase phosphatase (PNKP), is subsequently recruited to the AP site to remove the 3'P. PNKP, which is absent in *E. coli* and abundant in mammalian cells, is a bifunctional enzyme with both 5'-kinase and 3'-phosphatase activities catalyzed by two distinct domains. This enzyme can thereby act as a phosphatase or kinase depending on conditions that will activate one domain to a greater extent than the other (Caldecott, 2002;Jilani *et al.*, 1999). PNKP will act as a 3'-

phosphatase during the repair pathway to remove 3'P and prepare the strand for DNA synthesis by POL β and ligation by LIGIII/XRCC1 complex (Wiederhold *et al.*, 2004).

Thus, the products of β,δ-elimination activity in mammalians is processed by PNKP and not by APE1 as in the case for the two other branches described earlier. PNKP does not seem to interact directly with NEIL enzymes, but it has been suggested that PNKP could associate indirectly with them through a large complex consisting of XRCC1, POL β and LIGIII (Das *et al.*, 2006).

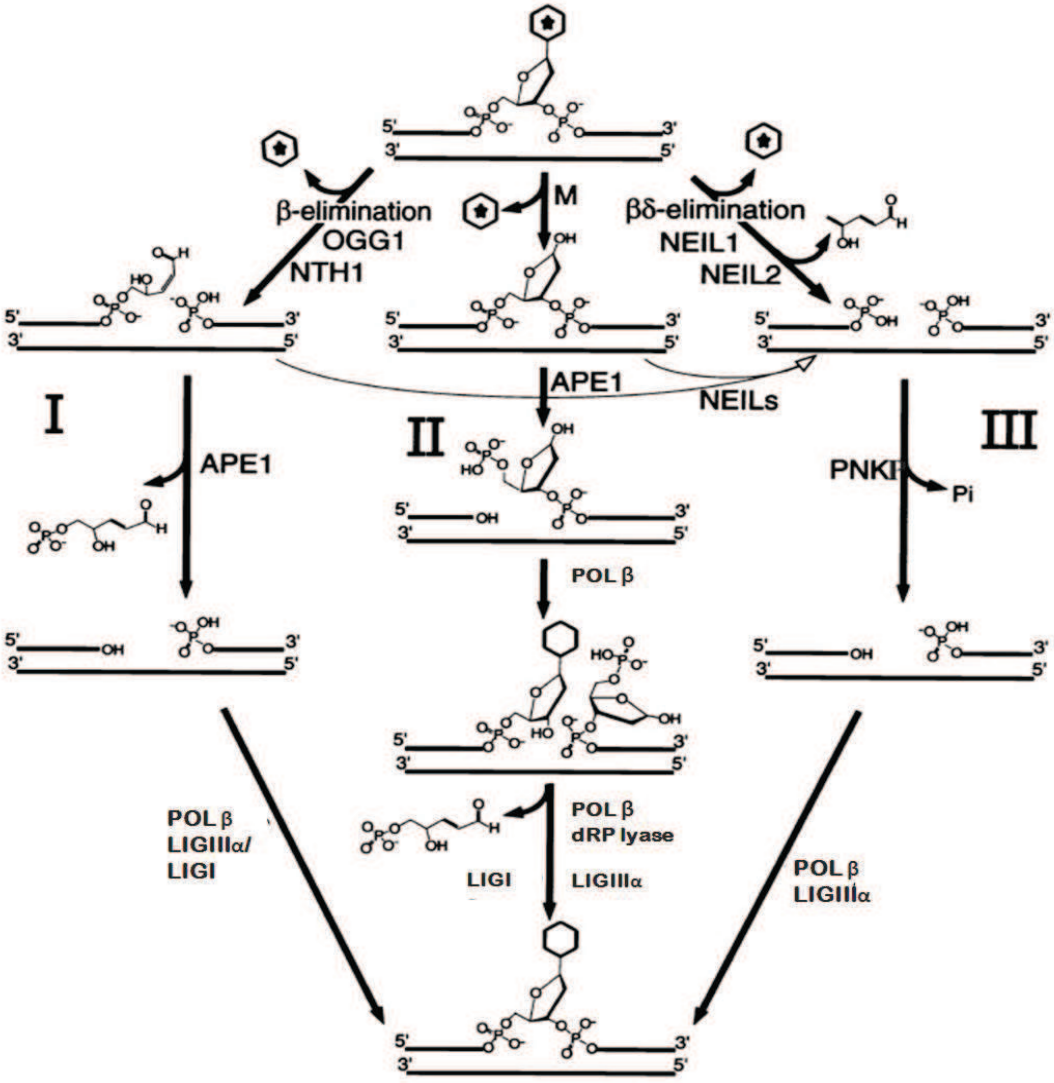

Figure 1.3. Schematic representation of the different branches of APE- and PNKP-dependent BER pathways in human cells. Each branch is (I, II, III) is defined by the type of DNA glycosylase that initiates the pathway. (Pathway I) After the β-elimination step of a bifunctional DNA glycosylase, APE1 removes the resulting 3'dRP by generating a 3'OH that can be further processed by POL β. (Pathway II) M = Monofunctional DNA glycosylase, generates an AP site, which is cleaved by APE1. POL β removes the resulting 5'dRP terminus and process the single nucleotide gap. (Pathway III) NEIL DNA glycosylases generates 3'P terminus, that is further processed by PNKP. Adapted from (Wiederhold *et al.*, 2004).

1.2.2 Short-patch and long-patch BER

A branching point has also been observed after recognition and removal of the damaged base that divide the BER pathway in two different subpathways: the short-patch (SP) and the long-patch (LP) BER. Of these two pathways, the SP-BER is currently thought to represent the major subpathway initiated either by a lesion-specific mono- or bifunctional DNA glycosylase (Almeida and Sobol, 2007). While the gap-filling step in SP-BER requires insertion of a single nucleotide and the action of POL β as described in section 1.2.1, LP-BER involves removal and replacement of longer patches of 2-10 nucleotides to fill the gap (David and Williams, 1998).

The LP-BER is initiated in a similar way to SP-BER, but the 5'dRP is replaced as a part of single-stranded flap generated by the strand displacement DNA synthesis by POL β and polymerase δ/ε (POL δ/ε) in complex with proliferating cell nuclear antigen (PCNA) (Figure 1.4). To complete the repair, flap endonuclease 1 (FEN1) processes the resulting 5' flap, leaving a nick that has been transferred 2-10 nucleotides downstream of the original base lesion.

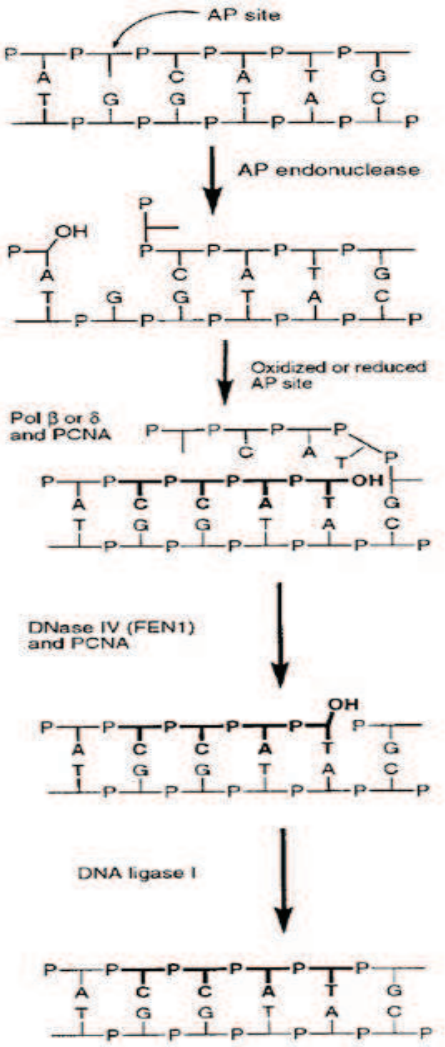

Figure 1.4. Schematic illustration of the long-patch BER pathway. Adapted from (David and Williams, 1998).

The choice of whether SP- or LP-BER is initiated has not yet been completely understood. However, in mammalian cells normal AP sites are processed by the SP-BER, whereas LP-BER occurs in the presence of a 5'dRP blocking group that is refractory towards the lyase activity of POL β. Thus, the nature of the 5' terminus at the AP site dictates whether SP-BER or LP-BER is initiated (Sung and Demple, 2006). Furthermore, whereas bifunctional DNA glycosylases initiate SP-BER, the repair initiated by monofunctional DNA glycosylases may follow either pathway (Fortini *et al.*, 1999).

1.2.3 Special cases of BER

Over the past several years, additional alternate repair mechanisms have been described in both prokaryotic and eukaryotic cells that utilize many of the same proteins as BER but work in different combinations to repair base damage. Thus, they can be considered as minor subpathways of BER. For example an alternate DNA glycosylase-independent repair pathway defined as "nucleotide incision repair" (NIR) is initiated by APE1 instead of DNA glycosylases in repair of oxidized pyrimidines and α-deoxynucleotides (Zharkov, 2008). APE1 cleaves 5' to the lesion, in the same manner as during regular BER, but it bypasses the DNA glycosylase step. That generates a 3'OH end and a 5'P end which also contains the damaged nucleotide, making the 5'end unable to be processed by the 5'dRP lyase activity of POL β. Thus, the repair proceeds via LP-BER (Sung and Demple, 2006).

The biological importance of NIR remains unclear, but it has been argued that NIR allows the cell to avoid the formation of toxic AP site intermediates, although SSB generated during NIR may be as toxic as an AP site (Ischenko and Saparbaev, 2002).

In addition, the SSB repair (SSBR) pathway utilizes many of the same proteins as BER such as APE, POL β, LigIII along with scaffold proteins PARP1 and XRRC1 (Figure 1.5). SSBR is responsible for mainly the repair of SSB in DNA caused by ROS, irradiation or incomplete topoisomerase action (Almeida and Sobol, 2007 ;Friedberg, 2006). The initiation step is the main difference between regular BER pathway and SSBR. PARP1 recognizes the SSB, thereby signaling recruitment of repair proteins to the damaged site (Caldecott *et al.*, 1996). In both BER and SSBR, repair may occur at a single nucleotide level or as a longer patch of repair. In addition these two repair pathways have common gap-filling and nick sealing steps, but SSBR also involves several end-processing enzymes which is perhaps the most diverse enzymatic step in BER and SSBR due to the variety of termini generated (Hegde *et al.*, 2012).

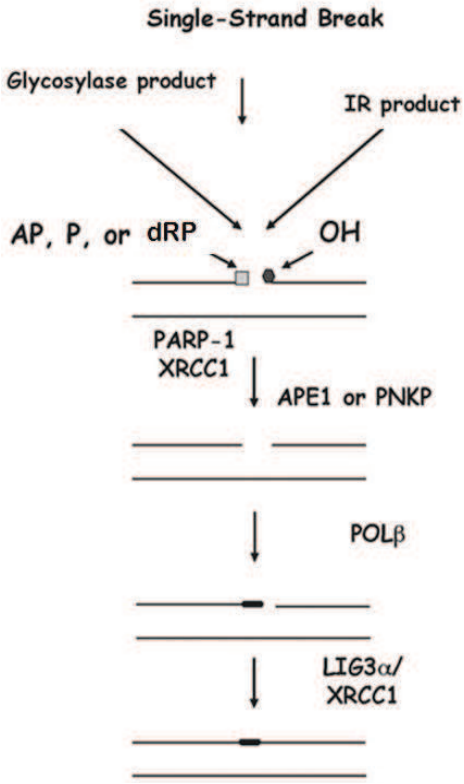

Figure 1.5. SSBR subpathway where the SSB is induced by either a DNA glycosylase or for example by ionizing radiation (IR). AP= AP site; P = phosphate; dRP= deoxyribose-phosphate OH=hydroxyl group. Figure modified from (Wilson *et al.*, 2007).

1.2.4 Role of tyrosyl-DNA phosphodiesterase 1 in APE-independent repair

In section 1.2.1, an APE-independent BER pathway initiated by a DNA glycosylases with associated β,δ-elimination activity was described. Recent studies confirm that APE-independent BER pathways play an important role in the regulation of DNA repair mechanisms.

Tyrosyl-DNA phosphodiesterase 1 (Tdp1) is a 68.5 kDa repair enzyme and was discovered in *Saccharomyces cerevisiae*. Tdp1 is a member of the phospholipase D superfamily which includes a diverse group of enzymes that catalyzes the cleavage of the phosphodiester bond on different substrates ranging from phospholipids to DNA (Interthal *et al.*, 2001). Tdp1 catalyzes primarily the cleavage of protein-DNA complexes by hydrolysis of a phosphodiester bond between an O-4 atom of tyrosine residues and a DNA 3'-phosphate. This type of linkage, a 3'-phosphotyrosine linkage, is typical for the transient covalent intermediate produced by the action of topoisomerase 1 (Top1) upon cleavage of a DNA strand (Lebedeva *et al.*, 2011;Yang *et al.*, 1996).

The enzymatic activity of Tdp1 was proposed to be associated with the repair of DNA lesions that developed from irreversible Top1-DNA cleavage complex (Yang *et al.*, 1996). Top1 is a ubiquitous enzyme that relaxes positive and negative supercoiling in DNA and thereby regulates the DNA topology.

Generation of a covalent complex between Top1 and DNA requires a reversible transesterification reaction (Figure 1.6). This transient DNA strand break, produced upon formation of Top1-DNA complex, allows removal of any local helical tension and thereby relaxes the DNA. Once this happen, the covalent intermediate is reversed by a second transesterifiaction reaction. Under normal circumstances, the transient break in DNA caused by Top1-DNA complex will get resealed since the rate of religation is much greater than the rate of cleavage (Champoux, 2001;Dexheimer *et al.*, 2008). However, different conditions or chemicals such as camptothecin (CPT) can reduce or inhibit the religation reaction. If this transient break in DNA is not resealed, the SSB caused by Top1 linkage to the DNA, will get transformed into a prolonged double-stranded (ds) break followed by a collision of the replication fork (Dexheimer *et al.,* 2008;Pommier *et al.,* 2006).

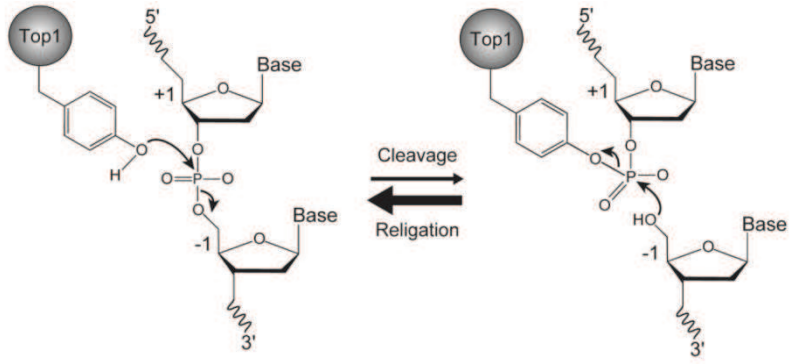

Figure 1.6. Reversible transesterification reaction that generates a covalent complex between Top1 and DNA that removes helical tension and relaxes the DNA (Dexheimer *et al.*, 2008).

The enzymatic activity of Tdp1 requires prior denaturation of the Top1 bond to DNA which presumably results in enhanced steric access of the phosphodiester bond. Thus, it has been suggested that in order to maintain efficient Tdp1 activity Top1 must go through proteolysis. This is in agreement with studies demonstrating that the efficiency of Tdp1 processing increases as the length of Top1 polypeptide is shortened by the ubiquitin-proteosome pathway (Debethune *et al.*, 2002;Dexheimer *et al.*, 2008).

The efficiency of Tdp1 activity is not only constricted to Top1-DNA complex or single tyrosine residues, although Tdp1 is less efficient with other substrates. Indeed, recently it was suggested that Tdp1 in *Schizosaccharomyces pombe* (*S. pombe*) act in an APE-independent branch of BER by removing the 3'dRP generated by bifunctional DNA glycosylase Nth1 (Nilsen *et al.*, 2012). The broad substrate specificity of Tdp1 is also demonstrated with the analysis of recombinant human Tdp1 (TDP1) which is capable of processing the 3'dRP terminus to 3'P terminus (Lebedeva *et al.*, 2011). In addition, analysis of TDP1 has also shown to hydrolyze other 3'-blocking lesions including 3'-phosohoglycolates, indicating that it may function as a general 3'-phosphodiesterase as well as a repair enzyme (Dexheimer *et al.*, 2008).

Furthermore, the 3'P terminus generated by TDP1 is further hydrolyzed to a 3'OH by the 3'-phosphatase activity of PNKP. The 3'OH terminus is then extended by a DNA polymerase. TDP1 has been shown to exist in complex with PNKP in human cells suggesting that TDP1 and PNKP function in the same repair way (Figure 1.7) (Lebedeva *et al.*, 2011;Plo *et al.*, 2003).

The importance of TDP1 is underscored by the fact that that a recessive mutation in *TDP1* gene is responsible for inherited neurodegenerative disorder, further discussed in section 1.4 (Takashima *et al.*, 2002).

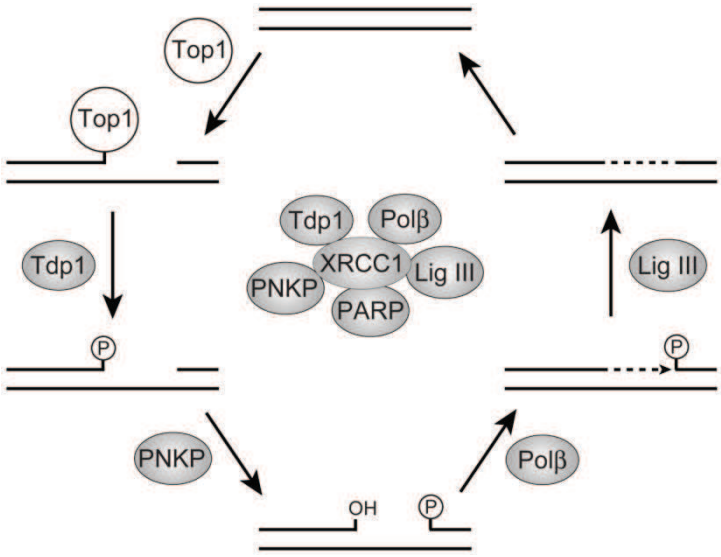

Figure 1.7. Tdp1-initiated repair of an irreversible Top1-DNA complex (Dexheimer *et al.*, 2008).

1.3 Major BER enzymes

Most of the BER enzymes that had been characterized in the early 1990's, provided an insight into mechanisms of lesion recognition and catalysis (Zharkov, 2008). Several DNA glycosylases and other BER proteins have been mentioned in previous sections without any further introduction. Thus, in this section, major BER enzymes will be described in more detail.

1.3.1 DNA glycosylases

Recognition of DNA damage in highly condensed chromatin is a critical step specially when the structures of the oxidized base lesions are not significantly different from the original base and almost normal basepairing is achieved with only minor perturbations in the DNA helix (Hegde *et al.*, 2010). Since DNA glycosylases initiate BER, their presence is essential to the recognition and removal of DNA base lesions. Their mechanism of actions has been extensively studied on a number of different levels. Regulation of DNA glycosylase activity via protein-protein interactions facilitate lesion recognition and ensure that initiated repair is completed through formation of lesion-specific repair complexes (Almeida and Sobol, 2007). While alkylated bases and uracil are excised by

monofunctional DNA glycosylases, all oxidized bases are removed by bifuntional DNA glycosylases with lyase activity (Mitra *et al.*, 2001).

DNA glycosylases utilize a mechanism of base excision that involves extrahelical flipping of modified, damaged or even normal base into the catalytic pocket of the enzyme. Thus, DNA glycosylases specificity depends on how the substrate lesion fits into the binding pocket and where the binding is stabilized by different types of interactions (Slupphaug *et al.*, 1996). However, since a large number of lesions are excised by the eleven DNA glycosylases in mammalian cells, the DNA glycosylases usually possess rather broad substrate specificities. In spite of this, DNA glycosylases also have distinct preferences and back-up functions (Hegde *et al.*, 2008;Hildrestrand *et al.*, 2009).

Furthermore, the overlapping substrate specificity of DNA glycosylases is most likely due to the fact that catalytic pockets of DNA glycosylases allows induced fit for the different substrates. This is also consistent with the general observation that the individual requirement of a specific DNA glycosylase is not essential for the general repair, nor is the deficiency of a specific DNA glycosylase lethal in most cases (Hegde *et al.*, 2012;Klungland *et al.*, 1999).

There has been some discussion about how DNA glycosylases are able to detect base lesions within the DNA helix. Questions like whether the DNA glycosylases actively contributes to baseflipping and if the damaged or even the normal bases are passively trapped into the catalytic pocket of the enzymes, have been raised. The last few years a number of studies have tried to answer these questions without being able to determine how DNA glycosylases search for and detect base lesions. There has however been suggested a passive role for DNA glycosylases in the baseflipping mechanism, where DNA glycosylases may catch the flipped base during a scanning process (Cao *et al.*, 2004;Dalhus *et al.*, 2009). Further experiments are clearly needed to clarify the details.

Currently most of the DNA glycosylases can be divided into three main superfamilies as described in greater detail below. However, there are several DNA glycosylases that do not belong to any of the three superfamilies. Each superfamily is organized around one or more core families that are characterized by a number of motifs and folds that are present in most members of the superfamilies (David and Williams, 1998;Zharkov, 2008).

Uracil DNA glycosylase superfamily

Uracil DNA glycosylase superfamily consists of at least five families of enzymes with similar substrate specificities, but low sequence similarities. The Udg family-1 DNA glycosylases are the most widely distributed members of this superfamily, and remove the main fraction of uracil from genomic DNA. Uracil DNA glycosylases (e.g. Ung in *E. coli*, UNG in humans and Ung1p in yeast) function by excising uracil from both single-stranded (ss) and ds DNA and do not produce breaks after base excision. However, they are inactive towards pyrimidines in DNA as well as uracil in RNA (David & Williams 1998;Zharkov, 2008).

Fpg/Nei superfamily

The superfamily of formamidopyrimidine DNA glycosylase (Fpg) and endonuclease eight (Nei) consists of homologous *E. coli* enzymes. Both are bifunctional DNA glycosylases with associated β,δ-elimination activity . Human DNA glycosylases named NEIL1 and NEIL2, mentioned previously, belongs to the same familiy as *E. coli* Fpg and Nei (Bandaru *et al.*, 2002). NEIL enzymes initially recognized oxidized pyrimidines like 5-hydroxyuracil (5-OHU), but was later observed to efficiently excise oxidized purines as well, such as 8-oxoG (Krishnamurthy *et al.*, 2008). In addition, NEIL enzymes have been to be more active with ss DNA as present in a bubble or a fork. Thus, NEIL enzymes preferentially function in the repair during DNA replication or transcription (Dou *et al.*, 2003). Table 1.1 summarizes a list of some base lesions recognized and removed by NEIL1 and NEIL2.

Table 1.1. Oxidized base lesions recognized and removed by human bifunctional DNA glycosylase NEIL1 and NEIL2 with associated β,δ-elimination. Adapted from (Svilar *et al.*, 2011).

Gene symbol	*Gene name*	*Gene ID*	*Uniprot accession number*	*Organelle expressed*	*Known substrate*[a]
NEIL1	endonuclease eight (VIII)-like 1	79661	Q96FI4	Nucleus, cytoplasm and mitochondria	5-hyroxy-C; 5-hydroxy-U:A/T>G Guanidinohydantoin/ Spiroiminodihydantoin (double- and single-stranded) Iminoallantoin (double- and single-stranded) 5,6-Dihydro-T 5,6-Dihydro-U:G/C/A>T 2,6-diamino-4-hydroxy-5-formamidopyrimidine (FapyG):C 7,8-dihydro-8-oxoguanine (8-oxoG):C/G>T>A 4,6-diamino-5-formamidopyrimidine (FapyA):T
NEIL2	Nei endonuclease eight (VIII)-like 2	252969	Q969S2	Nucleus and cytoplasm	5-hydroxy-U:G>T>A 5-hyroxy-C 5,6-Dihydro-U:G/A 7,8-dihydro-8-oxoguanine (8-oxoG):C/A Guanidinohydantoin/ Spiroiminodihydantoin (double- and single-stranded) Iminoallantoin (double- and single-stranded)

[a]*References: (Bjelland and Seeberg, 2003;Hailer et al., 2005)*

Nth superfamily

The family of DNA glycosylases related to endonuclease three (Nth) is the most diverse group of DNA glycosylases (Zharkov, 2008). The originally identified activity of Nth, encoded by the *nth* gene in *E. coli,* was DNA strand scission. However, it was soon recognized that Nth had both DNA glycosylase activity and AP lyase activity that cleaved the phosphodiester backbone 3' to an AP site.

This family of bifunctional DNA glycosylases has the widest substrate specificity amongst BER glycosylases, and is also specific for a large number of oxidized pyrimidines including thymine glycol (Tg) and urea. Most of these substrates derive from oxidative reactions at the 5,6-double bond in thymine or cytosine such as Tg and 5-hydroxycytosine (5-OHC). However, they are mainly known to be active upon ds DNA (David and Williams, 1998;Katcher and Wallace, 1983).

It is important to underscore the fact that many of the DNA glycosylases such as human endonuclease three- like 1 (NTH1) and NEIL have overlapping substrate specificities, and therefore often processes the same substrates (Hegde *et al.*, 2012). Some lesions processed by NTH1 in humans, are listed in Table 1.2.

Table 1.2. Oxidized base lesions recognized and removed by human bifunctional DNA glycosylase NTH1 with associated β-elimination. Adapted from (Svilar *et al.*, 2011)

Gene symbol	*Gene name*	*Gene ID*	*Uniprot accession number*	*Organelle expressed*	*Known substrate*[a]
NTHL1 (NTH1)	endonuclease three (III)-like 1	4913	P78549	Nucleus and mitochondria	T-glycol C-glycol 4,6-diamino-5-formamidopyrimidine (FapyA) 5,6-dihydro-U:G/A 5-formyl-U 5,6-dihydroxy-C 5,6-dihydro-T urea 5-hydroxy-U:G 5-hydroxy-C:G>A 5-hydroxy-5,6,-dihydro-T 7,8-dihydro-8-oxoguanine (8-oxoG)

[a]*References: (Bjelland and Seeberg, 2003;Matsumoto et al., 2001)*

Since the discovery of Nth in *E. coli*, similar enzyme homologues have been identified in different organisms including yeast and mammals (Gossett *et al.*, 1988;Higgins *et al.*, 1987). Ntg1p and Ntg2p in yeast and NTH1 in humans are close homologues to *E. coli* Nth with similar substrate specificities and extensive sequence similarities (David and

Williams, 1998). The *NTHL1* gene encodes NTH1 with an open reading frame that translates a protein of 34.3 kDa and 312 amino acids (Aspinwall *et al.*, 1997).

The crystal structure of *E. coli* Nth consists of two α-helical domains which contain a helix-hairpin-helix motif, and an iron-sulfur cluster (Kuo *et al.*, 1992). According to several recently studies the iron-sulfur cluster plays a role in DNA binding, but does not participate in catalysis (Fromme and Verdine, 2003). DNA binds to the binding pocket of the enzyme between the two domains while a single lysine residue (Lys-120) and an aspartic residue (Asp-138) in the active site catalyzes the reaction. When the enzyme carries out β-elimination, it forms a Schiff base between the active site Lys-120 and the deoxyribose in DNA formed after base excision (Dodson *et al.*, 1994). A three-dimensional structure of Nth in a complex with damaged DNA is presented (Figure 1.8).

Figure 1.8. A three-dimensional structure of *E. coli* Nth with the two domains in blue and green. The iron-sulfur cluster is shown in yellow and rust, respectively. The duplex DNA is shown in gold with the lesion nucleoside in grey and the complementary estranged nucleoside in red (Fromme and Verdine, 2003).

Compared to DNA glycosylases homologues in lower organisms, mammalian DNA glycosylases possess unique structural features such as an unfolded extension or a tail which participate in protein-protein interactions (Hegde *et al.*, 2010;Sarker *et al.*, 1998). The sequence alignment of NTH1 with *E. coli* Nth for instance revealed an N-terminal extension segment of 10 kDa in NTH1 which is absent in *E. coli* (Figure 1.9). The N-terminal segment is however not required for the enzymatic activity. It has although been demonstrated that the N-terminal segment may affect the glycosylase activity by increasing the enzymes affinity towards the DNA product generated after the glycosylase and lyase activity. Such terminal extentions with unconserved polypeptide sequence are not unusual amongst mammalian glycosylases or APEs (Izumi *et al.*, 2003;Liu and Roy, 2002).

Figure 1.9. Simplified illustration of *E. coli* Nth and NTH1, showing extensions. Boxes and lines indicate conserved and unconserved segments, repectively. Total amino acids are shown at right and the number with arrow define the border between the conserved and unconserved segments (Izumi *et al.*, 2003).

Until recently, excision of the base by a DNA glycosylase and catalysis to generate a β-elimination product were thought to occur subsequently. However, studies with bifunctional glycosylases such as NTH1 suggest that this not may be the case. Studies of NTH1 where activity and binding affinity to Tg-containing DNA were investigated revealed enhanced glycosylase activity and abrogation of the NTH1's β-elimination activity upon activation of APE1. This was supported by the fact that only the product of APE1, 5'dRP, was detectable not the product of β-elimination. Therefore, under physiological conditions where APE1 is abundant, NTH1 may act as a monofunctional glycosylase on Tg:A damaged DNA, thereby circumventing the β-elimination step and forwarding the damage directly towards cleavage by APE1 which has a greater capacity to cleave 5' to the AP site than 3' to the β-elimination product (Almeida and Sobol, 2007;Marenstein *et al.*, 2003).

Studies with other DNA glycosylase such as 8-oxoguanine DNA glycosylase (OGG1) showed similar results, suggesting that the circumvention of the β-elimination upon activation of APE1 is commonly observed for bifunctional glycosylases *in vivo* (Vidal *et al.*, 2001).

1.3.2 AP endonuclease

The second step in BER process after base excision is catalyzed by APEs that recognizes the AP sites and incises the DNA 5' to the AP site. Not only do they incise DNA at AP sites, but they also efficiently removes the products of β-elimination to produce 3'OH terminus required for the gap-filling step by a DNA polymerase (Wiederhold *et al.*, 2004). In human cells, APE1 is responsible for more than 95% of the AP site incision activity, underscoring its importance in AP site repair (Chen *et al.*, 1991). In addition, APE1 possesses a number of minor functions as 3'-phosphatase, 3'-phosphoglycosylase, 3'-phosphodiesterase and 3'→5' exonuclease activities (Almeida and Sobol, 2007).

In general, one or two AP endonucleases are present in each organism, and they can in turn be divided into two groups. Exonuclease three (Xth) and endonuclease four (Nfo) are two *E. coli* enzymes which are the prototypic members of these two groups. Although they share similar functions, they are unrelated on a structural level. The major human AP endonucleases, APE1 and APE2 are both Xth's homologues. Xth and its homologoues are described as metalloenzymes that relies on Mg^{2+} to be fully active (Zharkov, 2008).

Many of the different functions of APE described above are important in the repair pathways since they are involved in the gap-tailoring step of the 3'-blocked terminus, although the efficiency of each enzymatic activity may vary in different organisms. APE1 also interact physically with a number of BER proteins such as LIGI and LIGIII, FEN1, PCNA, POL β and most importantly XRRC1. By physically interacting with XRCC1, APE1 enhances the rate of endonucleolytic incisions and coordinates AP site repair initiation with other gap-tailoring enzymes (Almeida and Sobol, 2007).

1.3.3 POL β- a DNA polymerase and a 5'dRP processing enzyme

The major 5'dRP removing activity in mammals belongs to the classical BER enzyme POL β. Although POL β seems to be responsible for the primary 5'dRP lyase activity in mammalian BER, both DNA polymerase lambda (POL λ) and DNA polymerase iota (POL ι) have also been shown capable of removing the 5'dRP lesion subsequent to APE1 strand cleavage, however much less efficiently. POL ι and POL β are the main gap-filling DNA polymerases involved in DNA resynthesis in eukaryotes. However, POL δ or POL ε also play an important role in DNA resynthesis, especially in LP-BER (Bebenek and Kunkel, 2004;Zharkov, 2008).

1.3.4 DNA ligases

The reaction which completes BER by resealing the single-stranded nick in DNA is catalyzed by DNA ligases. All cells possess at least one type of DNA ligase that is required for joining of Okazaki fragments during replication. In addition, these enzymes are involved in most aspect of DNA metabolism and use the energy relieved in hydrolysis of phosphoanhydrid to make a phosohodiester bond. Most of the DNA ligases are ATP dependent, while some for instance in *E. coli* are NAD^+ dependent. Human genomes contain three genes for DNA ligases; *LIGI*, *LIGIII and LIGIV*. *LIGIII* encodes two isoforms of the mature enzyme, DNA ligase IIIα (LIGIIIα) and DNA ligase IIIβ (LIGIIIβ). LIGIIIα is ubiquitously expressed while LIGIIIβ in only found in testes.

LIGIIIα seems to be predominant in SP-BER, while LIGI is the main ligase involved in LP-BER and replication (Tomkinson *et al.*, 2006;Zharkov, 2008).

1.3.5 Scaffolds proteins in BER

The major BER enzymes discussed above constitute a core BER pathway and they are sufficient to successfully repair damage *in vitro*. However, several accessory proteins such as XRRC1, PARP1 and PARP2 usually functions as a scaffold for these core enzymes and stimulate the BER pathway *in vitro* and are most likely involved in BER processes *in vivo*. XRRC1 is probably the most important BER scaffold protein and is necessary for normal functioning BER pathways. It interacts with most, if not all, components of BER. Scaffolds proteins in general are believed to be involved in every step of the BER pathways effecting the recruitment of the core BER enzymes by generating multiprotein complex intermediates (Zharkov, 2008).

1.4 BER in context with genomic instability and diseases.

There is increasing evidence that BER is involved in repair of age-associated and neurodegenerative diseases, as well as cancer. Mouse whole-cell extracts and cellular knockout and knockdown models have been major tools for investigating and understanding the cellular and biological role of many BER proteins beyond the biochemical characterization of substrate specificity. There can however be differences in cellular response between mouse and other mammalian cells, as well as different response from different organs in general (Almeida and Sobol, 2007).

Mice models are also widely used in research to study human genes and diseases since 99% of the human genes are known to be conserved in mouse (Rosenthal and Brown, 2007). In fact, recently studies of DNA glycosylase deficient mice did not demonstrate significant increased cancer frequencies or mutation rates. In addition, no severely altered phenotypes or genomic instability was observed. This might be due to overlap in functions between DNA glycosylases as well as the fact that other alternative pathways may take over the repair. One exception was however observed in *OGG1*-deficient mice that exhibited up to 6-fold higher spontaneous mutation frequency in some tissues.

Cancer and genomic instability have also been demonstrated in mouse models where at least two DNA glycosylases were knocked out. In addition, deletion or deficiency of enzymes that work in steps downstream of DNA glycosylases are lethal in many cases

(Friedberg and Meira, 2000;Nilsen and Krokan, 2001). This has been demonstrated in knockout mouse models of Ape1 and Pol β (Zharkov, 2008).

Imbalances of BER proteins have also been demonstrated to significantly affect the rates of spontaneous mutation. Overexpression could lead to the removal of normal, non-damaged bases (Nemec *et al.*, 2010). Mutations in BER enzymes or other repair enzymes can also be a critical factor in development of diseases. A homozygous mutation in human *TDP1* gene results in a histidine to arginine mutation in the active site of TDP1. This mutation leads to the rare autosomal recessive neurodegenerative disease, spinocerebellar ataxia with axonal neuropathy (SCAN1). In contrast to other diseases associated with defective repair enzymes, SCAN1 patients do not have increased cancer frequency, but develop symptoms that are restricted to nervous system during puberty (Takashima *et al.*, 2002). In addition, it has also been demonstrated that OGG1 is often mutated in Alzheimer's disease patients, leading to reduced repair and increased oxidative damage in brain tissue (Zharkov, 2008).

1.5 Aims of this study

The overall aim of this project was to gain further insight into processing of AP sites in mammalian cells. Better understanding of DNA repair pathways and mechanisms might contribute to understand the causes of human diseases and hence improve the development in treatment strategies. Thus, gene targeted mouse models and down-regulation of targeted protein in human cells have been extensively used to study the roles of proteins involved in BER.

In this study the role of NEIL1 and NEIL2 in processing of AP sites was elucidated by using human immortal cell lines and knockout (KO) mice of Neil1 and Neil2. The use of KO mice and human cell lines also made it possible to further investigate and map the contribution of NTH1, which represent the only remaining bifunctional DNA glycosylase working on oxidized pyrimidines, in the absence of NEIL enzymes (Takao *et al*., 2002).

In addition, Nilsen *et al.*, 2012 recently showed that Nth1 provides the major AP site incision activity in *S. pombe* and that the generated 3'dRP is further processed to 3'P by the actions of Tdp1. Tdp1 working downstream of Nth1 in *S. pombe* was an interesting discovery and indicated an important back-up repair pathway of AP sites in *S. pombe*. An interesting question was whether a similar mechanism also is present in mammalian cells. Thus, one of the aims of our study was also to examine whether similar APE-independent repair pathway involving TDP1 and NTH1 could be observed in mammalian cells.

2 Materials

2.1 Bacterial strains

Strain	Characteristics	Genotype	Manufacturer
BL21 Codon Plus RIL	*E. coli*	B F^- *ompT hsdS*(r_B^- m_B^-) *dcm*$^+$ Tet_r *gal* λ(DE3) *endA* Hte [*argU ileY leuW* Cam_r]	Stratagene

2.2 Plasmid

Plasmid	Manufacturer
pET28b	Novagen

2.3 Enzymes

Enzyme	Buffer	Manufacturer
Uracil DNA glycosylase (Udg)	5xReaction buffer	Biolabs New England
Endonuclease III (Nth)	5xReaction buffer	Biolabs New England
T4 polynucleotide kinase	10xT4 Polynucleotide Kinase Reaction buffer	Biolabs New England
TURBO™ DNase	10xTURBO™ DNase buffer	Ambion

2.4 Antibody

Antibody	Host	Dilutions	Manufacturer
Anti-TDP1 Antibody	Rabbit	1:2,000	Novus biological
Anti-NTH1 Anti body	Rabbit	1:500	Novus biological
Anti-beta Actin antibody - Loading Control	Rabbit	1:2,000	AbCam
Goat polyclonal Secondary Antibody to Rabbit IgG - H&L (HRP)	Goat	1:30,000	AbCam

2.5 Primers

Primers id[1]	Discription	Sequence 5`→ 3`
14847	Forward, *NTHL1*	GATGGCACACCTGGCTATG
14848	Revers, *NTHL1*	GTCTCCTCTGGGGACTTGGT
13162	Forward, *ACTB*	CCCTAACACCAGCCTAACCA
13161	Revers, *ACTB*	GGGCTAGAGAAAAATTTGGAGAAGT

[1] Primers id is provided by the common primer database at Rikshospitalet, Oslo University hospital.

2.6 Cell types

Cell type	Description	Source[1]
HeLa S3	Human cervical carcinoma	LGC promochem /ATCC
HaCaT	Human immortalized keratinocytes	LGC promochem /ATCC

[1] American Type Culture Collection (ATCC)

2.7 siRNA

siRNA	Maufacturer	Concentrations
NTHL1-siRNA	Santa Cruz Biotech	10 µM
TDP1-siRNA	Santa Cruz Biotech	10 µM
Control siRNA	Santa Cruz Biotech	10 µM

2.8 Isotopes

Isotopes	Description	Specific Activity	Concentration	Manufacturer
[γ-^{32}P]ATP	Adenosine triphosphate [γ-^{32}P], NEG502A	3000Ci(111TBq)/mmol	10mCi/mL	Amersham
[α^{32}P]dATP	Deoxyadenosine 5'-triphosphate, 3'-[α-^{32}P]- (Cordycepin 5'-triphosphate)	5000Ci(185TBq)/mmol	10mCi/mL	Perkin Elmer

2.9 DNA substrates

Sequence length	DNA damage	Sequence[1] 5'→3'
40 mer	5-OHC	GCATGCCTGCACGG[**5-OHC**]CATGGCCAGATCCCCGGGTACCGAG
40 mer	U	GCATGCCTGCACGG[**U**]CATGGCCAGATCCCCGGGTACCGAG
40 mer	5-OHU	GCATGCCTGCACGG[**5-OHU**]CATGGCCAGATCCCCGGGTACCGAG
40 mer	Tg	GCATGCCTGCACGG[**Tg**]CATGGCCAGATCCCCGGGTACCGAG
20 mer	Phosphotyrosine	CTACGTCAGATCTGAGGATG-**pTyr**
24 mer	U	GGCGGCATGACCC[**U**]GAGGCCCATC

[1]Listed DNA substrates and their complementary strands were purchased at: The Midland Certified Reagent Company, Incorporated.

2.10 Molecular markers

Standard	Manufacturer
MagicMark™ XP Western Protein Standard	Invitrogen
SeeBlue® Plus2 Prestained Standard (1x)	Invitrogen
GeneRuler™ DNA Ladder Mix	Thermo Scientific

2.11 Kits

Kit	Manufacturer	Section
PCR Mycoplasma Test Kit	PromoKine	3.2.4
Immun-Star™ WesternC™ Kit	BioRad	3.4.1
High capacity RNA-to-cDNA Kit	Applied Biosystems	3.4.2

2.12 Softwares

Software	Source	Section
Image Lab	Biorad	3.4.1
StepOne™ Software v2.1	Applied biosystems	3.4.2
Typhoon Scanner Control	Amersham Biosciences	3.5
ImageQuant TL	Amersham Biosciences	3.5

2.13 Mice

Genotype	Strain	Manufacturer[1]
Wild-type	Black-six C57BL/6	Charles River
Neil1 single KO (*Neil1*-/-)	Black-six C57BL/6	Laboratory
Neil2 single KO (*Neil2*-/-)	Black-six C57BL/6	Laboratory
Neil1/Neil2 double KO (*Neil1*-/-*Neil2*-/-)	Black-six C57BL/6	Laboratory

[1]KO mice were generated in the laboratory by others (Unpublished material). Animal experiments were approved by the National Animal Research Authority (NARA) in Norway. Mice were housed and handled in accordance with the European Council Directive.

2.14 Buffers and solutions

Ordered by sections. Recipes are given in Appendix A.

Buffers and solutions	Section
LB-sorbitol medium	3.1.1
Buffer A/B/C	3.1.2
Coomassie Blue stain solution	3.1.3
Destaining solution	”
Culture medium	3.2.1
Cryomedium	3.2.3
Protein-cracking buffer	3.3.1
Lysis buffer	3.3.3
PBS-Tween buffer	3.4.1
PBS buffer	“
Stripping buffer	“
5xReaction buffer	3.5
Dilution buffer	”
20xTaurine buffer	”
Tris-sucrose/MOPS buffer	”
5x TDP1 buffer	”
1xTBE	”
Formamide loading dye	”

2.15 Chemicals

In alfabetical order

Chemicals/ Reagents[1]	Purity/ Concentrations	Manufacturer
β-mercaptoethanol	>99%	Sigma Aldrich
Acetic acid	100%	Merck
Ammoniumpersulphate (APS) (s)	-	BioRad
Betaine hydrochloride (s)	>99%	Sigma Aldrich
BioRad Protein Assay	5x	BioRad
Boric acid	>99.5%	Fluka
Bovine Serum Albumin (BSA)	10 mg/ml	BioLabs® Inc.
Bromophenol Blue (s)	-	Sigma Aldrich
Chloroform	>99.8%	Sigma Aldrich
Coomassie blue (s)	-	Sigma Aldrich
Dimethyl sulfoxide (DMSO)	>99.5%	Sigma Aldrich
Difco Luria Bertani (LB)-Broth	-	Miller
Dulbecco's Modified Eagle Medium with 4.5 g/l Glucose (DMEM)	-	Lonza
Dithiothreitol (DTT) (s)	-	Sigma Aldrich
Ethanol	100%	Kemityl
Ethylenediaminetetraacetic acid (EDTA)	>98%	Sigma Aldrich
Fetal Bovine Serum (FBS)	-	PAA Laboratories GmbH
Formamide	>99%	Sigma Aldrich
GlutaMAX™	100x	Gibco Invitrogen
Glycerol	>99.5%	Sigma Aldrich
Hepes (pH 7.4) (s)	-	Saveen Werner
Hydrogen chloride (HCl)	>99%	Sigma Aldrich
Imidazole (s)	>99%	Sigma Aldrich
IPEGAL® CA-630	-	Sigma Aldrich
Isopropanol	99.8%	Merck
Isopropyl β-D-1-thiogalactopyranoside (IPTG) (s)	>99%	Sigma Aldrich
Kanamycin (s)	50 mg/ml	Sigma Aldrich
Lipofectamine™ RNAiMAX	-	Invitrogen
Long Ranger™ Gel Solution	-	Lonza
Magnesium chloride ($MgCl_2$) (s)	>98%	Sigma Aldrich
Methanol	98.5%	VWR
Myricetin (s)	>96%	Sigma Aldrich
3-(N-morpholino) propanesulfonic acid (MOPS) buffer (s)	>99.5%	Sigma Aldrich
N,*N*,*N*′,*N*′-Tetramethylethylenediamine (TEMED)	99%	Sigma Aldrich
Ni-NTA agarose	50%	Qiagen
NuPAGE® LDS Sample Buffer	4x	Invitrogen
NuPAGE® MOPS SDS Running Buffer	20x	Invitrogen
NuPAGE® Transfer Buffer	20x	Invitrogen
Penicillin-streptomycin (Pen-Strep)	5000 U Pen/ml 5000 U Step/ml	Lonza
Phenyl methane sulfonyl fluoride (PMSF) (s)	-	Applichem
Potassium chloride (KCl)	-	Sigma Aldrich
Proteinase K (s)	-	Sigma Aldrich
Power SYBR® Green, PCR master mix		Applied Biosystems

Skim milk Powder	-	Fluka
Sodium acetate	-	Sigma Aldrich
Sodium borohydride (s)	90%	Sigma Aldrich
Sodium chloride (NaCl) (s)	>99%	Sigma Aldrich
Sodium Deoxy cholate (DOC)	>97%	Sigma Aldrich
Sodium dodecyl sulphate (SDS)	99%	Sigma Aldrich
Sodium hydrogen phosphate dehydrate (Na_2HPO_4) (s)	>99%	Merck
Sodium hydroxide (NaOH) (s)	>99%	Merck
Sodium orthovanadate (s)	99.8%	Sigma Aldrich
Sorbitol (s)	-	VWR
SYBR® Safe DNA gel stain	-	Lonza
Taurine (s)	>99%	Sigma Aldrich
Transfer RNA (tRNA)	10 mg/ml	Ambion
Tris Base (s)	-	Sigma Aldrich
Tris-HCl	>99%	Sigma Aldrich
TRIzol® Reagent	-	Invitrogen
Trypan Blue Stain	0.4%	Invitrogen
Trypsin-EDTA	170 000 U Trypsin/L 200 mg/l EDTA	Lonza
Tween®20		Sigma Aldrich
UltraPure™ Agarose	-	Invitrogen
Urea	>99.0 %	Duchefa BioChemicals
Xylene Cyanol	-	Sigma Aldrich

[1]s=solid

2.16 Equipment and instruments

Type	Manufacturer
Centrifuges:	
Allegra ™ X-22R Centrifuge	Beckman Coultier
PCR Capsulefuge PMC-860	Tomy
Spectrafuge mini	Labnet
Spectrafuge maxi	Hitachi
Avanti™ J-25 Centrifuge	Beckman
Megafuge	Heraeus
Biofuge Fresco	Heraeus
Spectrophotometer:	
UV- visible spectrophotometer UV-160 I	Shimadzu
NanoDrop ND-1000	Saveen Werner
Incubator:	
Innova 400 incubator shaker	New Brunswic scientific
Innova 4300 incubator shaker	New Brunswic scientific
Termaks incubator	Termaks
Forma Steri-cycle CO_2	Thermo scientific
Waterbath	KeboLab AS
Gel electrophoresis:	
Electrophoresis power supply EPS 60	Amersham pharmacia biotech
Electrphoresis power supply ECPS 3000/150s	Amersham pharmacia biotech
Electrophoresis unit: Hoefer He33	Amersham pharmacia biotech
Hoefer™ SQ3 Sequencer	Amersham pharmacia biotech
PCR:	
PTC-200 Peltier Thermal Cycler	MJ research
StepOnePlus Real-time PCR	Applied biosystems
Sterile hood	
Holten Lamin air	Holten
Diverse:	
3 MM Chromotography paper	Whatman®
BioRad Molecular Imager PhosphorImager	BioRad
Countess™ Automated Cell Counter	Invitrogen
Glass plate set for s2001/s2 (sequencing gel)	AH diagnostics/biometra
Heat block: QBT1	Grant
Multiple well Plate, MicroTest™ 96-well Tissue culture	Becton Dickinson Labware
Multiple well Plate, MicroTest™ 24-well Tissue culture	Becton Dickinson Labware
Multiple well Plate, MicroTest™ 6-well Tissue culture	Becton Dickinson Labware
Nitrogen tank: Cryo biological storage system	Thermolyne
Novex® Semi-Dry Blotter	Invitrogen
Nunclon™ 75 cm^2 Treated flask, blue filter cap	Thermo scientific
NuPAGE®10 % Bis-Tris gel	Invitrogen
Phosphor screen	Amersham Biosciences
Polyvinylidene difluoride (PVDF) (pore size 0,45 µm)	Amersham Biosciences
Shaker: Edmund Buhler	Hechingen
Sonicator: LabSonic™ M	Sartorius Stedim Biotech
Typhoon 940 Variable Mode PhosphorImager	Amersham Biosciences
Weighing scale: AT261 Delta Range	Mettler Toledo
Weighing scale: BP 4100	Sartorius
Vacuum dryer: Maxi dry Iyo,	Medinor

3 Methods

If not stated otherwise, enzymes, DNA and protein extracts were kept on ice during the experiments. DNA and proteins were stored at -20 ˚C and -70 ˚C, respectively. Recipes of solutions are listed in Appendix A.

3.1 Protein purification of NTH1

NTH1 was expressed and purified for biochemical activity assays. Protein expression can be achieved by cloning the gene of interest into a suitable plasmid expression vector, and transforming it into a host, such as an *E. coli* strain. Cell cultures are then grown and proteins are purified after induced expression. Protein purification was performed using nickel-nitrilotriacetic (Ni-NTA) agarose coloumn. This method is based on affinity purification of recombinant proteins tagged with six tandem histidine residues (6xHis-Tag) at the C- or N-terminal. The protein of interest will bind to Ni-NTA resin with its 6xHis-Tag, while other proteins pass through the column. Proteins bound to the resin are then eluted with a suitable buffer containing imidazole in excess that competes with the 6xHis-Tag for binding to the Ni-NTA (QIAGEN®, 2003). Purification of NTH1 can be performed using this method (Aspinwall *et al.*, 1997).

3.1.1 Expression of NTH1

The full-length NTH1 cDNA (Luna *et al.,* 2000) was cloned in into pET28b vector. This NTH1/pET28b construct with a C-terminal 6xHis-Tag, transformed into *E. coli* BL21 Codon Plus RIL strain, was a gift from Professor Lars Eide, Department of Medical Biochemistry, Rikshospitalet.

Procedure:

1. The cells were streaked out on Luria-Bertani (LB)-kanamycin (50 µg/ml) medium plates and incubated at 37˚C over night (ON).
2. ON culture was made by inoculating transformants in 20 ml LB-medium containing 50 µg/ml kanamycin. The ON culture was incubated at 37 ˚C ON with vigorous shaking.
3. 10 ml of ON culture was transferred to 1 l LB-sorbitol medium and incubated with shaking at 37 ˚C until OD_{600} reached ~0.6.
4. The protein expression was induced by adding 1 ml IPTG to a final concentration of 1 mM, and the cells were further grown at 37 ˚C for 4 h.
5. Cells were harvested by centrifugation at 6,000 rpm for 5 min at 4 ˚C and resuspended in 15 ml buffer A per liter cell culture.

3.1.2 Protein purification

Procedure:

1. *Sonication:*

   The cell suspension was sonicated on ice for 3x30 seconds at 60% amplitude, with a 30 second cooling period between each burst.

2. The cell suspension was centrifuged at 13,000 rpm for 20 min at 4 ˚C to pellet the cellular debris, and the supernatant was transferred to a fresh tube and kept on ice.

3. *Pre-equilibration:*

   A 20 ml purification column was packed with 2 ml of Ni-NTA agarose that consists of 50 % ethanol and 50% Ni-NTA. The resin was settled by gravity, and pre-equilibrated with 6 ml buffer A that resuspended the resin. The resin was allowed to settle for 5-10 min using gravity.

4. *Purification on Ni-NTA column:*

   The supernatant, containing protein of interest was loaded on the column and incubated for 30 min at 4 ˚C under shaking to keep the resin and supernatant suspended.

5. The resin was then settled by gravity, allowing the supernantant to flow through the column. The flow-through (FT) was saved at 4 ˚C for gel analysis.

6. *Wash:*

   The column was washed twice with buffer A and B using 3x column volume and the wash fractions were stored at 4 ˚C for electrophoresis analysis.

7. *Elution:*

   Bound proteins were eluted with 3x column volume of buffer C and collected in fractions of 1 ml. The purified protein fractions were analyzed by gel analysis, and aliquoted into 30 µl fractions with 20% glycerol for storage at -70 ˚C. Protein concentrations were determined using BioRad Protein Assay with BSA as standard.

3.1.3 SDS polyacrylamide gel electrophoresis (SDS-PAGE)

Protein gel electrophoresis is a method used to separate proteins according to their size, where the smaller proteins migrate faster through the gel than the larger proteins. Since proteins neither have a uniform negative charge nor a uniform secondary structure, the strong ionic detergent SDS is added in the polyacrylamid gel. The proteins are denatured by heating, applied to the SDS-containing gel and subjected to an electrical field. The binding of negatively charged SDS to the denatured proteins provides an equal mass to charge ratio upon which proteins are separated. The mass of the protein can be determined by comparing the protein movements to molecular markers with known migration patterns (Watson *et al.*, 2004).

Procedure:

1. FT, wash fractions and the eluted protein fractions were prepared for gel electrophoresis as follows:

Fraction	5.0 µl
NuPAGE® LDS Sample Buffer (4x)	4.0 µl
DTT (1 M)	1.0 µl
MQ	5.0 µl
Total	10.0 µl

2. Samples were incubated at 95 ˚C for 3 min and loaded at 10% NuPAGE® Bis-Tris gel in 1xNuPAGE® MOPS buffer.
3. 5 µl SeeBlue® Plus2 Prestained Standard was used as a molecular marker. The gel ran at 200 V for 35 min.
4. After the electrophoresis, the gel was stained and destained for 1-2 h by Coomassie Blue staining solution and destaining solution, respectively.
5. The gel was dried under vacuum on Whatman 3MM paper at 80 ˚C for 45 min.

3.2 Culturing and maintaining cell cultures.

A cells culture is a major tool used in molecular and cell biology that represent the biological model system of the intended experiment. Normal mammalian cells stop dividing after a limited number of cell division, and lose their ability to proliferate. However, some mammalian cells that have undergone transformations either spontaneously, chemically or virally can proliferate indefinitely (Alberts *et al.*, 2008). Thus, such immortals cells are often used in biological studies to achieve successful transfection and gene knockdown.

Human epithelial cervical carcinoma (HeLa) cells are cancer cells and the oldest permanent human cell line. Human immortalized keratinocytes (HaCaT) and HeLa cells are described as immortal since they can divide an unlimited number of times in a cell culture as long as fundamental growth conditions are present (Lucey *et al.*, 2009). These cells are adherent, meaning that they can grow as a monolayer on an artificial substrate that is suitable for cell adhesion and spreading.

Sterile and aspetic work area is required when working with different cell lines. All incubations were performed in a humified atmosphere at 37 ˚C with 5.5% CO_2. Cells were regularly passaged and monitored in microscope to maintain exponential growth and determine cell confluency. Dulbeccos's Modified Eagle medium (DMEM) containing 4.5 g/l glucose, 10% fetal bovine serum (FBS), 2% L-glutamine and 2% penicillin-streptomycin, is further referred as culture medium. Phosphate buffered saline (PBS), culture medium, and trypsin, otherwise kept at 4˚C, should be room tempered when added to the cells. Detailed guidelines and and procedures are refered in (Invitrogen®, 2012).

3.2.1 Initiating cell culture from a freezing stock

Procedure:

1. The cell culture was initiated from common frozen seeding stock, by immediately thawing the cells at 37 ˚C water bath and mixing the contents gently with 10 ml culture medium. The solution was then centrifuged at 1,200 rpm for 3 min.
2. The pellet was resuspended in 1 ml culture medium and mixed gently by pipetting up and down.
3. The cell suspension was transferred to a Nunclon™ 75 cm^2 (T75)-flask and diluted with culture medium up to 15 ml. The cells were examined on the microscope and incubated at 37 °C for 2-4 days until cell confluency reached 70-80%.

3.2.2 Passaging cells

Procedure:

1. When cell confluency reached 70-80%, the culture medium was removed. Since only the adherent cell lines were used, the cells remained stuck to the flask bottom.
2. The cells were gently washed with 1xPBS to remove residual medium.
3. 2 ml Trypsin-EDTA, just enough to cover the cell surface, was added to the T75-flask and incubated for 5 min to detach the cells.
4. Trypsin was then inactivated by trypsin inhibitors found in FBS, by adding 8 ml culture medium, which was vigorously pipetted up and down to detach all cells. Detached cells were observed under the microscope.
5. The cell suspension was then transferred to a fresh tube and centrifuged at 1,200 rpm for 3 min to remove trypsin and EDTA.
6. The pellet was resuspended in 1 ml culture medium.
7. Counting of viable cells are not necessary when passaging cell cultures, however this additional step is required to determine the seeding density in dishes before transfection. 10 µl of the cell suspension was added to 10 µl 0.4% Trypan Blue Stain. Amount of cells in a cell culture was then determined by using Countess™ Automated Cell Counter" according to the manufacturer's instructions.
8. The cells suspension was split in 1:10, 1:5 or 1:4 fractions and diluted with culture medium up to 15 ml in a T75-flask every 2-5 days depending on the confluency. The cell cultures were incubated at 37 ˚C.

3.2.3 Preparation of frozen seeding stocks

Procedure:

1. To prepare freezing stocks for storage and future use, step 1-5 in section 3.2.1 was followed.
2. The pellet was resuspended in 1 ml prepared cryo medium containing 10% dimetylsulfoxide (DMSO) that reduces the freezing point of the medium and prevents the formation of ice crystals that could cause damaged cells or cell death. The cryovial was stored at -70 ˚C for few days before transferring the vial to liquid nitrogen tank at –130 ˚C for long time storage.

3.2.4 Detecting contamination in cell lines

Cell health is essential to achieve successful experiments, however contaminated cells represent a major problem when working with biological material since they may alter cellular characteristics. For example mycoplasma, a simple bacteria that is considered to be the smallest self-replicating organism, is difficult to detect until they reach extremely high frequency (Invitrogen®, 2012;van Kuppeveld *et al.*, 1994).

To check for mycoplasma contamination in cell cultures PromoKine's PCR mycoplasma Test Kit II- protocol, designed for detecting mycoplasma in biological materials was followed (Appendix B).

3.3 Transfection of cells with siRNA and gene knockdown

Transfection is the process used to deliver foreign nucleic acid into mammalian cells that can be used to down-regulate the gene of interest. One technique used to transfect cells, rely on cationic liposomes that interact with the negatively charged foreign nucleic acid, resulting in liposome-nucleic acid complexes. This complex will get transfected into the cell by endocytosis and release the foreign nucleic acid. When small interfering RNA (siRNA) are used to transfect the cells, they are released in the cytoplasma, where they become a part of the RNA-induced silencing complex (RISC) and denatured (Figure 3.1) (Felgner *et al.,* 1987). The presence of ss siRNA will direct the complex to a complementary messenger RNA (mRNA), resulting in inhibition of translation and degradation of that specific mRNA (Watson *et al.*, 2004).

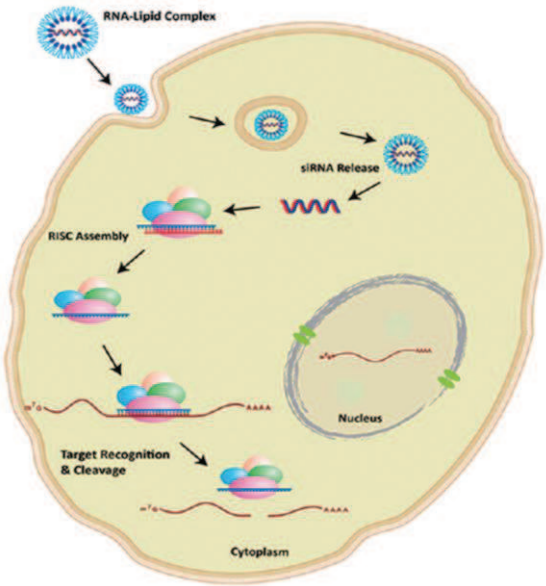

Figure 3.1. Schematic illustration of transfection of siRNA and its assembly in RISC (Li and Rana, 2012).

Another aspect to consider is whether the transfection should be transient or stable. Stable transfection ensures that foreign DNA is integrated in the genome permanently. Transient transfections on the other hand requires less time, however the effect is only temporary (Felgner *et al.*, 1987;Sambrook and Russel, 2001).

To achieve down-regulation of NTH1 and TDP1 in mammalian cells, different cell lines were transiently transfected with siRNA specific to *NTHL1* and *TDP1* genes using cationic liposomes to transfect cells. Additional cells were also transfected with non-targeting control siRNA, designed as a negative control.

3.3.1 Optimizing transfection conditions and evaluating knockdown

Procedure:

1. To determine when the highest transfection efficiencies were achieved, different transfection conditions were optimized using varying combinations of siRNA and Lipofectamine™ RNAiMAX Reagent.

2. $4x10^4$ cells/well were seeded in a 24-well plate in a total volume of 500 µl culture medium without antibiotics.
3. When indicated, 0, 1.2, 6 and 30 pmol siRNA was transfected in combination with 0.5, 1.0 and 1.5 µl Lipofectamine™ RNAiMAX in a total volume of 100 µl DMEM. All combinations were replicated twice.
4. The cells were transfected at 50-70% confluency as described in "Forward Transfection Protocol" from Invitrogen (Appendix C).
5. Cells were washed and harvested 48 h after transfection by 100 µl 1xPBS and 50 µl protein-cracking buffer, respectively. The samples were sonicated using a microtip for 3x20 second, at 30% amplitude under 0.6 seconds cycles.
6. The samples were incubated at 95˚C for 3 min and centrifuged at 13,000 rpm for 5 min.
7. Since protein concentrations could not be measured, 25 µl of the sample were loaded onto a 10% NuPAGE® Bis-Tris gel for Western Blot analysis, described in section 3.4.1, to evaluate down-regulation of NTH1 and TDP1.
8. The proteins were separated at 170 V for 60 min and 3 µl µl MagicMark™ XP Western Protein Standard was used as a molecular marker.

3.3.2 Transient Transfection assay

The various amounts of Lipofectamine™ RNAiMAX, siRNA and medium used are in proportion to the relative surface area of the culture plates used (Appendix C). Thus, the amounts of concentrations and cell densities used in a 6-well plate corresponds to $4x10^4$ cells/well, 1.2 pmol siRNA and 1.5 µl Lipofectamine™ RNAiMAX used in the 24-well plate in section 3.3.1.

Procedure

1. Different cell lines were seeded in 6-well plates at a density of $2x10^5$ cells/well using a total volume of 2.5 ml culture medium without antibiotics. The cells were incubated at 37 ˚C until confluency reached 50-60%.
2. Cells were transfected by adding 7.5 µl Lipofectamine™ RNAiMAX Reagent and 6 pmol of *NTHL1*-siRNA or *TDP1*-siRNA in a total volume of 500 µl DMEM. Additional cells were also transfected with control siRNA in the same manner, using the same amount of control siRNA. Each transfection was replicated twice.
3. The cells were incubated for 48 h and further assayed for gene knockdown.

3.3.3 Preparation of whole-cell protein extracts

Procedure:

1. Transfected cells were washed in 500 µl 1xPBS, harvested by trypsinization using 500 µl Trypsin-EDTA and incubated for 2-3 min.
2. 1 ml of culture medium was subsequently added, mixed gently and the cell suspension from each well was transferred to a microcentrifuge tube, which was then centrifuged at 13,000 rpm for 2 min.
3. The pellets were washed once in 1xPBS and resuspended in 1 ml lysis buffer on ice.
4. The samples were incubated on ice for 15 min, sonicated for 2x30 second at 30% amplitude under 0.6 seconds cycles and centrifuged at 13,000 rpm for 15 min.
5. The supernatant containing proteins was transferred to a fresh microcentrifuge tube and kept one ice.
6. Total protein concentrations were determined by BioRad Protein Assay.
7. 25 µg proteins were loaded onto a 10% NuPAGE® Bis-Tris gel in a total volume of 25 µl containing 1x LDS Sample buffer and 100 mM DTT.
8. 3 µl MagicMark™ XP Western Protein Standard was used as a molecular marker.
9. The proteins were separated by electrophoresis for 60 min at 170 V and the gel was further used in Western blot analysis.

3.4 Evaluation of gene knockdown

To determine the success of gene knockdown by transfecting siRNA into cell lines, Western blot and real time-polymerase chain reaction (RT-PCR) can be performed.

3.4.1 Western blotting

Western blotting is a method used to transfer electrophoretically separated proteins to a membrane by applying an electric field through the gel that is in direct contact with the membrane. Once the proteins are transferred, the non-specific binding sites are blocked by incubating the membrane in a blocking buffer containing proteins unrelated to the protein of interest. The membrane is then incubated in a solution of a primary antibody that specifically recognizes and can only bind to the target protein. A chromogenic enzyme that is artificially attached to a second antibody that binds the primary antibody is used to visualize the target protein (Watson *et al.*, 2004).

Procedure:

1. The electrophoretically separated proteins were transferred to a polyvinylidene difluoride (PVDF) membrane using Novex® Semi-Dry Blotter at 20 V for 30 min (Appendix D).

   Post-transfer:
2. The membrane was washed in 1xPBS for 2 min and subsequently blocked in PBS-Tween buffer containing 5% skim-milk, on a shaker for 1 h in room temperature (RT) or ON at 4 ˚C.
3. PBS-Tween buffer was used to wash the membrane 3x5 min on a shaker.
4. The membrane was incubated with primary antibody in PBS-Tween buffer containing 3% skim-milk buffer ON at 4 ˚C or 1-3 h at RT. Different antibodies required different dilutions as listed in section 2.4.
5. The membrane was washed in PBS-Tween buffer for 5x10 min in RT under strong agitation.
6. 1:30,000 dilution of a horseradish peroxidase (HRP)-conjugated secondary antibody, was added and the membrane incubated for 1 h on a shaker at RT.
7. PBS-Tween buffer was used to wash the membrane 6x10 min under strong agitation.
8. Immun-Star™ WesternC™ Kit from BioRad was used according to the manufacturer's instructions, and the membrane was immediately visualized in BioRad Molecular Imager.

Antibodies can be removed from the membrane by stripping when detection of more than one protein on the same membrane is wanted. This was performed by removing primary and secondary antibodies from the membrane and re-incubating with an antibody specific for a protein that is expected to occur in equal amounts, thereby acting as a loading control.

Procedure:

9. Stripping-buffer containing β-mercaptoethanol was pre-heated to 50 °C and added to the membrane, which was then incubated for 45 min at 50 °C with some agitation.
10. Traces of β-mercaptoethanol can damage the antibodies. Thus, the membrane was washed extensively with MQ under strong agitation for 1-2 h, before repeating step 1-8 and using Anti β-Actin antibody as the primary antibody.

3.4.2 RT-PCR

RT-PCR is a technique based on PCR, a method that amplifies segments of DNA up to few thousand base pair. PCR is a cyclic process and can be summarized in three steps; denaturation of the original DNA, annealing of primers to the DNA template strand and polymerization by DNA polymerases. However, standard PCR have its limitations since the product is only detected at the end of the reaction on an agarose gel. In RT-PCR on the other hand, the products can be measured continuously and during the exponential phase of the reaction providing accurate and fast quantification of DNA and RNA levels in cells.

For quantification of mRNA, RT-PCR is often combined with reverse transcription that yields a complementary DNA (cDNA) copy from the total isolated RNA. Gene expression for a target gene can then be detected by using RT-PCR to amplify the cDNA. Detection is obtained by adding fluorescent probes, such as SYBR Green that will bind non-specifically to the minor grove of ds DNA, resulting in increased intensity of fluorescence. As the ds DNA is amplified, the level of fluorescence increases proportionally, making it possible to accurately determine the precise amount of target mRNA present in the cells (Valasek and Repa, 2005).

Isolation of RNA from transfected cells

Procedure:

1. HeLa S3 cells transfected with siRNA specific to *NTHL1* were harvested 48 h after transfection by trypsinization and centrifugation, as described in step 1-2 in section 3.3.3.
2. Each pellet was resuspended in 750 µl TRIzol® Reagent to homogenize the samples and incubated at RT for 5 min.
3. 150 µl chloroform was added and the tube was shaken vigorously for 15 seconds.
4. The samples were incubated for 2-3 min at RT, and then centrifuged at 12,000 rpm for 15 min at 4 °C, which resulted in a colorless upper aqueous phase, an interphase and a lower red phenol-chloroform phase.
5. The aqueous phase, containing RNA, was transferred to a fresh tube.
6. 375 µl 100% isopropanol was added to the aqueous phase, incubated at RT for 10 min and centrifuged at 12,000 rpm for 10 min at 4 °C.
7. The pellet, containing RNA, was washed in 750 µl 75% ethanol, before centrifuging the tube at 7,500 rpm for 5 min at 4 °C.

8. The supernatant was discarded and the pellet was air-dried for 15 min.
9. The RNA pellet was resuspended in 30 µl RNAse free water and incubated at 55 °C for 10 min.
10. 3.3 µl 10xTURBO™ DNase buffer and 0.5 µl TURBO™ DNase was added to remove any remaining residual DNA.
11. The samples were incubated at 37˚C for 30 min and reaction was subsequently stopped at 75˚C for 10 min.
12. Concentration of RNA was measured using NanoDrop® ND-100.

cDNA synthesis

Procedure:

1. 1 µg of the total RNA from each sample was used for cDNA synthesis. The samples were prepared by using "High Capacity RNA-to-cDNA Kit" from Applied Biosystems as instructed by the manufacturer's protocol (Appendix E).
2. The samples were incubated in a thermal cycler at 25˚C for 10 min, subsequently followed by 37˚C for 2 h. The reactions were then stopped by raising the temperature to 85˚C for 5 seconds and the samples were subsequently held at 10˚C.
3. The remaining RNA samples were stored at -70 ˚C.

Preparing standard curves to determine the amount of cDNA to use

The cytoskeletal protein β-Actin, encoded by the gene *ACTB*, was used as the housekeeping gene for normalization. To determine the amplification efficiencies of the target gene, primers specific for target gene and β-Actin were used to generate standard curves.

Procedure:

1. Two standard curves of 5 points were generated by making five standard solutions with 1:5 dilutions of cDNA prepared from control cells transfected with non-targeting siRNA.
2. Triplicates were made of each standard solution.
3. To generate each standard curve, primers for the target gene; *NTHL1* and *ACTB* were used. Primers are listed in section 2.5. For sequence information of *NTHL1* gene, see GeneBank: National Center for Biotechnology Information (NCBI), accession number NM_002528.5.

4. Following reaction mixture was prepared for each of the primerpairs.

1:5 serial dilution of control cDNA	1.0 µl
Forward primer (100 nM)	0.2 µl
Revers primer (100 nM)	0.2 µl
Power SYBR® Green PCR master mix	8.0 µl
MQ	10.6 µl
Total	20.0 µl

5. RT-PCR was performed using program: Comparative method of relative quantification in StepOne™ v2.1 Software, provided by Applied Biosystems.

Assaying gene knockdown in RT-PCR

Procedure:

1:10 dilutions of control cDNA samples and cDNA samples obtained from cells transfected with *NTHL1*-siRNA were prepared in triplicates, using primerpairs specific to the *ACTB* and *NTHL1* as previously described in step 4-5 above.

3.5 Biochemical activity assays

To investigate the activity of an enzyme of interest on a specific damage, biochemical activity assay can be performed. This is achieved by radioactively labeling the DNA substrate, containing base damage of interest, on the 5'-end with [γ-^{32}P]adenosine triphosphate (ATP) and T4 polynucleotide. The DNA substrate can also be labeled at the 3'-end with [α-^{32}P]deoxyATP (dATP) (Tu and Cohen, 1980). The principle is based on radioactively labeling the DNA substrate only one end, so the location of any break in the strand can be determined by the size of the resulting labeled substrate (Figure 3.2). To stop the enzymatic reactions on the radioactively labeled DNA substrate, a formamide loading dye is added that denaturates the DNA. The DNA products can then be separated on a denaturing polyacrylamide gel (Alberts *et al.*, 2008). The radioactive DNA products are typically visualized and quantified by phosphorimaging by exposing the gel to a phosphor screen. When the screen is scanned by a laser, it will emit light in proportion to the amount of radioactivity in the samples (Amersham Biosciences®, 2012).

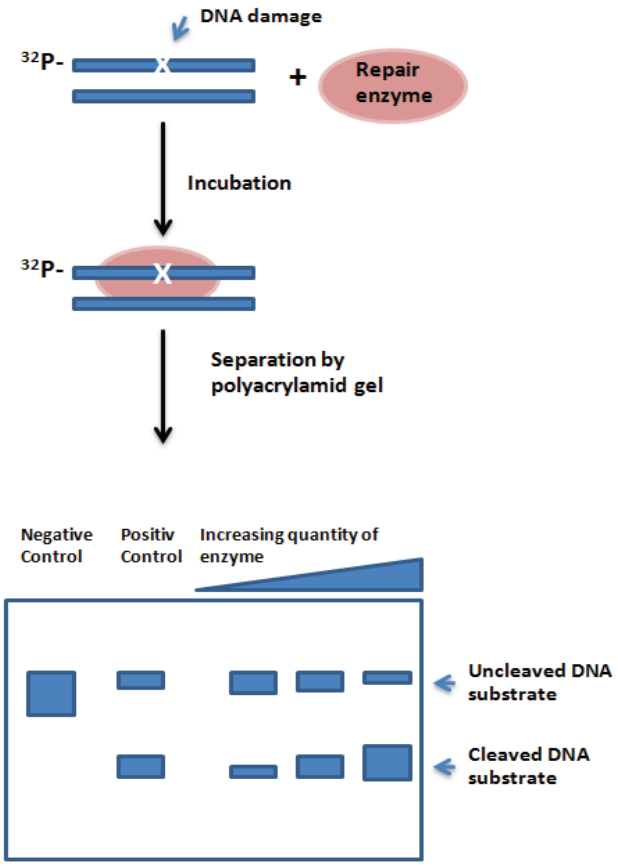

Figure 3.2. Simplified schematic presentation of 5'end-labeled activity assay.

3.5.1 Activity assays performed on [^{32}P]-5'-labeled DNA substrates

Purified enzymes like *S. pombe* Tdp1, *E. coli* Nth, human APE1 and NEIL1, used as controls, were provided from common stocks in the laboratory and diluted in dilution buffer as indicated. Ss and ds DNA substrates containing single base damages were radioactively labeled at 5'end or 3'end as described in (Nilsen *et al*., 2012) by Alseth and Erik Sebastian Vik.

Whole-cell protein extracts of heart, liver and brain from five wild-type (WT) mice, six Neil1 single KO (S-KO) mice, six Neil2 S-KO mice and six Neil1/Neil2 double KO (D-KO) mice were prepared as described in (Yndestad *et al*., 2009), and were a gift from Susanne Vetlesen. Serial dilutions of the whole-cell protein extracts were made by using

Tris-sucrose/MOPS buffer. The sequences of DNA substrates used in these studies are listed in section 2.9.

Procedure:

1. 10 µl of a reaction mixture was prepared by mixing following components:

Enzyme[1]	1.0 µl
DNA substrate (10 fmol)	1.0 µl
5xReaction buffer	2.0 µl
MQ	6.0 µl
Total	10.0 µl

2. The reaction samples were incubated at 37 ˚C for 30 min.
3. The reactions were stopped by adding equal volume of formamide loading dye in volume ratio.
4. The samples were denatured at 90 ˚C for 3 min.
5. The reactions products were separated on a 20% polyacrylamid gel at 200 V for 1 h in 1xTaurine buffer, by applying 4 µl of the reaction sample. To achieve single nucleotide resolution, the DNA products were also separated on 20% sequencing gel at 40 W for 2.5 h using Hoefer™ SQ3 Sequencer.
6. The gel was dried under vacuum for 45 min at 80 ˚C and exposed to phosphoscreen ON.
7. The radiolabeled products were visualized by using Typhoon PhosphorImager and ImageQuant TL software was used for quantification.
8. The remaining samples were stored at -20 ˚C.
9. When intact AP sites were processed 1 µl 50 ng/µl Proteinase K and 1 µl 5% SDS was also included in the reaction mixture after the incubation step, followed by additional incubation at 65 ˚C for 15 min. This was done to improve the detection of the cleaved DNA substrate since Proteinase K degrades redundant proteins in the native state.
10. When indicated:
    - 1 µl of 0.5 M NaOH was added after the incubation step to hydrolyze uncleaved AP sites and the incubation continued for additional 10 min at 70 ˚C, followed by neutralization with 1 µl 0.5 M HCl.

[1] Purified recombinant proteins or whole-cell extracts from WT and KO mice or HeLa S3 cells.

— Different amount of inhibitors like myricetin and sodium orthovanadate were included in the reaction mixtures, notably before the enzymes were added to the DNA substrates. 5xTDP1 buffer was used instead of 5xReaction buffer for optimal TDP1 activity.

3.5.2 Preparation of AP site using [^{32}P]-5'-labeled DNA substrates

Procedure:

1. DNA substrates with an intact AP site were produced by pre-treating the uracil-containing ss and ds 40-mer DNA substrate Uracil DNA glycosylase (Udg) as described below:

5xReaction buffer	0.25 µl	Multiplied with the number of total reaction samples
Udg (5,000 U/ml)	0.05 U	
DNA substrate (10 fmol)	1.00 µl	
Total	1.25µl	

2. When indicated, 0.1 U *E .coli* Nth (10,000 U/ml) was also included to generate a nicked AP site with a 3'dRP terminus.
3. The mixture was incubated at 37 ˚C for 30 min, subsequently followed by additional incubation at 55 ˚C for 10 min.
4. 1 µl of the Udg-treated DNA substrate was added to each sample of reaction mixture. The reaction mixtures are prepared and separated on gel as described previously through step 1-8 in section 3.5.1.

3.5.3 Sodium borohydride-mediated trapping assay

A ^{32}P-5'end-labeled ds DNA substrate containing 5-OHU opposite G was used in trapping assay.

Procedure:

1. 10 µl of reaction mixtures were prepared as described in step 1 in section 3.5.1 with 1 µl of 1 M sodium borohydride.
2. The samples were incubated at 37 ˚C for 30 min, and the reaction were stopped by adding 2.5 µl 4xNuPAGE® LDS Sample buffer and 1 µl 1 M DTT.
3. The samples were denatured at 95 ˚C for 3 min.
4. 5 µl of the samples were applied and separated on 10% NuPAGE® Bis-Tris gel at 150 V for 1 h. Step 6-8 in section 3.5.1 was further followed to visualize the gel.

3.5.4 Activity assays perfomed on [^{32}P]-3'-labeled DNA substrates

The enzyme activities were investigated using ^{32}P-3'end-labeled 24-mer ds DNA substrate. The reaction products were separated on 20% sequencing gel at 45 W for 3-4 h in 1xTBE buffer.

Procedure:

1. Intact AP site opposite C on the 14th position from the 5'end was produced by pre-treating the DNA substrate with Udg as described in section 3.5.2.
2. When indicated:
   - 2 mM $MgCl_2$ was added in reaction samples, before incubating them at 37 ˚C for 30 min.
   - AP site was nicked by adding 4 ng APE1 subsequent to *E. coli* Udg addition, and incubated for additional 30 min at 37 ˚C.
3. The samples, after incubation, are added 2 µl of the reducing agent sodium borohydride.
4. For effective precipitation of DNA products are following reagents added and the samples are briefly centrifuged between each addition.

— tRNA (1 µg/µl)	1.0 µl
— sodium acetat (3 M, pH 5.5)	1.3 µl
— 96% ethanol	30.0 µl

5. The samples were mixed thoroughly and incubated at -20 ˚C for 30 min, before centrifuging them at 13,000 rpm for 30 min at 4 ˚C to pellet the DNA products.
6. 30 µl of 70% ethanol was used to wash the pellet and the samples were centrifuged for 5-10 min.
7. The pellet was air-dried for 10-15 min and resuspended in 10 µl formamide loading dye. The samples were denatured at 75 ˚C for 2 min.
8. 3 µl of the samples were applied on the 20% sequencing gel and separated using Hoefer™ SQ3 Sequencer.

4 Results

Mutagenic and cytotoxic AP sites are amongst the most frequently formed lesions in DNA. To gain better understanding of how AP sites are processed and repaired in mammalian cells, recombinant NTH1, KO mice models and immortalized human cell lines have been used.

4.1 Purification of recombinant NTH1 using Ni-NTA column

The protein NTH1, expressed in *E. coli* BL21 Codon Plus RIL strain using NTH1/pET28b construct, was purified using Ni-NTA column. 5 µl of protein fractions were separated on 10% NuPAGE® Bis-Tris gel, and an induction of a protein of ~39 kDa was observed that corresponded to the expected size of NTH1 (Figure 4.1). Engineers in the laboratory had earlier analyzed the expressed protein isolated from NTH1/pET28b construct by mass spectroscopy. Thus, no further purification or analysis was necessary. Consistent with the presence of an iron-sulfur cluster within NTH1, the purified protein had a yellow coloration. FT and wash fractions showed no substantial loss of protein of interest during purification. The eluted protein fraction in lane 3 was used in further experiments. The protein concentration was determined to 930 ng/µl by BioRad Protein Assay using BSA as a reference.

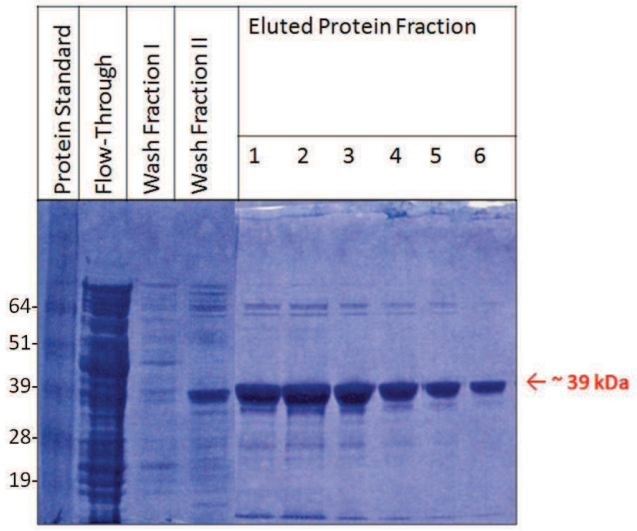

Figure 4.1. Detection of recombinant NTH1 protein after IPTG induction by SDS-PAGE using 10% NuPAGE® Bis-Tris gel and Coomassie Blue staining. The red arrow indicates the presence of NTH1 at ~39 kDa. SeeBlue® Plus2 Prestained Standard (1x) was used as a molecular marker. The purified protein NTH1 was eluted from Ni-NTA column in six fractions using 300 mM imidazol. Flow-through was collected and the two wash fractions were derived from washing the Ni-NTA column with 10 mM and 30 mM imidazol, respectively.

4.2 Cleaving activity of NTH1

Recombinant NTH1 was used in biochemical activity assays to gain better understanding of its DNA cleaving activity upon various DNA damages.

4.2.1 Processing of 5-OHC by NTH1

The activity of purified NTH1 was measured using a 5'end-labeled DNA substrate containing 5-OHC, which is a known substrate for NTH1. When indicated, 0.5 M NaOH that hydrolyzes AP sites, was also added to determine whether the glycosylase or AP lyase activity is coupled.

Cleaving activity was observed in both 40-mer ss and ds DNA substrate containing 5-OHC, although the ss DNA substrate was cleaved less efficiently. Indeed, the ds DNA substrate was cleaved approximately twice as efficiently as the ss DNA substrate (Figure 4.2).

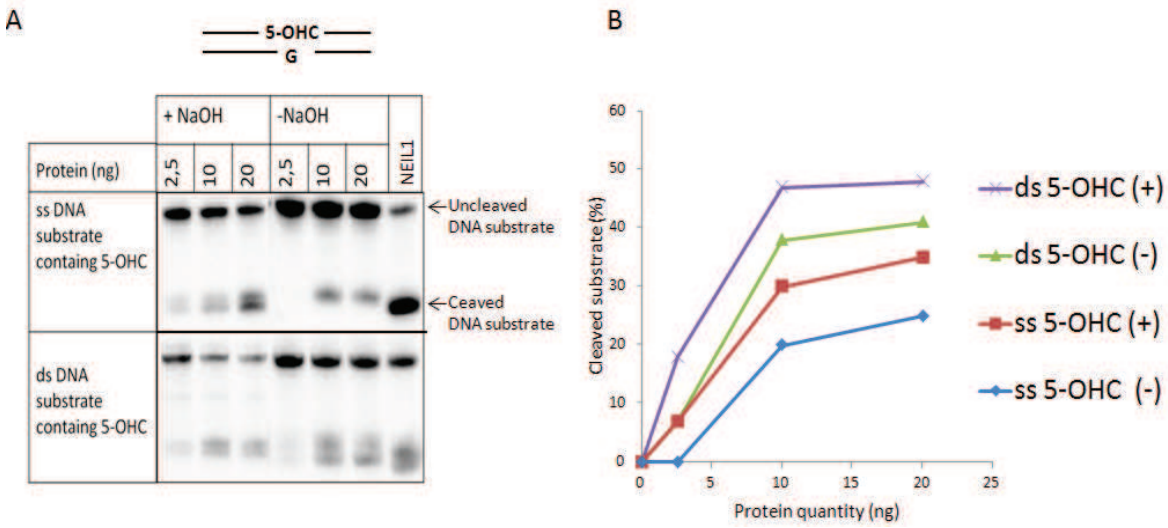

Figure 4.2. The activity of NTH1 upon ^{32}P-5'end-labeled 40-mer DNA substrate containing 5-OHC. (A) Different amounts of NTH1 are indicated and were incubated with ss and ds DNA substrate containing 5-OHC (10 fmol) for 30 min at 37 °C. Cleaved DNA substrates were separated from intact DNA substrates by 20% denaturing PAGE and visualized by phosphorimaging. Purified NEIL1 (10 ng) was used as control for 3'OH terminus. Experiments were repeated twice, one representative experiment is shown. (B) Cleaved substrate (%) was plotted against different amounts of NTH1 (2.5, 10 and 20 ng). The cleavage products were quantified using ImageQuant TL and the background was subtracted during quantification. "+" and "-" denotes reactions with and without 0.5 M NaOH, respectively.

Only ~10% increase in cleaved substrate was observed when NaOH was added to the reaction, which represents the fraction of bases that are removed without any subsequent AP lyase incision. Thus, most of the activity of NTH1 seems to be coupled, meaning that if NTH1 removes the damaged base, a subsequent incision 3' to the AP site will follow in

most cases, at least when NTH1 is the only enzyme acting upon the damaged substrate. However, as the results indicate, in ~10% of the cases, NTH1 will act only as a monofunctional DNA glycosylase.

4.2.2 Processing of AP sites using recombinant NTH1

A 5'end-labeled ss DNA substrate containing an AP site on the 15th position from the 5'end was used to investigate in what extent the recombinant NTH1 is able to incise AP sites. AP site opposite A, C, T or G was used to determine whether the activity of NTH1 was affected by the opposite base.

A 15-mer product was generated when NTH1 nicked 3' to the AP site, producing a 3'dRP terminus. The different bases opposite the AP site did not affect the rate of incision. 20 ng NTH1 was able to cleave ~60% of the ds DNA substrate, but only ~15% of ss DNA substrate, demonstrating that ds DNA are better substrates than ss DNA for NTH1 (Figure 4.3).

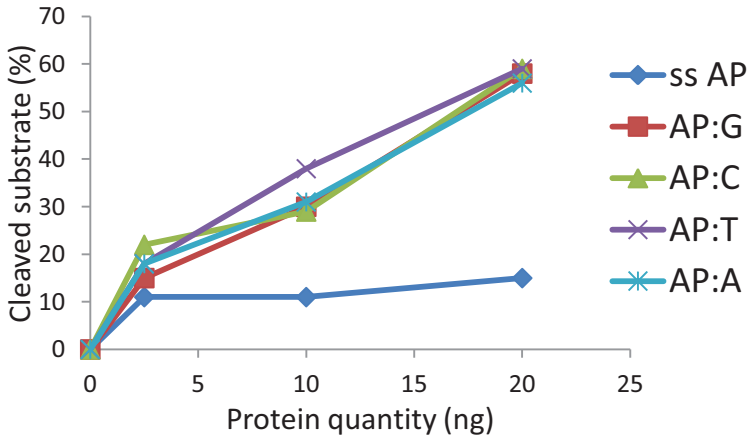

Figure 4.3. The activity of NTH1 upon ^{32}P-5'end-labeled 40-mer DNA substrate containing intact AP site opposite G, C, T or A. Cleaved substrate (%) was plotted against different amount of NTH1 (2.5, 10 and 20 ng) that were incubated with ss and ds DNA substrate containing (10 fmol) for 30 min at 37 °C. Experiments were replicated twice, one representative experiment is shown.

4.2.3 Processing of 5'dRP by recombinant NTH1

The activity of NTH1 upon a 5'dRP terminus generated by APE1 was also investigated by adding serial dilutions of NTH1 to 3'end-labeled DNA substrate containing either intact or nicked AP site. The AP site was nicked by APE1 to generate a 5'dRP terminus and 2 mM Mg^{2+} was included for optimal APE1 activity.

10 ng NTH1 was sufficient to efficiently cleave the intact AP site to produce 5'P product, whereas 100 ng was required to generate corresponding amount of 5'P product from an APE1-nicked AP site (Figure 4.4). As 10-fold more enzymes are required to generate the corresponding cleavage product from a 5'dRP terminus compared to an intact AP site, suggest that 5'dRP is a poor substrate for NTH1.

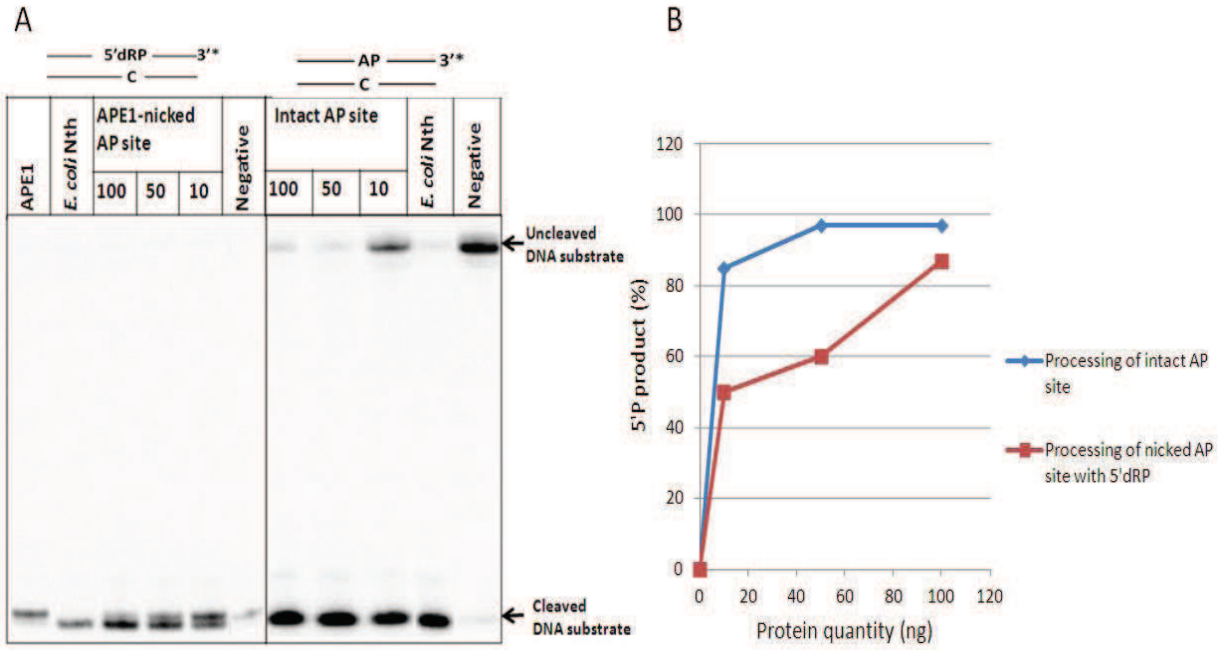

Figure 4.4. Processing of 5'dRP terminus and intact AP site opposite C by NTH1 using ^{32}P-3'end-labeled 24-mer DNA substrate. (A) The different amounts of NTH1 used are indicated and were incubated with intact or APE1-nicked AP site (10 fmol) for 30 min at 37 °C. Cleaved DNA substrates were separated from intact DNA substrates by 20% denaturing PAGE and visualized by phosphorimaging. Purified APE1 (10 ng) and *E. coli* Nth (2 U/µl) were used as positive controls for 5'dRP and 5'P termini, respectively. Experiments were repeated twice, one representative experiment is shown. (B) Generated 5'P product (%) was plotted against different amounts of NTH1 (10, 50 and 100 ng). The cleavage products were quantified using ImageQuant TL and the background was subtracted during quantification.

4.3 Processing of AP sites in mice

KO mouse models were used to study the biological role of Neil1, Neil2 and Nth1 in the processing of AP sites. Here, various biochemical activity assays were performed on whole-cell protein extracts prepared from either liver, heart or brain of six months old WT and KO mice. The lack of Neil1 and Neil2 in S-KOs or D-KOs has been established by engineers in the laboratory by genotyping and RT-PCR (unpublished material).

4.3.1 Processing of intact AP sites

Whole-cell extracts prepared from liver were used to compare the cleaving activity of Neil1 S-KO, Neil2 S-KO, Neil1/Neil2 D-KO and WT upon a 5'end-labeled ds DNA substrate containing AP site on the 15th position opposite G, T, C or A (Figure 4.5). Furthermore*, E. coli* Nth and NEIL1 were used as markers for β-elimination and β,δ-elimination product, respectively. One cleavage product was observed when WT, D-KO or S-KO were used that migrated between the β-elimination and β,δ-elimination product, suggesting that the detected product was generated by the activity of Ape1. In addition, processing of AP site opposite A, C, G or T produced similar results, demonstrating that the processing occurs independent of the base in the complementary strand. Thus, only one representative substrate is shown, as indicated in each figure.

No statistical significant differences between the cleavage products in neither the S-KO and D-KO, nor WT and D-KO ($p > 0.1$) were observed. These results suggest a non-essential role of Neil enzymes in AP site strand incision since the lack of either both Neil enzymes or just one, do not affect the incision of the AP site substantially compared to WT mice (Figure 4.5). Thus, only WT and Neil1/Neil2 D-KO were included in further experiments. The statistical significance was determined by performing a statistical T-test, using a 90% confidence interval. A p value higher than 0.1 was considered to be statistical insignificant. The cleavage products were quantified first using ImageQuant TL and the background was subtracted during quantification. Five or six parallels from each genotype were used to calculate means and standard deviations for the cleaving activity.

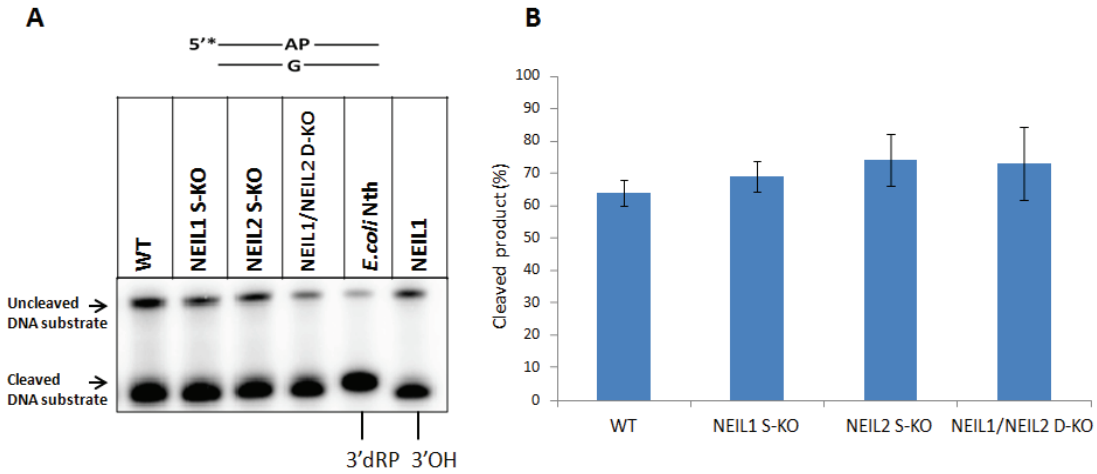

Figure 4.5. Total product generated (%) from a ^{32}P-5'end-labeled 40-mer DNA substrate containing an intact AP site opposite G, was compared for whole-cell liver extracts prepared from all four genotypes. AP site opposite other bases showed similar results as well. (A) 1.5 µg liver extracts were incubated with DNA substrate containing intact AP site (10 fmol), for 30 min at 37 °C. Cleaved DNA substrates were separated from intact DNA substrates by 20% denaturing PAGE and visualized by phosphorimaging. Purified *E. coli* Nth (2 U/µl) and NEIL1 (10 ng) were used as markers for β-elimination and β,δ-elimination activity, respectively. Experiments were repeated twice, one representative experiment is shown. (B) Means and standard deviations were calculated using five or six parallels of each genotype. *p* values were calculated using statistical two-tailed T-test and a 90% confidence interval. The results were quantified using ImageQuant TL and the background was subtracted during quantification.

To achieve single nucleotide resolution, DNA products were separated on 20% denaturing sequencing gels that made it possible to distinguish between products generated by different enzymes. Nth1 incises the 5'end labeled DNA substrate 3' to the AP site, generating a product that migrates slower than the product generated by Ape1. Neil1 and Neil2, on the other hand generates the 3'P product through a β,δ-elimination step that migrates fastest through the gel, even though it is not the shortest fragment due to the negative charge provided by the phosphate group on the 3'end.

The experiments performed on whole-cell extracts from liver, heart and brain, using WT and D-KO mice, all demonstrated that intact AP sites are mainly processed by the activity of Ape1, as expected (Figure 4.6). The product from Nth1's activity, 3'dRP, was also observed in both WT and D-KO in all three organs, although to a lesser extent than the 3'OH product generated by Ape1. In addition, within the three organs tested, the AP site processing in liver extracts was twice as efficient as compared to heart and brain. This is demonstrated by the fact that 0.5 µg liver extracts were sufficient to process the AP site efficiently, whereas 1.8 and 2.0 µg of heart and brain extracts were required to observe corresponding processing of AP sites, respectively.

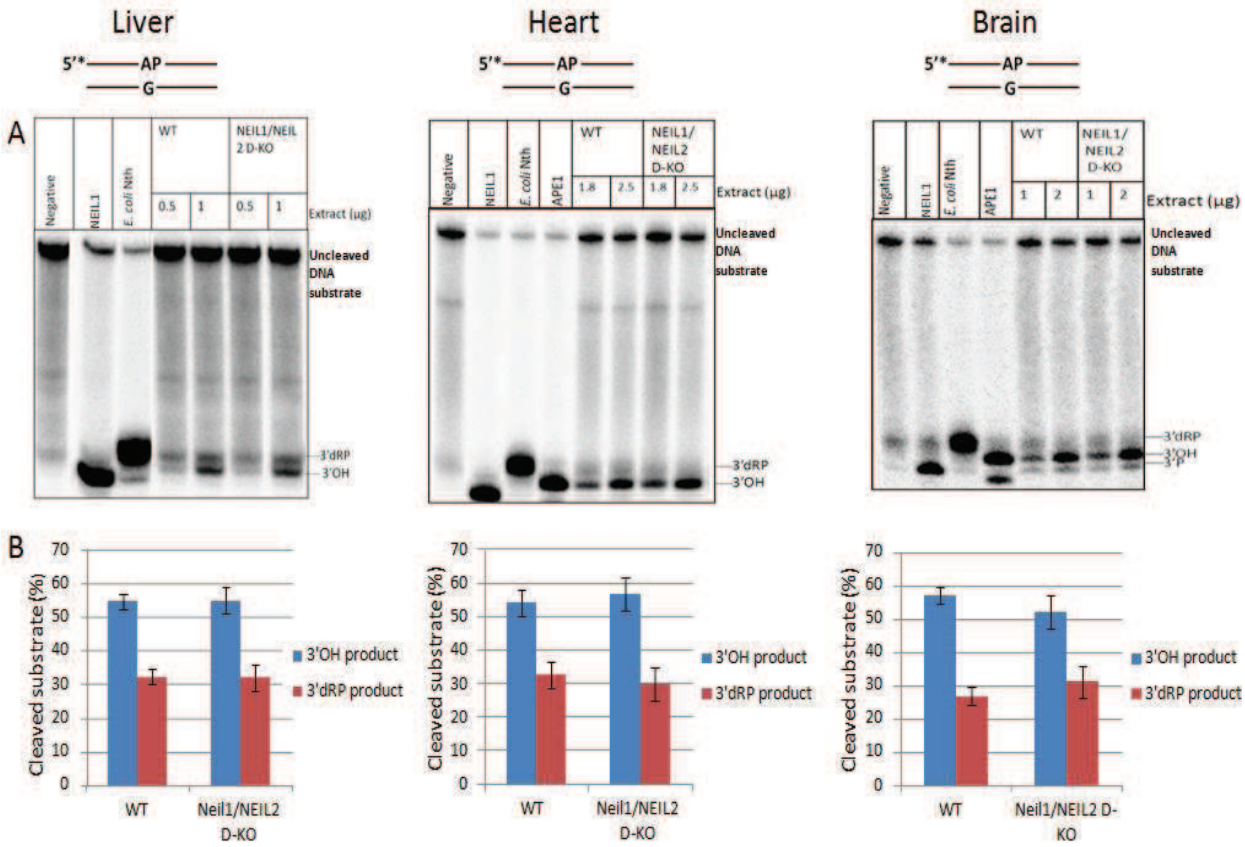

Figure 4.6. Processing of intact AP site opposite G using whole-cell extracts from liver, heart and brain. (A) Different amounts of extracts that were incubated with a ^{32}P-5'end-labeled 40-mer DNA substrate containing intact AP site (10 fmol), for 30 min at 37 °C, are indicated in each figure. Cleaved DNA substrates were separated from intact DNA substrates by 20% denaturing PAGE and visualized by phosphorimaging. *E. coli* Nth (2 U/µl), NEIL1 (10 ng) and APE1 (10 ng) were used positive controls for 3'dRP, 3'P and 3'OH termini, respectively. Experiments were repeated twice, one representative experiment is shown. (B) The charts represent the observed 3'dRP and 3'OH products in liver, heart and brain when 1.0, 1.8 and 2.0 µg whole-cell extract was used, respectively. Blue and red bars denote the activity of generated 3'OH and 3'dRP products, respectively. The fraction of 3'dRP and 3'OH product was compared with each other. The results were quantified using ImageQuant TL and the background was subtracted during quantification. Means and standard deviations were calculated using five or six parallels of each genotype. *p* values were calculated using statistical two-tailed T-test and a 90% confidence interval. AP site opposite other bases showed similar results as well.

The high abundance of the 3'OH product compared to the 3'dRP is consistent with the fact that Ape1 is mainly responsible for the AP site cleaving activity in mammalian cells (Chen *et al.*, 1991). Results also showed no change in 3'dRP product in Neil1/Neil2 D-KO compared to the WT, indicating no change in the level of Nth1 in the absence of Neil enzymes.

To further investigate any up-regulation of Nth1 in the absence of Neil enzymes on a quantitative level, Western blot analysis was performed on 20 µg of WT and Neil1/Neil2

D-KO extracts from all three organs. Although several bands of different sizes were detected, one band represented the expected size of target protein, as indicated. No up-regulation of Nth1 was observed in Neil1/Neil2 D-KO extracts compared to WT in any of the three organs, suggesting that the amount of Nth1 does not increase noteworthy when Neil enzymes are absent (Figure 4.7A). β-Actin was used as loading control, and the gel was also stained by Coomassie Blue after blotting to demonstrate equal amounts of WT and Neil1/Neil2 D-KO extracts loaded (Figure 4.7B). Different amount of β-Actin was observed in brain and liver, whereas β-Actin was not even detected in heart, which was unexpected. However, equal amounts of β-Actin were detected within each organ, making it possible to compare WT with Neil1/Neil2 D-KO.

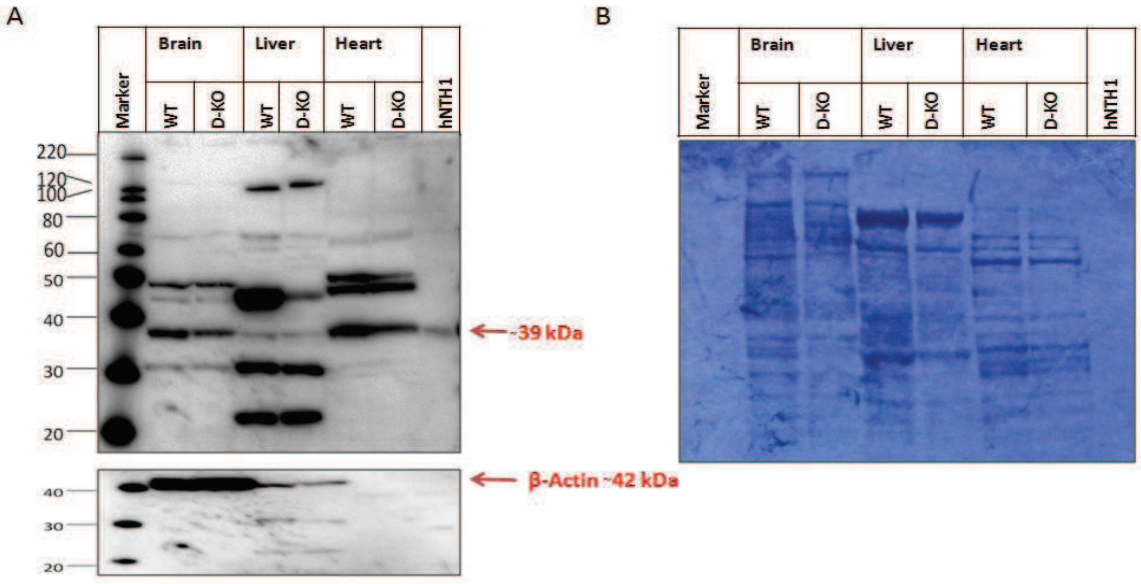

Figure 4.7. (A) Western blot performed on 20 µg of whole-cell extracts prepared from brain, liver and heart, using WT and Neil1/Neil2 D-KO mice. Endogenous NTH1 was detected using 1:500 dilution of Anti-NTH1 antibody. MagicMark™ XP was used as Western protein standard. β-Actin was used as loading control and detected with 1:2,000 dilution of Anti-β Actin antibody. (B) 10% NuPAGE® Bis-Tris gel was stained with Coomassie Blue after blotting procedure to detect the remaining proteins and to determine whether equal amounts of extracts were loaded.

In contrast to liver and heart extracts, faint bands representing 3'P product were observed in both WT and Neil1/Neil2 D-KO when intact AP site was processed using brain extracts (Figure 4.6). No significant differences ($p > 0.1$) were observed in the intensity of the 3'P product between WT and Neil1/Neil2 D-KO, suggesting that enzymes other than Neil1 and Neil2 are responsible for producing the 3'P product. This was further investigated using nicked AP sites with a 3'dRP terminus.

4.3.2 Processing of nicked AP sites

To investigate how the β-elimination product was further processed in BER, 5'end-labeled DNA substrates containing AP sites on the 15th position were nicked with *E. coli* Nth to produce a 3'dRP terminus.

When WT and Neil1/Neil2 D-KO whole-cell extracts prepared from liver, heart or brain were added to nicked AP site substrate, the 3'dRP terminus was further processed to both 3'OH and 3'P products (Figure 4.8). In contrast to the processing of intact AP sites where the 3'P product was only observed using brain extracts, the 3'dRP terminus was further processed to generate the 3'P product in extracts from all three organs. However, the abundance of 3'P product is substantially higher in brain when compared to liver and heart. No significant differences in the yielded 3'P product ($p > 0,1$) was observed between WT and Neil1/Neil2 D-KO, suggesting that enzymes other than Neil1 and Neil2 are responsible for processing the 3'dRP.

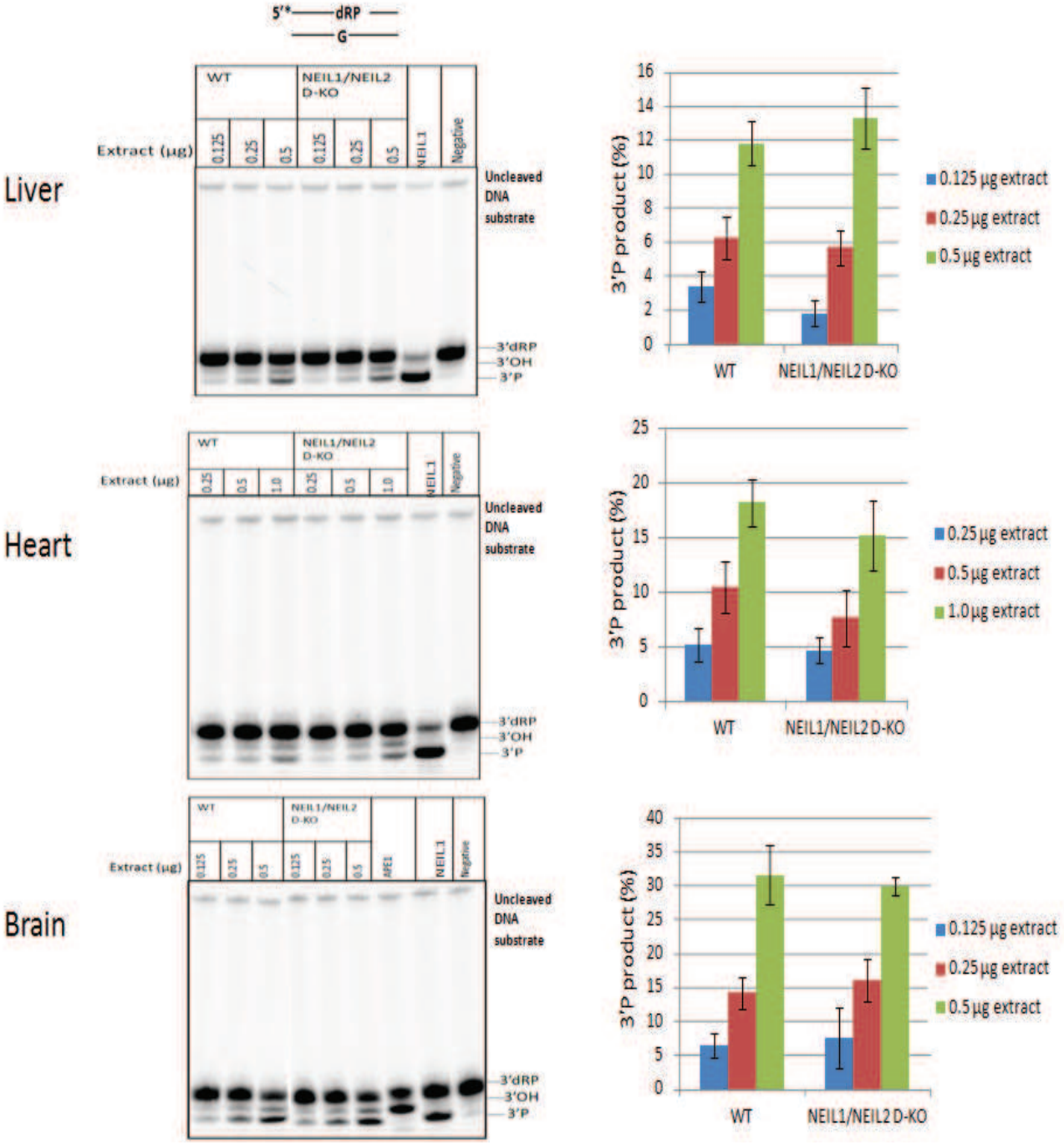

Figure 4.8. 3'P product (%) generated from ^{32}P-5'end-labeled 40-mer DNA substrate containing nicked AP site with a 3'dRP terminus opposite G. AP site opposite other bases showed similar results as well. The different amounts of extracts that were incubated with a DNA substrate containing nicked AP site (10 fmol) for 30 min at 37 °C, are indicated. Purified APE1 (10 ng) NEIL1 (10 ng) were used as positive controls for 3'OH and 3'P termini, respectively. Experiments were repeated several times, one representative experiment is shown. Cleaved DNA substrates were separated from intact DNA substrates by 20% denaturing PAGE and visualized by phosphorimaging. The results were quantified using ImageQuant TL and the background was subtracted during quantification. Means and standard deviations were calculated using five or six parallels of each genotype. *p* values were calculated using statistical two-tailed T-test and a 90% confidence interval.

A possible candidate for generation of the 3'P product is Tdp1, which is shown to act on different 3'blocking lesions (Dexheimer *et al.*, 2008;Nilsen *et al.*, 2012). To further investigate whether the generated 3'P products were caused by Tdp1, 5 mM sodium orthovandate was used to inhibit the activity of Tdp1. The inhibition resulted in the abrogation of the 3'P product, indicating that Tdp1 was indeed responsible for generating the 3'P terminus. The extracts of WT and D-KO prepared from liver with and without 5 mM sodium orthovanadate are shown (Figure 4.9). Similar results were obtained when extracts from heart and brain were used, however, only one representative experiment is presented. 1 ng *S. pombe* Tdp1 was also included to observe the inhibition efficiency, showing that 5 mM sodium orthovandate is sufficient to achieve full inhibition.

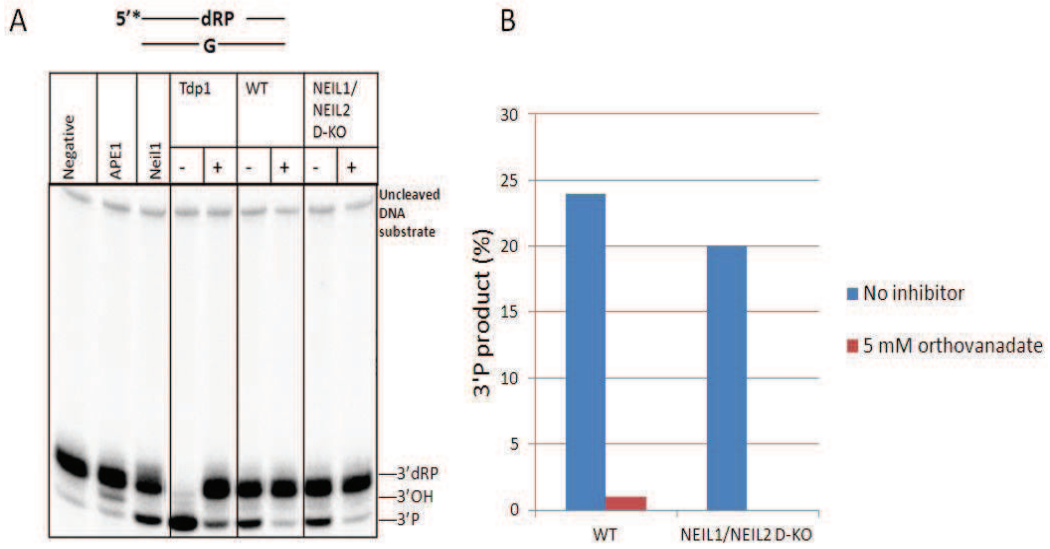

Figure 4.9. Inhibition of the activity of Tdp1 upon ^{32}P-5'end-labeled 40-mer DNA substrate containing nicked AP site with a 3'dRP terminus opposite G. (A) 1 µg whole-cell extracts derived from WT and Neil1/Neil2 D-KO liver and 5 mM sodium ortho vanadate were mixed and incubated with a DNA substrate containing nicked AP site (10 fmol). "+" and "-" denotes reactions with and without 5 mM sodium orthovanadate, respectively. Cleaved DNA substrates were separated from intact DNA substrates by 20% denaturing PAGE and visualized by phosphorimaging. Purified APE1 (10 ng) NEIL1 (10 ng) were used as positive controls for 3'OH and 3'P termini, respectively. *S. pombe* Tdp1 (1 ng) was also used as a control to investigate the efficiency of the inhibitor. Experiments were repeated twice, one representative experiment is shown. (B) Schematic representation of (A). The results were quantified using ImageQuant TL and the background was subtracted during quantification. The blue and red bars denote the fraction of 3'P product in reactions without and with inhibitor, respectively.

4.3.3 Processing of intact AP site using 3'end-labeled DNA substrate

The 3'end-labeled experiments were performed to better evaluate the contribution of Nth1 in AP site incision.

Whole-cell extracts from WT and D-KO were incubated with ^{32}P-3'end-labeled DNA substrate containing an intact AP site opposite C, and the DNA products were analyzed using 20% denaturing sequencing gels. Since the 24-mer DNA substrate was ^{32}P-labeled on the 3'end, the product of Nth1 upon cleavage represented the shortest fragment with a 5'P terminus. This is in contrast with the 5'end-labeled substrates, where the activity of Nth1 produced the largest fragment with a 3'dRP terminus. Thus, when using 3'end-labeled DNA substrates, Ape1, represents the largest fragment with a 5'dRP. The activity of Neil enzymes, if any, will appear as a 5'P product, since the β-elimination step is performed closest to the 3'end prior to the δ-elimination step.

When 2 mM Mg^{2+} was included, Ape1 was responsible for the main incision activity, representing ~65% of the total cleaving activity in heart and ~100% in liver and brain. However in the absence of Mg^{2+}, the 5'dRP and 5'P product was detected in approximately 50/50 distribution independent of organ (Figure 4.10). Although Nth1 is primarily responsible for generating the 5'P product, one cannot disregard the possibility that Pol β may also contribute to some extent in the processing of 5'dRP to 5'P product. In addition, only 1/10 amount of extracts were sufficient to detect the products when Mg^{2+} was included, compared to the samples without Mg^{2+} stimulation.

No statistical tests were performed to determine any significant differences between WT and Neil1/Neil2 D-KO, since only two extracts from each genotype was used during experiments with 3'end-labeled substrates. However, quantification analysis suggested no substantial differences between the WT and Neil1/Neil2 D-KO, which are consistent with the results obtained by using 5'end-labeled DNA substrates, suggesting that the contribution of Neil enzymes is not substantial compared to Ape1 and Nth1 in mice.

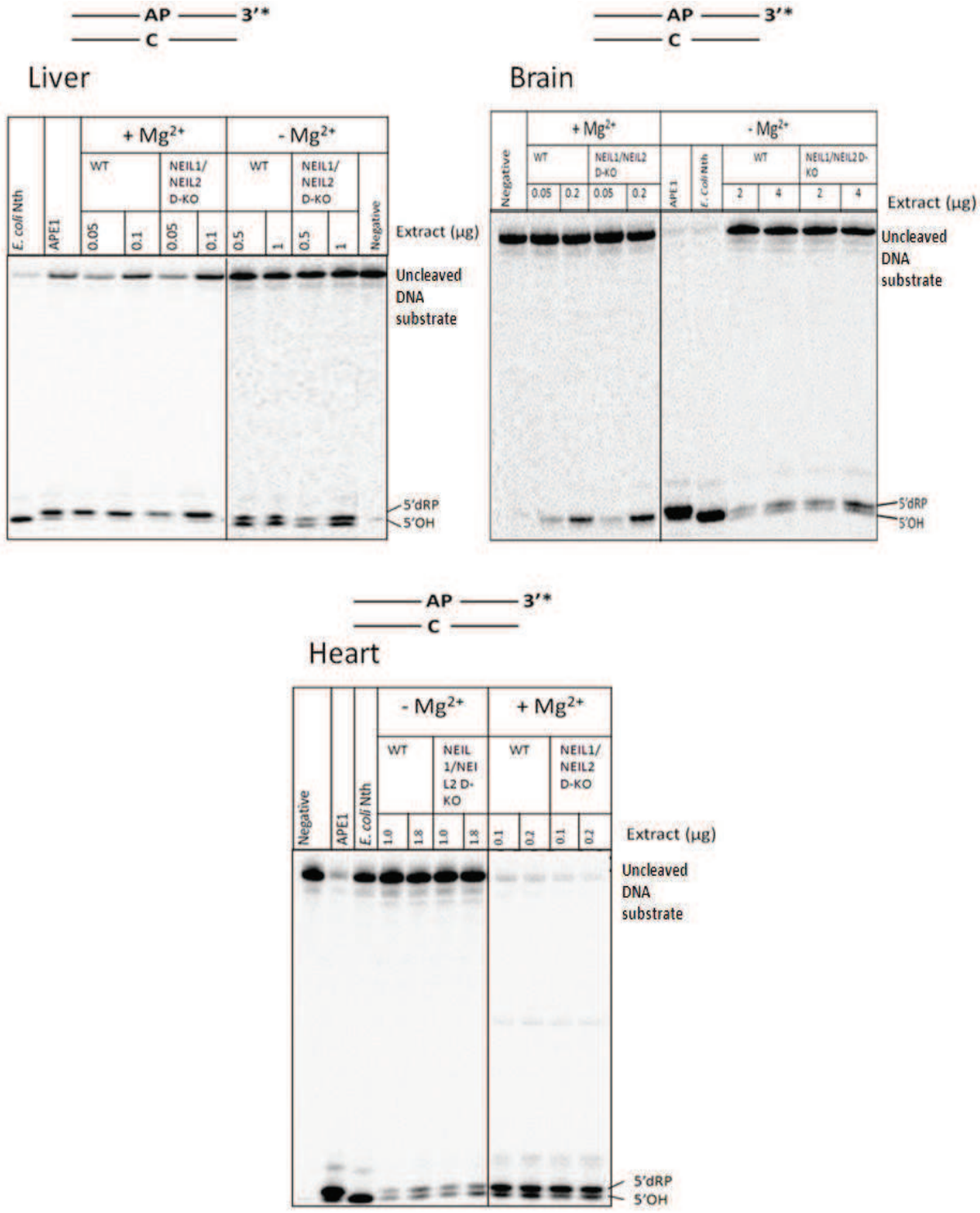

Figure 4.10. Processing of intact AP site opposite C using ^{32}P-3'end-labeled 24-mer DNA substrate in WT and Neil1/Neil2 D-KO whole-cell extracts prepared from liver, heart and brain. The different amounts of extracts are indicated and were incubated with a DNA substrate containing intact AP site (10 fmol) for 30 min at 37 °C. 2 mM Mg^{2+} was included when indicated. Cleaved DNA substrates were separated from intact DNA substrates by 20% denaturing PAGE and visualized by phosphorimaging. Purified APE1 (10 ng) and *E. coli* Nth (2 U/µl) were used as positive controls for 5'dRP and 5'P termini, respectively. Experiments were repeated twice, one representative experiment is shown.

4.4 Down-regulation of NTH1 and TDP1

To determine the effect on processing of AP sites when the expression of NTH1 or TDP1 were down-regulated in humans, different cell lines like HeLa S3 and HaCaT were used. In order to achieve knockdown of NTH1 and TDP1, transfection with siRNA specific to the respective genes was performed.

4.4.1 Optimization of transfection conditions

Transfection conditions, like the amount of siRNA, Lipofectamine™ RNAiMAX and cell type, were optimized to achieve highest possible transfection efficiencies and maximum knockdown.

Optimal transfection conditions were first determined in HeLa S3 cells, by using 1.2-30 pmol siRNA in combination with 0.5, 1.0 and 1.5 µl Lipofectamine™ RNAiMAX. Transfected cells were harvested in protein-cracking buffer and used in Western blot analysis to evaluate reduction in protein quantities. Only the combination of 1.5 µl Lipofectamine™ RNAiMAX and 1.2 pmol of *NTHL1*-siRNA exhibited substantial down-regulation of NTH1 (Figure 4.11A). In contrast, TDP1 was down-regulated under several combinations, including the combination where 1.5 µl Lipofectamine™ RNAiMAX and 1.2 pmol *TDP1*-siRNA was used (Figure 4.11B). Relative quantity analysis in ImageLab BioRad indicated ~50% down-regulation of NTH1 in cells transfected with *NTHL1*-siRNA, and ~65% down-regulation of TDP1 in cells transfected with *TDP1*-siRNA. Control cells transfected with non-targeting siRNA were used as reference. Different amount of siRNA used in combination with 1.5 µl Lipofectamine™ RNAiMAX are shown (Figure 4.11). Experiments where either 0.5 or 1.0 µl Lipofectamine™ RNAiMAX was used in combinations with various amount of siRNA, indicated similar results. The presence of endogenous NTH1 and TDP1 was demonstrated in the control samples. Although several bands of different sizes were detected, one band represented the expected size of target protein, as indicated. Parallels were made for each combination, and included as quality control.

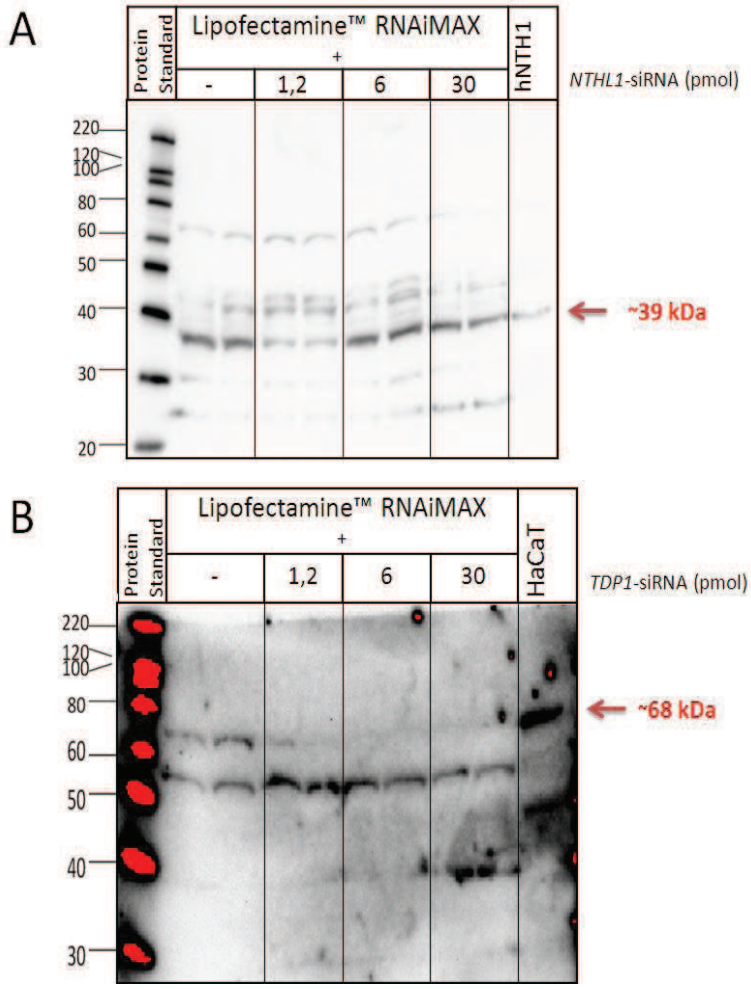

Figure 4.11. Determination of optimal transfection conditions using HeLa S3 cells line. Different amount of siRNA was used in combination with 1.5 µl Lipofectamine™ RNAiMAX, to determine which combination resulted in down-regulation. Combination where 0.5 and 1.0 µl Lipofectamine™ RNAiMAX was used indicated similar results. 4x10^{4}cells were seeded and transfected cells were harvested in protein-cracking buffer and used in Western blot analysis. (A) NTH1 and (B) TDP1 was detected using 1:500 and 1:2,000 dilution of Anti-NTH1 antibody and Anti-TDP1 antibody, respectively. The red arrow indicates the bands of interest. (A) NTH1 (20 ng) and (B) HaCaT cell lysate (30 µg) was included as positive controls. "-" denotes HeLa S3 cells used as control for endogenous (A) NTH1 and (B) TDP1. Dublicates were made for each transfection condition. MagicMark™ XP was used as Western protein standard.

4.4.2 Transfection of HeLa S3 cells to down-regulate NTH1 or TDP1

To investigate the processing of AP sites when NTH1 or TDP1 was down-regulated, whole-cell protein extracts were prepared from newly transfected cells. Based upon the testing of the transfection conditions, 1.5 µl Lipofectamine™ RNAiMAX and 1.2 pmol siRNA resulted in successful down-regulation of NTH1 and TDP1 in 4x10^4 cells. Thus, this ratio was further used to achieve down-regulation, using five times more cells.

Western blot was performed on 25 µg of NTH1 knockdown (KD) extracts, TDP1 KD extracts and control extracts. Relative quantity analysis in ImageLab BioRad indicated approximately 65 % down-regulation of TDP1 in TDP1 KD extracts (Figure 4.12A). However, down-regulation of NTH1 was not successful (Figure 4.12B), which was somewhat unexpected since down-regulation of NTH1 was achieved during optimization.

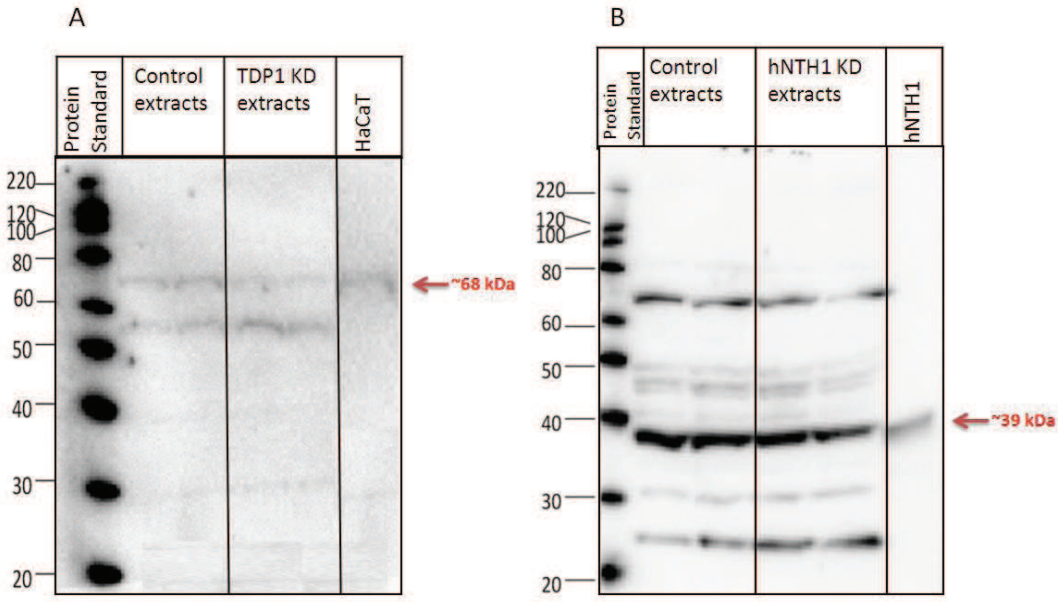

Figure 4.12. Western blot performed on 25 µg (A) TDP1 and (B) NTH1 KD extracts prepared from transfected HeLa S3 cells. 7.5 µl Lipofectamine™ RNAiMAX and 6 pmol siRNA was used to transfect 2x10^5 cells. Biological duplicates were prepared when targeted gene were down-regulated. (A) TDP1 and (B) NTH1 was detected using 1:500 and 1:2,000 dilution of Anti-NTH1 antibody and Anti-TDP1 antibody, respectively. The red arrow indicates the bands of interest. (A) HaCaT cell lysate (20 µg) and (B) NTH1 (20 ng) was included as positive controls. MagicMark™ XP was used as Western protein standard.

Even though bands of expected size for NTH1 and TDP1 were detected in Western, they may represent false positive bands, due to unspecific binding of the antibody to proteins with similar masses as the target proteins. Thus, biochemical approaches was also used to verify the results obtained from Western blot analysis.

4.4.3 Evaluating down-regulation of NTH1 by biochemical analysis

Although the NTH1 KD extracts showed no down-regulation of NTH1, a sodium borohydride-mediated trapping assay was performed to verify the results. The β-elimination activity of NTH1 occurs via a Schiff base intermediate. In the presence of the reducing agent, sodium borohydride, the enzyme-DNA complex is irreversibly linked and thus migrate slower than the free DNA substrates (Fromme and Verdine, 2003). Trapped products of the same size as purified NTH1, used as positive control, were observed in

both control and NTH1 KD extracts, indicating the presence of NTH1-DNA complex (Figure 4.13). In addition, the intensity of the bands is not reduced in NTH1 KD extracts compared to control extracts, indicating no substantial down-regulation of NTH1. This is consistent with the results obtained from Western blot analysis.

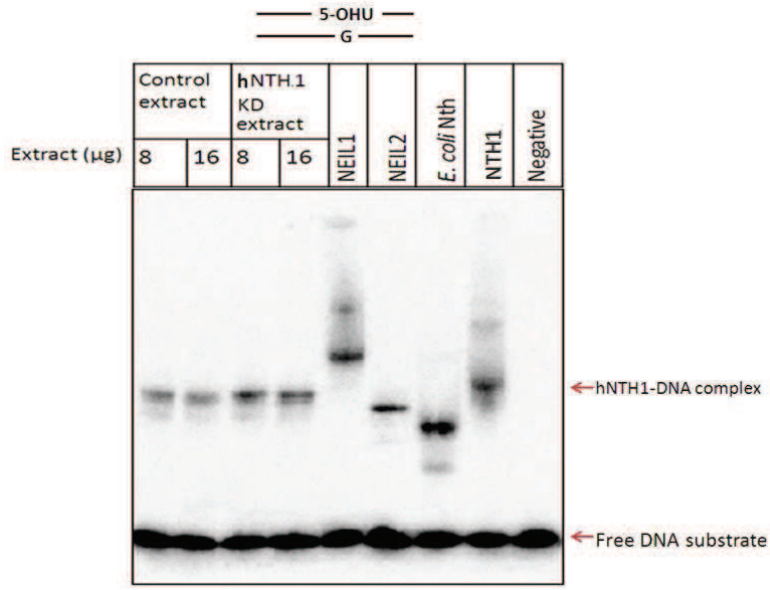

Figure 4.13. Formation of trapped complexes of protein and 5'end-labeled DNA substrate containing 5-OHU opposite G. DNA substrate (10 fmol) and different amounts of extract indicated were incubated at 37 °C for 30 min in the presence of 100 mM sodium borohydride. NEIL1 (50 ng), NEIL2 (50 ng), *E. coli* Nth (2 U/µl) and NTH1 (50 ng) was included as positive controls. Protein-DNA substrate complexes were separated from DNA substrate by SDS-PAGE using 10% NuPAGE® Bis-Tris gel. The position of the trapped complex is indicated. Experiments were repeated with biological dublicate extracts, one representative experiment is shown.

4.4.4 Evaluating down-regulation of TDP1 by biochemical analysis

TDP1 KD extracts indicated down-regulation of TDP1 by ~65%, using Western blot. To verify this down-regulation, the TDP1 KD extracts were tested against a 5'end-labeled DNA substrate containing phophotyrosine at the 3'end, which is known to be efficiently processed by TDP1 (Yang *et al.*, 1996).

When using control extracts, phosphotyrosine was efficiently processed to 3'P terminus, as expected. However, the removal of phosphotyrosine was reduced by ~55% when using the TDP1 KD extracts, indicating that TDP1 levels in KD extracts are reduced compared to the control extracts (Figure 4.14), as also seen in Western blot analysis. Thus, the TDP1 KD extracts and control extracts were further used to investigate the processing of AP site, addressed in section 4.5.

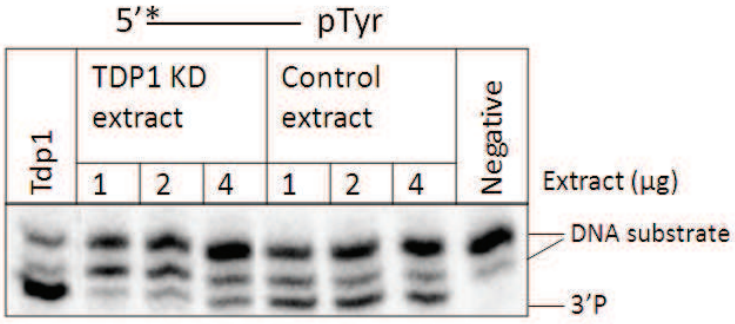

Figure 4.14. Processing of ^{32}P-5'end-labeled 20-mer DNA substrate containing phosphotyrosine (pTyr) on the 3'end. The different amounts of extracts incubated with DNA substrate (10 fmol), for 30 min at 37 °C, are indicated in each figure. Cleaved DNA substrates were separated from intact DNA substrates by 20% denaturing PAGE and visualized by phosphorimaging. The results were quantified using ImageQuant TL and the background was subtracted during quantification. *S. pombe* Tdp1 (1 ng) was used as positive control for 3'P terminus. Experiments were repeated with biological dublicate extracts, one representative experiment is shown.

4.4.5 Further attempts to down-regulate NTH1

After several unsuccessful attempts to down-regulate NTH1 in HeLa S3 cells, different combinations of Lipofectamine™ RNAiMAX and *NTHL1*-siRNA were also tested in HaCaT cells. However, no down-regulation of NTH1 was observed in the HaCaT cells either (data not shown). Meanwhile, mycoplasma contamination was detected in both HeLa S3 and HaCaT cell lines during a routine control, which could explain the unsuccessful down-regulation of NTH1 (Appendix F).

Thus, a healthy HeLa S3 cell line was used to down-regulate NTH1 again. The absence of mycoplasma was confirmed (data not shown). In addition, this time the success of down-regulation was evaluated not only by Western Blot but also by RT-PCR.

4.4.6 Evaluation of down-regulation using RT-PCR

Total RNA was first isolated from the transfected cells and converted to cDNA by reverse transcription. The gene for β-Actin, *ACTB*, was chosen as the endogenous reference for normalization.

To determine the amplification efficiencies of the target genes; *NTHL1* and *ACTB*, series of 1:5 dilutions were prepared from the control cDNA sample using gene-specific primers. Positive controls and negative controls were also included. Each sample was amplified in a two-step RT-PCR and standard curves were constructed by plotting different C_T values of standard dilutions against the logarithm of the amount of cDNA template (Appendix G). Amplifications efficiencies for *NTHL1* and the reference gene

were determined to 85% and 99%, as expected. The amplification efficiencies between reference and target genes are usually different due to unequal primer annealing.

Based on the information gained from the standard curves, 1:10 dilution of the cDNA samples prepared from control cells and cells transfected with siRNA specific for *NTHL1,* were used to evaluate down-regulation of *NTHL1*. Gene knockdown efficiency was calculated by an automated relative quantification method in the StepOne™ v2.1 Software, where the ratio between the amount of target gene and the reference gene in a control sample was determined. This ratio was then used to compare cDNA from KD cells extracts and control cells. Melting curves for each target gene were analyzed for quality control and the clear peak demonstrate the absence of primer-dimers and the presence of one specific PCR product (Appendix G).

The analysis showed no down-regulation of *NTHL1* gene in transfected cells compared to control cells (Figure 4.15A), which was also confirmed using Western blot analysis on 25 µg NTH1 KD extracts and control extracts (Figure 4.15B).

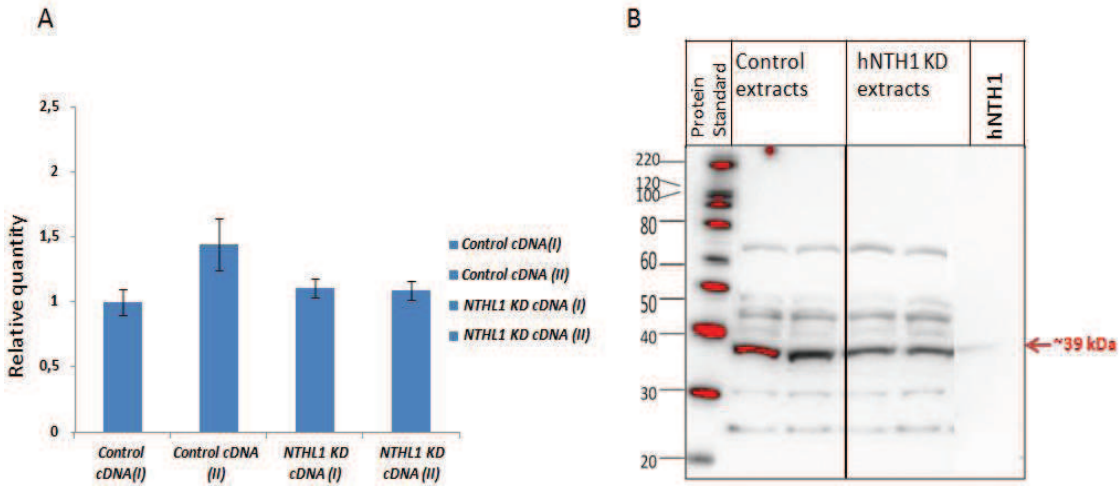

Figure 4.15. Evaluation of the gene down-regulation of NTH1. (A) RT-PCR: relative mRNA levels of *NTHL1* were calculated by comparative method of relative quantification using StepOne™ V2.1 Software. The relative expression of mRNA levels of *NTHL1* gene is shown in control cells and *NTHL1*-siRNA transfected cells. (I) and (II) represent biological duplicates, included as quality control. The mRNA expression levels of *NTHL1* in control cDNA (I) is set as reference. Triplicates were made from each extract and normalized to β- Actin, used as the endogenous reference. Error bars indicate standard deviations of the means of three technical replicates. (B) Western blot performed on 25 µg biological duplicates of control extracts NTH1 KD extracts prepared from *NTHL1*-siRNA transfected HeLa S3 cells. Endogenous NTH1 was detected using 1:500 Anti-NTH1 antibody. The red arrow indicates the bands of interest. NTH1 (10 ng) was included as positive controls for endogenous NTH1. MagicMark™ XP was used as Western protein standard.

4.5 Biochemical assays performed on TDP1 KD extracts

Control and TDP1 KD extracts, from section 4.4.4 were used to investigate the processing of 5'end-labeled DNA substrates containing intact or nicked AP sites. Due to the dominating activity of APE1 in the processing of AP sites, an APE1-inhibitor was used to reduce its activity, which could provide better insight in the roles of TDP1 and NTH1.

4.5.1 Processing of intact AP sites using APE1 inhibitor

When 1 µg control extract was used, ~65% of the intact AP sites were processed to 3'OH, whereas ~20% of the total cleavage product was observed as 3'dRP product. The remaining ~15% were processed to 3'P product.

The band of 3'OH products represent the total amount of 3'OH generated mainly by the activity of APE1 that either incise the AP site to generate 3'OH directly or further processes the 3'dRP terminus produced by the actions of NTH1. However, one must also take into consideration that PNKP is also capable of processing the 3'P product to 3'OH, even though its contribution is not significant compared to APE1.

To determine the fraction of the 3'OH products that are generated from 3'dRP, the activity of APE1 was inhibited using 500 µM myricetin, an APE1 inhibitor. 1 µg control extract was sufficient to reduce the intensities of the 3'OH bands from representing ~65% of the total activity to ~35% of the total activity (Figure 4.16A). This is consistent with the fact that the intensity of the 3'dRP band increased by ~30% when myricetin was added, suggesting that ~30% of the 3'dRP generated by NTH1 is further processed to 3'OH by APE1.

In addition, when myricetin was added to control extracts, a reduction in the intensity of the 3'P product was also observed, suggesting that the action of TDP1 is also inhibited by myricetin. Indeed, this was confirmed when the activity of 1 ng of *S. pombe* Tdp1 was inhibited by 500 µM myricetin. In fact, myricetin is capable of inhibiting TDP1 in approximately the same extent as sodium orthovanadate (Figure 4.16B).

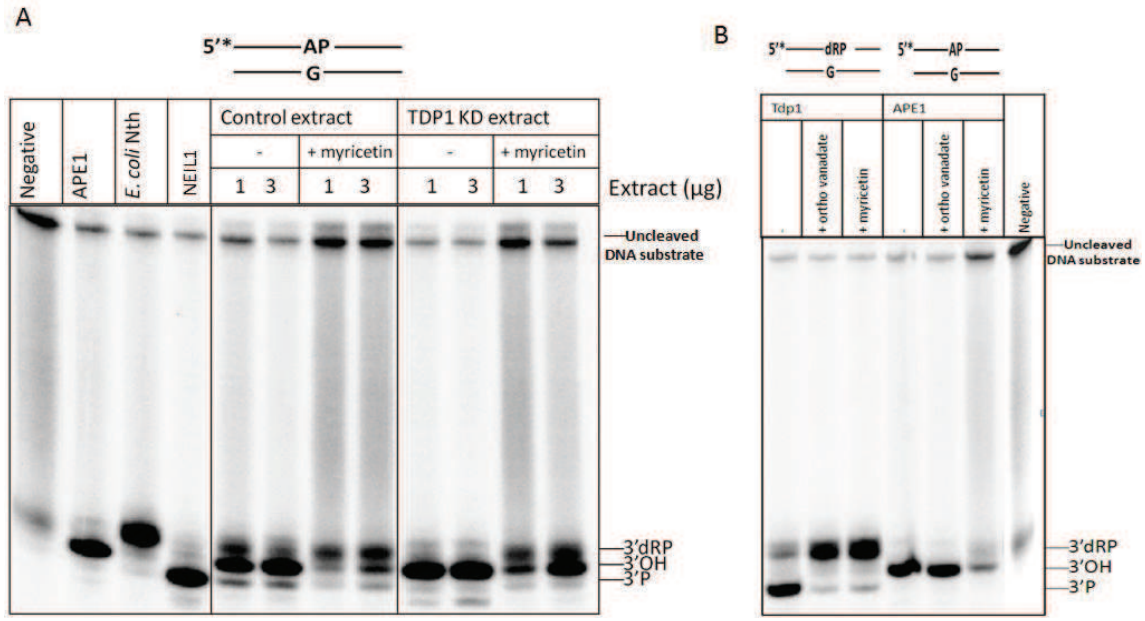

Figure 4.16. Processing of AP site opposite G using ^{32}P-5'end-labeled 40-mer DNA substrate. Cleaved DNA substrates were separated from intact DNA substrates by 20% denaturing PAGE and visualized by phosphorimaging. The results were quantified using ImageQuant TL and the background was subtracted during quantification. (A) Different amounts of extracts were incubated with a DNA substrate containing intact AP site (10 fmol), for 30 min at 37 °C, and are indicated. "-" and "+myricetin" denotes reactions with and without 500 µM APE1 inhibitor, respectively. Purified *E. coli* Nth (2 U/µl), NEIL1 (10 ng), APE1 (10 ng) were used as markers for 3'dRP, 3'P and 3'OH termini, respectively. Experiments were repeated twice, one representative experiment is shown. (B) The activity of *S. pombe* Tdp1 (1 ng) and APE1 (10 ng) was inhibited using either 5 mM sodium orthovanadate or 500 µM myricetin. *S. pombe* Tdp1 (1 ng) and APE1 (10 ng) was incubated, for 30 min at 37 °C, with DNA substrate containing nicked AP site or intact AP site. Experiments were repeated twice, one representative experiment is shown.

The 3'P products were detected in reduced quantity in TDP1 KD extracts compared to control extracts, which was expected. In addition, when TDP1 KD extracts were used, the 3'dRP product was observed to represent only ~10% of the total cleavage product, whereas the 3'OH product represent the remaining ~90%. This increase in the 3'OH product might suggest an up-regulation of APE1 in TDP1 KD extracts.

When 500 µM myricetin was added the intensity of the 3'dRP band increased by ~35%, due to the accumulation of the 3'dRP product when APE1 is inhibited, which is consistent with the increase observed in control extracts.

4.5.2 Processing of nicked AP site using APE1 inhibitor

To demonstrate that the 3'dRP is in fact further processed by either APE1 or TDP1, a 5'end-labeled DNA substrate containing a nicked AP site was used. Both 3'OH and 3'P product were generated in control extracts (Figure 4.17). To ensure that the 3'P product was indeed produced by the actions of TDP1, the activity of TDP1 was inhibited by 5

mM sodium orthovanadate in control extracts, resulting in reduction of the 3'P products by ~80%. Thus, the reduction of the 3'P product was seen in both TDP1 KD extracts and by the use of sodium orthovanadate, suggesting that the 3'P product indeed result from TDP1 activity, and that NEIL1 and NEIL2 in HeLa S3 cells have a non-essential role in AP site processing.

In addition, when TDP1 KD extracts were used, reduced 3'P and increased 3'OH products were observed when compared to control extracts, supporting the idea that APE1 might be up-regulated when TDP1 is down-regulated.

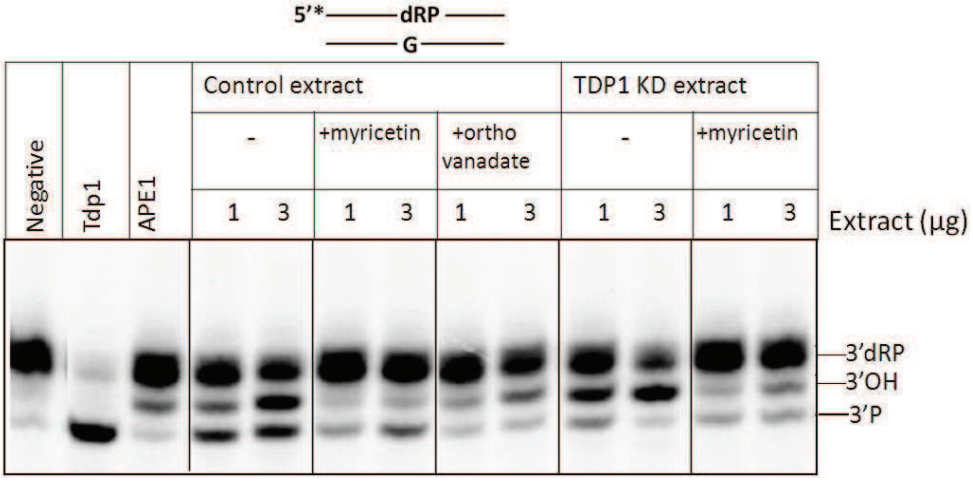

Figure 4.17. Processing of AP site nicked with *E. coli* Nth opposite G using TDP1 KD extract. The different amounts of extracts incubated with nicked DNA substrate (10 fmol) for 30 min at 37 °C, are indicated. Cleaved DNA substrates were separated from intact DNA substrates by 20% denaturing PAGE and visualized by phosphorimaging. The results were quantified using ImageQuant TL and the background was subtracted during quantification. Purified *S. pombe* Tdp1 (1 ng) and APE1 (10 ng) were used as markers for 3'P and 3'OH, respectively. Experiments were repeated twice, one representative experiment is shown.

5 Discussion

AP sites are one of the most frequent lesions in cellular DNA and their repair is essential for genomic stability. In this study, the processing of AP sites were investigated by using recombinant NTH1, KO mice models and knockdown of immortalized human cell lines.

5.1 Cleaving activity of recombinant NTH1

Initially, the cleaving activity of recombinant NTH1 was demonstrated upon ss and ds DNA substrate containing either an AP site or 5-OHC. These assays revealed that NTH1 was active upon ds and ss DNA substrate containing AP site, however, the processing of ss DNA substrate was observed to be 4-fold less than processing of ds DNA substrate. With 20 ng NTH1, the ss DNA substrate was cleaved only ~15% compared to ~60% for the corresponding ds DNA substrate. Also when 5-OHC was processed by NTH1, only ~20% of the ss DNA substrate was cleaved. These results show that NTH1 primarily is active only upon ds DNA, and can to some extent also process an AP site or 5-OHC in ss DNA substrates. Thus, the activity of NTH1 upon ss DNA substrates is probably of less biological importance *in vivo*. This is in agreement with the fact that NTH1 is known to be only active with ds DNA, as described in the introduction (Hegde *et al.*, 2012).

Although NTH1 possess both DNA glycosylase and AP lyase activities, these two activities can occur at different rates. For instance, the DNA glycosylase activity of NTH1 has been shown to be 7-fold greater than its AP lyase activity when the DNA substrate contains a Tg opposite A (Tg:A) (Marenstein *et al.*, 2003). Thus, the efficiency of DNA glycosylase and AP lyase activities seem to depend on not only the damaged base but also on the complementary base.

The DNA glycosylase and AP lyase activities of NTH1 were found to be mostly coupled when 5-OHC was processed. However, the ~10% increase in cleaving activity when NaOH was added, represent the fraction of NTH1's activity that only removed the base to generate an AP site, which in turn was hydrolyzed by NaOH. The appearance of two bands when NaOH was added to the reactions can be explained by NaOH's ability to cleave on both the 5' and 3' sides of the AP site.

Furthermore, the processing of ds DNA substrates containing AP site was not affected when different bases were used opposite the AP site. This was somewhat unexpected

since the activity of NTH1 has been demonstrated to be affected by the nature of the opposite base. For instance, NTH1 acts only as a monofunctional DNA glycosylase upon Tg:G, but demonstrate both DNA glycosylase and AP lyase activity upon Tg:A (Marenstein *et al.*, 2003). The dependency on the complementary base for DNA glycosylase and AP lyase activities is supported by the fact that NTH1 probably interacts with both DNA strands upon binding and processing, as revealed by the three-dimensional structure of *E. coli* Nth (Fromme and Verdine, 2003). An important aspect to consider is that the opposite base may have a greater role when it forms hydrogen bonds with the damaged base. In the case of AP sites, however, the opposite base may not have a great importance, due to lack of base pairing.

In addition, it was tempting to speculate whether NTH1 was also capable of acting downstream of APE1 in BER to process the 5'dRP terminus either parallel with POL β or as a back-up for POL β. This was investigated by using a 3'end-labeled DNA substrate containing an APE1-nicked AP site to generate a 5'dRP terminus. Our results demonstrated that 5'dRP was a poor substrate for NTH1, requiring 10-fold more enzyme than for the intact AP site. Thus, NTH1 manages to process the 5'dRP terminus when the system is pushed and the protein is added in excess, but the contribution of NTH1 in processing of 5'dRP have probably little, if any, biological importance *in vivo*.

5.2 Repair of AP sites in mice

Neil1/Neil2 D-KO and WT mice have been used to investigate the repair of AP sites using whole-cell extracts from heart, liver and brain.

Contribution of Neil enzymes

No statistical significant differences in cleaving activity were ever observed between WT and Neil1/Neil2 D-KO, suggesting a non-essential role of Neil1 and Neil2 in AP site incision. Even though the Neil enzymes cleave AP sites, their actions might be of minor importance in the presence of Ape1. However, it is important to consider the possibility that Neil enzymes may contribute more significantly in the repair of base damages than AP sites. Indeed, this can be supported by the fact that recombinant NEIL1 and NEIL2 have the ability to initiate repair of 5-OHU in the absence APE1 by removing the damaged base and then processing the generated AP site (Das *et al.*, 2006). Thus, one may speculate whether Neil enzymes need their DNA glycosylase activity, in order to

further proceed with their AP lyase acitivity. If the damaged base is already removed, other enzymes are more likely to initiate the repair of the AP site, making the contribution of Neil enzymes not substantial enough to be detected. It is also a possibility that Neil enzymes may function as a back-up repair pathway for AP sites and contribute more in the absence of Ape1.

Nth1's activity in Neil1/Neil2 D-KO and WT

Processing of intact AP sites using WT and D-KO extracts showed that AP sites are mainly processed by the activity of Ape1. The 3'dRP product generated by Nth1 was also detected, although to a lesser extent than 3'OH. No change in the activity of Nth1 was observed when the cleavage products were compared between WT and Neil1/Neil2 D-KO, suggesting that the level of Nth1 was not changed by the absence of Neil enzymes. It was tempting to speculate whether the levels of Nth1 were up-regulated in Neil1/Neil2 D-KO mice, due to the fact that Nth1 represent the only remaining bifuntional DNA glycosylase in mammals acting on oxidized pyrimidines when Neil enzymes are absent (Takao *et al.*, 2002). However, no up-regulation of Nth1 was demonstrated on a quantitative level by Western blot analysis when Neil1/Neil2 D-KO was compared to WT. Nevertheless, the lack of up-regulation should also be confirmed by monitoring levels of gene expression.

In addition, β-Actin included as loading control showed equal amounts of β-Actin within each organ as expected, indicating that equal amounts of extracts were loaded. However, the levels of β-Actin were observed to differ between the organs (Figure 4.7A). To our knowledge β-Actin is expressed in all the organs, but with significant difference in their expression levels (Kouadjo *et al.*, 2007). The fact that β-Actin was not even detected in heart extracts, was unexpected. However, the Coomassie Blue-stained gel demonstrated that equal amount of heart extracts were loaded onto the gel, and thus made it possible to compare the Nth1 levels in heart extracts of WT and D-KO too.

Contribution of NTH1 in AP site repair

To determine the contribution of Nth1 to AP site repair in mice, the bands representing 3'dRP was quantified, which proved to be a challenge since the 3'dRP product appeared as diffused smears instead of clear bands. The software used to quantify the processed products overestimated the yield of the 3'dRP product, resulting in inaccurate

quantifications. Thus, there is an uncertainty in the estimated fractions that represent the abundance of 3'dRP compared to 3'OH products (Figure 4.6).

Regardless, based on the visual examination of the bands, it is clear that the 3'OH product is more abundant. However, a fraction on the total 3'OH product may also represent the activity of Nth1 indirectly. Indeed, the processing of DNA substrates containing nicked AP sites demonstrated that the 3'dRP terminus can be further processed to 3'OH or 3'P by the actions of Ape1 or Tdp1, respectively. One must also take into consideration that the product of Tdp1, 3'P, is also further processed to 3'OH by the actions of Pnkp. Thus, total 3'OH product generated when intact or nicked AP site are processed, is not only represented by the activity of Ape1, but also by Pnkp. However, it is important to emphasize that the contribution of Pnkp is not substantial compared to Ape1, due to the fact that Ape1 is responsible for ~95% of the AP site processing (Chen *et al.*, 1991).

Since Ape1 not only incise the AP site directly, but also further processes the 3'dRP, it is impossible to determine the total contribution of Nth1. Evaluation of the contribution of Nth1, as well as Tdp1, can therefore be complicated, due to the fact that there are several enzymes involved in the processing either directly or through protein-protein interactions.

To avoid the Ape1 processing of the 3'dRP products, DNA substrates were also ^{32}P-labeled on the 3'end to investigate the abundance of the 5'P generated by Nth1. One may speculate whether a fraction of the 5'P product can also result from the action of Pol β who is capable of processing the 5'dRP to 5'P. However, as shown by Allison *et al.*, 2001, Pol β acts in a coordinated manner subsequently to the activity of APE1, by adding a single nucleotide to the 3'end of the incised AP site, as it simultaneously removes the 5'dRP residue. In addition, Pol β has shown to process the 5'dRP terminus in a Mg^{2+}-dependent manner (Matsumoto and Kim, 1995). Thus, it seems like if Pol β requires incorporation of a single nucleotide, to process the 5'dRP product to 5'P. Since neither Mg^{2+} nor nucleotides were added to the reactions where 5'P product was observed, one can assume that the contribution of Pol β is of minor, if any, importance to the generated 5'P terminus in these assays.

Thus, based on the results obtained using 5'end-labeled and 3'end-labeled DNA substrates, it is only possible to establish that Nth1 is indeed involved in the AP site

processing in mice, but the total contribution of Nth1 cannot be determined. A better picture of the situation can be obtained by inhibiting the activity of either Pol β or Ape1. However, full inhibition of their activities, especially the activity of Ape1 is not possible to accomplish, without affecting other DNA repair processes, which in turn will provide inaccurate results. Indeed, the essential role of both Ape1 and Pol β in BER can be emphasized by the fact that Pol β-deficient mice have been shown to die immediately after birth, whereas Ape1-deficient mice die in the early embryonic stage (Sugo *et al.*, 2000;Zou *et al.*, 2007).

Contribution of Tdp1

As mentioned previously the 3'dRP product generated by Nth1 was shown to be further processed to 3'P by the activity of Tdp1. This was somewhat unexpected since the generated 3'P product was expected to result from the activities of Neil enzymes. Furthermore, Lebedeva *et al.,* 2011 had shown that recombinant human TDP1 is capable of processing the 3'dRP termini, however, the *in vivo* significance of this observation was not addressed.

When nicked AP site with a 3'dRP was processed by Ape1 and Tdp1, near equal amounts of the 3'OH and 3'P products were produced in all three organs, which is in contrast to when intact AP sites were processed. Interestingly, at least twice as much 3'P product was generated in brain as in liver and heart. Also when intact AP sites were being processed in different mice organs, the Tdp1's activity was only seen in brain. These findings suggest that Tdp1 may be present in larger quantities in brain or it may have some modifications that enhance its activity in brain. The importance of Tdp1 in brain function is also seen in the neurodegenerative disease, SCAN1, that is caused by a homozygous mutation in the TDP1 gene (Takashima *et al.*, 2002). It is believed that the absence of TDP1 in mammals can cause accumulation of the TOP1 SSB and hypersensitivity towards CPT, as well as increase the vulnerability of neurons due to high levels of oxidative stress and low level of antioxidant enzymes. Furthermore, TDP1 deficiency in mammalian cells have also shown reduced repair capacity for oxidative SSB, suggesting that the actions of TDP1 are not only restricted to Top1-DNA complexes (El-Khamisy *et al.*, 2005;Interthal *et al.*, 2005).

Differences observed between organs

One additional noteworthy observation was that processing of intact AP site using liver extracts required less amount of protein extract compared to heart and brain that required approximately twice as much protein extract to exhibit corresponding processing of AP sites. It is conceivable that the more efficient processing of intact AP sites in liver may be explained by the fact that liver is responsible for the main detoxification processes and thus requires more efficient repair of DNA damages. It can also be speculated in whether the proteins of interest are present in larger quantities in the protein extracts prepared from liver compared to the other organs, which in fact has not yet been determined. This can be determined by investigating expression levels of the target proteins in the different organs. Other reasons for observing more efficient AP site processing in liver can be that liver proteins may have different types of modifications compared to the other organs, as well as other protein partners that facilitate the processing by protein-protein interactions.

5.3 Down-regulation of NTH1 or TDP1 in HeLa S3 cells

To down-regulate the expression of NTH1 or TDP1, different cell lines were transfected with siRNA specific for *NTHL1* or *TDP1* gene.

Evaluation of transfected cells

Optimal transfection conditions were determined to 1.2 pmol siRNA and 1.5 µl Lipofectamine™ RNAiMAX, and cells were transfected at 50-70% confluency. It is important that cells are proliferating exponentially when transfected. In addition, cells should be harvested before they reach confluence, due to contact inhibition that prevents the cells from dividing when they come in contact with each other. Immortal cell lines, however, continue proliferating even after they reach confluence, but result in deterioration after two doublings. Thus, optimizing seeding densities and transfecting cells at suitable confluency is essential for achieving successful down-regulation.

When testing optimal transfection conditions in HeLa cells, several combinations of siRNA and transfection reagent resulted in down-regulation of TDP1. In contrast, only one combination resulted in down-regulation of NTH1, suggesting that the down-regulation of TDP1 was more robust than that of NTH1.

Even though successful down-regulation of both NTH1 and TDP1 was observed in at least one of the transfection conditions tested, down-regulation of NTH1 was not

achieved in later experiments. This was somewhat unexpected since the purchased siRNA, containing pools of three target-specific siRNAs, has been designed and tested solely to down-regulate gene expression of *NTHL1* (Santa Cruz®, 2012). TDP1 on the other hand, was estimated to be ~65% down-regulated by Western blot analysis. This down-regulation was, however, not confirmed on mRNA level using RT-PCR. Thus, biochemical approaches were used to evaluate down-regulation. Since the activity on a phosphotyrosine-containing DNA substrate was reduced by ~55% in the corresponding extracts, one can consider the down-regulation to be biological relevant. Biochemical approaches used to evaluate down-regulation are further discussed in the end of this section.

Furthermore, a routine contamination check detected the presence of mycoplasma in the HeLa cell line used to down-regulate NTH1. Mycoplasma contamination can influence the experimental results by causing alterations in growth characteristic, enzyme patterns, cell membrane composition and chromosomal abnormalities. This again can influence the experimental results obtained with cell lines and lead to misleading conclusions. Thus, the contaminated cells, may have affected the transfection and knockdown efficiencies, resulting in unsuccessful down-regulation of NTH1 (van Kuppeveld *et al.*, 1994).

Nevertheless, even when a fresh and uncontaminated HeLa S3 cell line was used, no down-regulation of NTH1 was observed. It is uncertain whether the unsuccessful down-regulation is caused by low transfection efficiencies due to low siRNA uptake in cells or by low knockdown efficiencies. The transfection efficiency, defined by the fraction of cells that manages to take up exogenous RNA or DNA successfully, can be determined by transfecting cells with a plasmid expressing green fluorescent protein (GFP). The expression of GFP can then be examined by using fluorescence microscopy. Another way to determine the fraction of siRNA uptake in cells is by fluorescently labeling siRNA and use flow cytometry to measure the fraction of cells containing fluorescent siRNA. These methods should be included in further studies.

The efficiency of knockdown is always less than the transfection efficiency, due to the fact that not all siRNA taken up by the cell will actively contribute to down-regulation of the target gene. Once the cells have taken in the siRNA-liposome complex, the fraction of siRNA released into the cells that is actually active, varies, since a portion of siRNA

released might either be inactivated, degraded or compartmentalized (Bartz *et al.*, 2011;Rossi, 2005)

It is also important to consider that transient transfections only provides down-regulation of the target gene for a limited time, since the transfected genetic material is not integrated into the genome. The effect of down-regulation is thus only transient, since the siRNA taken in by the cell will get diluted through mitosis or degraded. If the transfections efficiencies and knockdown efficiencies are not optimal, the time interval the target gene is down-regulated in, is also shortened. Thus, the time frame of the experiment is an important parameter to consider, since the effect of transfection only last for a limited time period.

Although several studies indicate successful down-regulation of both TDP1 and NTH1 using transient transfection, stable transfection is the best option especially during a long term experiment. However, due to limited time frame, transient transfection was chosen to down-regulate the proteins of interest.

Furthermore, in addition to cell health, a lot of other factors that can influence the transfection efficiency were also taken into consideration. Number of passages was kept at less than 10. The cells were transfected at the confluency recommended by the manufacturer and harvested 48 h after transfection as recommended. To ensure that the effect of down-regulation was not lost due to long incubation period after transfection, transfected cells were also once harvested after 24 h instead of 48 h, without observing any successful down-regulation.

To observe down-regulation on mRNA levels, uncontaminated HeLa S3 cells transfected with siRNA specific for *NTHL1* were also evaluated by RT-PCR, a method that is capable of determining if and to what extent mRNA levels of the target gene has been down-regulated. Western blot is only capable of evaluating down-regulation on protein level and is often supplemented with other methods like RT-PCR or biochemical assays, since Western blot may show false positive bands, due to unspecific binding of the antibody to proteins with similar masses as the target protein. However, no down-regulation of *NTHL1* was observed on mRNA levels either, which was consistent with the results obtained from Western blot analysis or biochemical analysis.

Use of RT-PCR to evaluate down-regulation of NTH1

The two biological replicates representing control cells are demonstrating somewhat different mRNA levels of the *NTHL1* gene, indicating individual variation in the biological system (Figure 4.15).

Since no primer-dimers were observed during the melting curve analysis, one can exclude their contribution to any inaccurate results. In addition, the calculated amplifications efficiencies were as expected and were used as an indication of how well the gene-specific primers are able to anneal to their respective genes. Although, the amplification efficiency of 100% indicates that the PCR product is doubled during each cycle which is optimal during an experiment, most amplification efficiencies are usually calculated to be below this due to experimental limitations, such as depletion of PCR components and renaturing of PCR products. In addition the difference between amplification efficiencies of the target and reference gene were as expected and are caused by various efficiency of primer annealing, GC-content of the sequence that are amplified and the size of PCR product. Since no fluorescence signal was detected in the negative control included in the experiment, any nucleic acid contamination in the samples that could have caused inaccurate results was also ruled out.

Use of biochemical approach to evaluate down-regulation

A biochemical approach was used to demonstrate that NTH1 was not down-regulated in NTH1 KD extracts. The trapped protein-DNA complex in both control and NTH1 KD extracts appeared to be at the same size as NTH1-DNA complex formed when recombinant NTH1 was used as positive control (Figure 4.13). However, the bands detected in the extracts seemed to have migrated slightly longer than the recombinant NTH1-DNA complex. One explanation may be that endogenous NTH1 in the extracts may have PTMs, which the recombinant NTH1 lacks.

Another observation made during the trapping assay was the absence of NEIL1-DNA and NEIL2-DNA complexes in control or NTH1 KD extracts, indicating that the levels of NEIL1 or NEIL2 were too low to be detected when 8 or 16 µg extracts were used. NTH1, on the other hand, was detectable, indicating that NTH1 might be present in larger quantities than the NEIL enzymes, which in turn could also help explain why we could not observe any susbstantial contribution in AP site processing from Neil enzymes in mice.

Down-regulation of TDP1 was also evaluated by observing the processing of a phosphotyrosine-containing DNA substrate. Less phosphotyrosine was processed in TDP1 KD extracts compared to control extracts, indicating successful down-regulation of TDP1. The high background signal detected by phosphorimaging, did not interfere with the obtained results, but indicates some level of impurity in the DNA substrate (Figure 4.14).

5.4 Processing of AP sites using HeLa S3 cell line

The processing of intact AP sites were also investigated using control and TDP1 KD extracts prepared from transfected HeLa S3 cells.

Intact AP sites were mainly processed to 3'OH termini, which is consistent with the observations made in mice. The fact that 3'dRP and 3'P was observed in less degree than 3'OH, confirms that APE1 is responsible for most of the AP site processing.

Just like in mice, the 3'P product was generated by the activity of TDP1 acting downstream of NTH1 on the 3'dRP termini. Indeed, the abrogation of the 3'P product in TDP KD extracts and when TDP1-inhibitor was added to control cells, suggest that NEIL1 or NEIL2 are not responsible for generating the 3'P product.

Since the 3'dRP can be further processed to 3'OH and 3'P, it was not possible to determine the total contribution of NTH1. In addition, the strong activity of APE1, overshadows the contribution of other enzymes involved in the processing of AP site. This issue was also raised when AP sites were processed in mice. Thus, in contrast to experiments where mice extracts were used, the activity of APE1 was inhibited to some extent in control and TDP1 KD extracts by using 500 μM myricetin. A ~30% increase was observed in the intensity of the 3'dRP band when the activity of APE1 was inhibited, suggesting that ~30% of the 3'dRP is further processed to 3'OH by APE1. This is consistent with other studies indicating that APE1 have a greater capacity to cleave 5' to the AP site, than 3' to the 3'dRP product. Indeed, Chen *et al.,* 1991 demonstrated that mammalian APE1 exhibits 100- to 200-fold higher AP endonuclease than 3'-phosphodiesterase activity, underscoring the fact that most of the 3'OH product generated has resulted from APE1's ability to cleave 5' to the AP site directly. However, due to the

high activity of APE1, it is not possible to achieve full inhibition of APE1, without affecting and inhibiting other essential DNA repair processes, as discussed earlier in section 5.2. Thus, the ~30% increase in the 3'dRP products can only provide an idea of how much of the 3'dRP product is in fact further processed, without determining the actual contribution of NTH1.

Another interesting observation was the increase in the 3'OH products in TDP1 KD extract compared to control extract, which might suggest an up-regulation of APE1. When TDP1 levels are down-regulated, it is likely that alternate repair enzymes, like for instance APE1 gets up-regulated that in turn could explain the increase in 3'OH products. Another possible explanation to the increase in the 3'OH may be that TDP1 competes with APE1 for binding of the substrate, resulting in less substrate available for APE1. When TDP1 is down-regulated, APE1 is able to process the substrate that would normally be handled by TDP1, which in turn result in an increase in the 3'OH products. However, to confirm any up-regulation of APE1, experiments must be performed on a quantitative and qualitative level too.

5.5 Comparison of AP site processing in mice and humans

The processing of intact AP site using mice extracts or extracts prepared from HeLa S3, showed similar results; The 3'OH product was most abundant, whereas the 3'P and 3'dRP products were observed to a lesser extent. The processing of a nicked AP site in both model systems suggests that enzymes other than APE1, such like TDP1 are capable of processing the 3'dRP terminus generated by NTH1.

As mentioned earlier, Lebedeva *et al.,* 2011 have already demonstrated that recombinant TDP1 processes the 3'dRP termini, however the *in vitro* significance was further addressed by using whole-cell extracts from mice and immortalized human cells in this study. Overall, the activity of Tdp1 in whole-cell extracts from mice not only supports the findings shown by Lebedeva *et al*., 2011 but also suggest that Tdp1 is capable of working downstream of Nth1 in a similar APE-independent manner as shown in *S. pombe* by Nilsen *et al.,* 2012. Similar TDP1 activity was also observed in HeLa S3 cells, suggesting that NTH1 may in concert with TDP1 and PNKP serve as back-ups for APE1 in the repair of AP sites (Figure 5.1). The *in vivo* significance of Tdp1 in *S. pombe* and chicken DT40 cells, have also been established using cell-based survival assays where Tdp1-deficient cells were hypersensitive to methyl methanesulfonate (MMS), underscoring the importance of Tdp1 in the AP site repair (Murai *et al.*, 2012;Nilsen *et al.*, 2012).

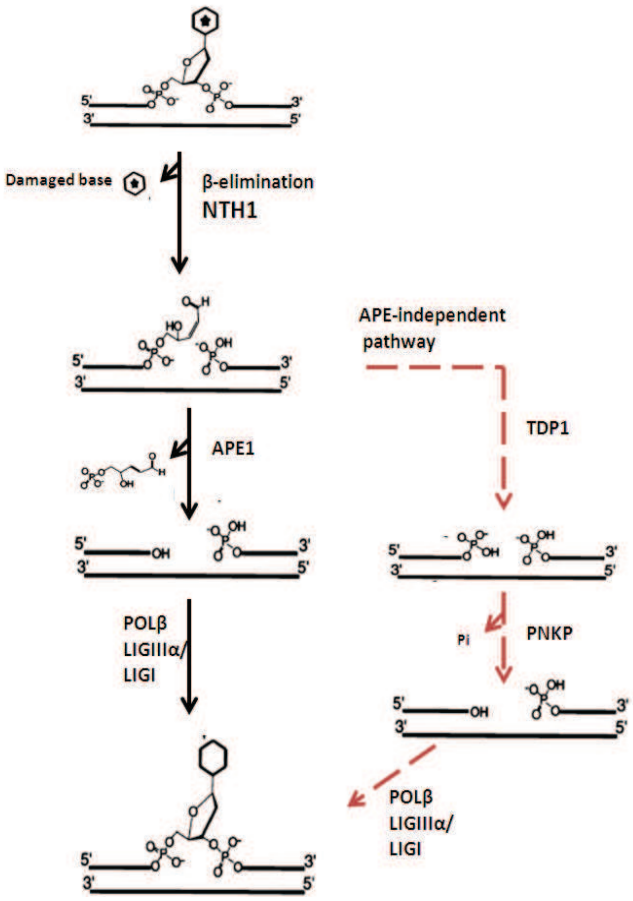

Figure 5.1. Possible BER of AP sites in mammals. When BER is initiated by NTH1, APE1 is mainly responsible for the further processing of the β-elimination product (Black arrows). However, an APE-independent pathway has been proposed in mammals where TDP1 can process the β-elimination product generated by NTH1, and thus act as a back-up for APE1. Figure modified from (Wiederhold *et al.*, 2004)

5.6 Conclusion

Processing of AP sites in mammalian cells was investigated to gain better insight in the actions of BER enzymes. Processing of AP site opposite different bases using either mice extracts or recombinant NTH1, indicates that the processing of AP site was not affected by the opposite base.

The processing of the intact AP site using mice extracts or extracts prepared from HeLa S3 cells showed that APE1 is responsible for the main AP site incision activity, whereas the roles of NEIL1 and NEIL2 in AP site processing was demonstrated to be non-essential. The product of NTH1 incision, 3'dRP, was also observed in both mice and HeLa S3 extracts, although in lesser extent than the 3'OH product, indicating that NTH1 is involved in AP site processing. In addition, NTH1 was shown to require 10-fold more enzyme to process the 5'dRP terminus than the intact AP site, indicating that NTH1 most likely do not compete with POL β for processing of the 5'dRP terminus, downstream of APE1.

Down-regulation of NTH1 was not achieved when siRNA specific for *NTHL1* gene was transfected into HeLa S3 and HaCaT cell lines. TDP1 was, however, successful down-regulated by ~65% in HeLa S3 cells, and biochemical analysis showed abrogation of the 3'P product , indicating that TDP1 is to some extent involved in AP site processing. The 3'dRP termini was shown also to be further processed to the 3'P termini by TDP1 in both HeLa S3 cells and mice extracts, indicating that TDP1 is capable of working downstream of NTH1 in an APE1-independent manner and thus may serve as a back-up for APE1 in the repair of AP site.

5.7 Future aspects

The total contribution of NTH1 in AP site processing was not possible to determine exactly, since the 3'dRP product is also further processed by other enzymes in the cellular extracts. Thus, to clarify the exact role of NTH1 in AP site repair, it is possible to use Nth1 KO mice models that have been used in several studies, and are viable with no obvious phenotypical changes (Takao *et al.*, 2002).

Although the processing of AP sites have been investigated and suggest that TDP1 may work downstream of NTH1 in an APE1-independent manner in both mice and humans, further investigations are required in KD or KO cells to establish its exact role in AP site repair. To our knowledge, the involvement of TDP1 in repair of AP sites induced by the classical alkylating agent MMS, has not been reported. However, cell-based survival assay performed on Tdp1-deficient DT40 cells in chicken demonstrated hypersensitivity towards MMS exposure (Murai *et al.*, 2012). MMS produces alkylated bases that are converted to AP sites by DNA glycosylases or by spontaneous base loss (McCullough *et al.*, 1999). Thus, similar cell-based studies should also be performed using KD or KO cells from human cell lines, to determine any changes in cell sensitivity towards MMS exposure. Such cell-based survival assay was intended to be performed on both NTH1 KD cells and TDP1 KD cells, but due to the unsuccessful down-regulation of NTH1 and the lack of time, these experiments were postponed.

Since the down-regulation of NTH1 was not reproduced after the initiating testing of transfection conditions, it is clearly a need to further optimize the transfection conditions and also to reconsider the use of the particular *NTHL1*-siRNA sequences used to down-regulate NTH1. In addition, cells transfected with either a plasmid expressing GFP or fluorescent labeled siRNA, should be included in the experiments to determine the transfection efficiencies. Another important factor to consider is whether one should rather invest in stable transfection, instead of transient, especially if the time frame provided allows it.

Overall, based upon our results, it is evident that although APE1 is responsible for the main AP site processing in mammalian cells, NTH1 and TDP1 are also involved. Further investigation of their role in different human and mouse models are thus required since increased knowledge of the AP site repair might contribute to unravel the causes of human diseases.

6 Reference List

Alberts,B., Johnson,A., Lewis,J., Raff,M., Roberts,K., and Walter,P. (2008). Molecular Biology of the Cell. 5th Edition. Garland Science. pp. 534-536, 600-604, 1059. ISBN 0-8153-4106-7.

Allinson,S.L., Dianova,I.I., and Dianov,G.L. (2001). DNA polymerase beta is the major dRP lyase involved in repair of oxidative base lesions in DNA by mammalian cell extracts. EMBO J. *20*, 6919-6926.

Almeida,K.H. and Sobol,R.W. (2007). A unified view of base excision repair: lesion-dependent protein complexes regulated by post-translational modification. DNA Repair (Amst) *6*, 695-711.

Amersham Biosciences®. (2012). Storage Phosphor Screens. http://wp1000855.wp002.webpack.hosteurope.de/screen/phoshpor%20screen.pdf

Aspinwall,R., Rothwell,D.G., Roldan-Arjona,T., Anselmino,C., Ward,C.J., Cheadle,J.P., Sampson,J.R., Lindahl,T., Harris,P.C., and Hickson,I.D. (1997). Cloning and characterization of a functional human homolog of Escherichia coli endonuclease III. Proc. Natl. Acad. Sci. U. S. A *94*, 109-114.

Bandaru,V., Sunkara,S., Wallace,S.S., and Bond,J.P. (2002). A novel human DNA glycosylase that removes oxidative DNA damage and is homologous to Escherichia coli endonuclease VIII. DNA Repair (Amst) *1*, 517-529.

Barnes,D.E., Tomkinson,A.E., Lehmann,A.R., Webster,A.D., and Lindahl,T. (1992). Mutations in the DNA ligase I gene of an individual with immunodeficiencies and cellular hypersensitivity to DNA-damaging agents. Cell *69*, 495-503.

Barnes,D.E., Lindahl,T., and Sedgwick,B. (1993). DNA repair. Curr. Opin. Cell Biol. *5*, 424-433.

Bartz,R., Fan,H., Zhang,J., Innocent,N., Cherrin,C., Beck,S.C., Pei,Y., Momose,A., Jadhav,V., Tellers,D.M., Meng,F., Crocker,L.S., Sepp-Lorenzino,L., Barnett,S.F. (2011). Effective siRNA delivery and target mRNA degradation using an amphipathic peptide to facilitate pH-dependent endosomal escape. Biochem. J. *435*, 475-487.

Bebenek,K. and Kunkel,T.A. (2004). Functions of DNA polymerases. Adv. Protein Chem. *69*, 137-165.

Berdal,K.G., Johansen,R.F., and Seeberg,E. (1998). Release of normal bases from intact DNA by a native DNA repair enzyme. EMBO J. *17*, 363-367.

Bjelland,S. and Seeberg,E. (2003). Mutagenicity, toxicity and repair of DNA base damage induced by oxidation. Mutat. Res. *531*, 37-80.

Caldecott,K.W., Aoufouchi,S., Johnson,P., and Shall,S. (1996). XRCC1 polypeptide interacts with DNA polymerase beta and possibly poly (ADP-ribose) polymerase, and DNA ligase III is a novel molecular 'nick-sensor' in vitro. Nucleic Acids Res. *24*, 4387-4394.

Caldecott,K.W. (2002). Polynucleotide kinase: a versatile molecule makes a clean break. Structure. *10*, 1151-1152.

Cao,C., Jiang,Y.L., Stivers,J.T., and Song,F. (2004). Dynamic opening of DNA during the enzymatic search for a damaged base. Nat. Struct. Mol. Biol. *11*, 1230-1236.

Champoux,J.J. (2001). DNA topoisomerases: structure, function, and mechanism. Annu. Rev. Biochem. *70*, 369-413.

Chen,D.S., Herman,T., and Demple,B. (1991). Two distinct human DNA diesterases that hydrolyze 3'-blocking deoxyribose fragments from oxidized DNA. Nucleic Acids Res. *19*, 5907-5914.

Dalhus,B., Laerdahl,J.K., Backe,P.H., and Bjoras,M. (2009). DNA base repair--recognition and initiation of catalysis. FEMS Microbiol. Rev. *33*, 1044-1078.

Das, A., Wiederhold, L., Leppard, J. B., Kedar, P., Prasad, R., Wang, H., Boldogh, I., Karimi-Busheri, F., Weinfeld, M., Tomkinson, A. E., Wilson, S. H., Mitra, S. and Hazra, T. K. (2006). NEIL2-initiated, APE-independent repair of oxidized bases in DNA: Evidence for a repair complex in human cells. DNA Repair (Amst) *5*, 1439-1448.

David,S.S. and Williams,S.D. (1998). Chemistry of Glycosylases and Endonucleases Involved in Base-Excision Repair. Chem. Rev. *98*, 1221-1262.

Debethune,L., Kohlhagen,G., Grandas,A., and Pommier,Y. (2002). Processing of nucleopeptides mimicking the topoisomerase I-DNA covalent complex by tyrosyl-DNA phosphodiesterase. Nucleic Acids Res. *30*, 1198-1204.

Demple,B. and Harrison,L. (1994). Repair of oxidative damage to DNA: enzymology and biology. Annu. Rev. Biochem. *63*, 915-948.

Dexheimer,T.S., Antony,S., Marchand,C., and Pommier,Y. (2008). Tyrosyl-DNA phosphodiesterase as a target for anticancer therapy. Anticancer Agents Med. Chem. *8*, 381-389.

Dodson,M.L., Michaels,M.L., and Lloyd,R.S. (1994). Unified catalytic mechanism for DNA glycosylases. J. Biol. Chem. *269*, 32709-32712.

Dou,H., Mitra,S., and Hazra,T.K. (2003). Repair of oxidized bases in DNA bubble structures by human DNA glycosylases NEIL1 and NEIL2. J. Biol. Chem. *278*, 49679-49684.

El-Khamisy,S.F., Saifi,G.M., Weinfeld,M., Johansson,F., Helleday,T., Lupski,J.R., and Caldecott,K.W. (2005). Defective DNA single-strand break repair in spinocerebellar ataxia with axonal neuropathy-1. Nature *434*, 108-113.

Falnes,P.O., Johansen,R.F., and Seeberg,E. (2002). AlkB-mediated oxidative demethylation reverses DNA damage in Escherichia coli. Nature *419*, 178-182.

Felgner,P.L., Gadek,T.R., Holm,M., Roman,R., Chan,H.W., Wenz,M., Northrop,J.P., Ringold,G.M., and Danielsen,M. (1987). Lipofection: a highly efficient, lipid-mediated DNA-transfection procedure. Proc. Natl. Acad. Sci. U. S. A *84*, 7413-7417.

Fortini,P., Parlanti,E., Sidorkina,O.M., Laval,J., and Dogliotti,E. (1999). The type of DNA glycosylase determines the base excision repair pathway in mammalian cells. J. Biol. Chem. *274*, 15230-15236.

Friedberg,E.C. and Meira,L.B. (2000). Database of mouse strains carrying targeted mutations in genes affecting cellular responses to DNA damage. Version 4. Mutat. Res. *459*, 243-274.

Friedberg,E.C. (2006). DNA Repair and Mutagenesis. 2nd Edition. Washington, D.C: ASM Press. pp. 27-28, 162-163. ISBN 1-55581-319-4.

Fromme,J.C. and Verdine,G.L. (2003). Structure of a trapped endonuclease III-DNA covalent intermediate. EMBO J. *22*, 3461-3471.

Gossett,J., Lee,K., Cunningham,R.P., and Doetsch,P.W. (1988). Yeast redoxyendonuclease, a DNA repair enzyme similar to Escherichia coli endonuclease III. Biochemistry *27*, 2629-2634.

Hailer,M.K., Slade,P.G., Martin,B.D., Rosenquist,T.A., and Sugden,K.D. (2005). Recognition of the oxidized lesions spiroiminodihydantoin and guanidinohydantoin in DNA by the mammalian base excision repair glycosylases NEIL1 and NEIL2. DNA Repair (Amst) *4*, 41-50.

Hegde,M.L., Hazra,T.K., and Mitra,S. (2008). Early steps in the DNA base excision/single-strand interruption repair pathway in mammalian cells. Cell Res. *18*, 27-47.

Hegde,M.L., Hazra,T.K., and Mitra,S. (2010). Functions of disordered regions in mammalian early base excision repair proteins. Cell Mol. Life Sci. *67*, 3573-3587.

Hegde,M.L., Mantha,A.K., Hazra,T.K., Bhakat,K.K., Mitra,S., and Szczesny,B. (2012). Oxidative genome damage and its repair: Implications in aging and neurodegenerative diseases. Mech. Ageing Dev.

Higgins,S.A., Frenkel,K., Cummings,A., and Teebor,G.W. (1987). Definitive characterization of human thymine glycol N-glycosylase activity. Biochemistry *26*, 1683-1688.

Hildrestrand,G.A., Neurauter,C.G., Diep,D.B., Castellanos,C.G., Krauss,S., Bjoras,M., and Luna,L. (2009). Expression patterns of Neil3 during embryonic brain development and neoplasia. BMC. Neurosci. *10*, 45.

Interthal,H., Pouliot,J.J., and Champoux,J.J. (2001). The tyrosyl-DNA phosphodiesterase Tdp1 is a member of the phospholipase D superfamily. Proc. Natl. Acad. Sci. U. S. A *98*, 12009-12014.

Interthal,H., Chen,H.J., Kehl-Fie,T.E., Zotzmann,J., Leppard,J.B., and Champoux,J.J. (2005). SCAN1 mutant Tdp1 accumulates the enzyme--DNA intermediate and causes camptothecin hypersensitivity. EMBO J. *24*, 2224-2233.

Invitrogen®. (2012). Handbook of Cell Culture Basics.
http://www.invitrogen.com/site/us/en/home/References/g ibco-cell-culture-basics.html

Ischenko,A.A. and Saparbaev,M.K. (2002). Alternative nucleotide incision repair pathway for oxidative DNA damage. Nature *415*, 183-187.

Izumi,T., Wiederhold,L.R., Roy,G., Roy,R., Jaiswal,A., Bhakat,K.K., Mitra,S., and Hazra,T.K. (2003). Mammalian DNA base excision repair proteins: their interactions and role in repair of oxidative DNA damage. Toxicology *193*, 43-65.

Jilani,A., Ramotar,D., Slack,C., Ong,C., Yang,X.M., Scherer,S.W., and Lasko,D.D. (1999). Molecular cloning of the human gene, PNKP, encoding a polynucleotide kinase 3'-phosphatase and evidence for its role in repair of DNA strand breaks caused by oxidative damage. J. Biol. Chem. *274*, 24176-24186.

Katcher,H.L. and Wallace,S.S. (1983). Characterization of the Escherichia coli X-ray endonuclease, endonuclease III. Biochemistry *22*, 4071-4081.

Kavli,B., Otterlei,M., Slupphaug,G., and Krokan,H.E. (2007). Uracil in DNA--general mutagen, but normal intermediate in acquired immunity. DNA Repair (Amst) *6*, 505-516.

Klungland,A., Rosewell,I., Hollenbach,S., Larsen,E., Daly,G., Epe,B., Seeberg,E., Lindahl,T., and Barnes,D.E. (1999). Accumulation of premutagenic DNA lesions in mice defective in removal of oxidative base damage. Proc. Natl. Acad. Sci. U. S. A *96*, 13300-13305.

Klungland,A. (2001). Life without DNA repair. Tidsskr. Nor Laegeforen. *121*, 41-49.

Kouadjo,K.E., Nishida,Y., Cadrin-Girard,J.F., Yoshioka,M., and St-Amand,J. (2007). Housekeeping and tissue-specific genes in mouse tissues. BMC. Genomics *8*, 127.

Krishnamurthy,N., Zhao,X., Burrows,C.J., and David,S.S. (2008). Superior removal of hydantoin lesions relative to other oxidized bases by the human DNA glycosylase hNEIL1. Biochemistry *47*, 7137-7146.

Kuo,C.F., McRee,D.E., Fisher,C.L., O'Handley,S.F., Cunningham,R.P., and Tainer,J.A. (1992). Atomic structure of the DNA repair [4Fe-4S] enzyme endonuclease III. Science *258*, 434-440.

Lange,S.S., Takata,K., and Wood,R.D. (2011). DNA polymerases and cancer. Nat. Rev. Cancer *11*, 96-110.

Lebedeva,N.A., Rechkunova,N.I., and Lavrik,O.I. (2011). AP-site cleavage activity of tyrosyl-DNA phosphodiesterase 1. FEBS Lett. *585*, 683-686.

Li,Z. and Rana,T.M. (2012). Molecular Mechanisms of RNA-Triggered Gene Silencing Machineries. Acc. Chem. Res.

Lindahl,T. (1993). Instability and Decay of the Primary Structure of Dna. Nature *362*, 709-715.

Liu,X. and Roy,R. (2002). Truncation of amino-terminal tail stimulates activity of human endonuclease III (hNTH1). J. Mol. Biol. *321*, 265-276.

Loeb,L.A. and Preston,B.D. (1986). Mutagenesis by apurinic/apyrimidinic sites. Annu. Rev. Genet. *20*, 201-230.

Lucey,B.P., Nelson-Rees,W.A., and Hutchins,G.M. (2009). Henrietta Lacks, HeLa cells, and cell culture contamination. Arch. Pathol. Lab Med. *133*, 1463-1467.

Luna,L., Bjoras,M., Hoff,E., Rognes,T., and Seeberg,E. (2000). Cell-cycle regulation, intracellular sorting and induced overexpression of the human NTH1 DNA glycosylase involved in removal of formamidopyrimidine residues from DNA. Mutat. Res. 460, 95-104.

Marenstein,D.R., Chan,M.K., Altamirano,A., Basu,A.K., Boorstein,R.J., Cunningham,R.P., and Teebor,G.W. (2003). Substrate specificity of human endonuclease III (hNTH1). Effect of human APE1 on hNTH1 activity. J. Biol. Chem. *278*, 9005-9012.

Matsumoto,Y. and Kim,K. (1995). Excision of deoxyribose phosphate residues by DNA polymerase beta during DNA repair. Science *269*, 699-702.

Matsumoto,Y., Zhang,Q.M., Takao,M., Yasui,A., and Yonei,S. (2001). Escherichia coli Nth and human hNTH1 DNA glycosylases are involved in removal of 8-oxoguanine from 8-oxoguanine/guanine mispairs in DNA. Nucleic Acids Res. *29*, 1975-1981.

McCullough,A.K., Dodson,M.L., and Lloyd,R.S. (1999). Initiation of base excision repair: glycosylase mechanisms and structures. Annu. Rev. Biochem. *68*, 255-285.

Mitra,S., Boldogh,I., Izumi,T., and Hazra,T.K. (2001). Complexities of the DNA base excision repair pathway for repair of oxidative DNA damage. Environ. Mol. Mutagen. *38*, 180-190.

Murai,J., Huang,S.Y., Das,B.B., Dexheimer,T.S., Takeda,S., and Pommier,Y. (2012). Tyrosyl-DNA Phosphodiesterase 1 (TDP1) Repairs DNA Damage Induced by Topoisomerases I and II and Base Alkylation in Vertebrate Cells. J. Biol. Chem. *287*, 12848-12857.

Neeley,W.L. and Essigmann,J.M. (2006). Mechanisms of formation, genotoxicity, and mutation of guanine oxidation products. Chem. Res. Toxicol. *19*, 491-505.

Nemec,A.A., Wallace,S.S., and Sweasy,J.B. (2010). Variant base excision repair proteins: contributors to genomic instability. Semin. Cancer Biol. *20*, 320-328.

Nilsen,H. and Krokan,H.E. (2001). Base excision repair in a network of defence and tolerance. Carcinogenesis *22*, 987-998.

Nilsen,L., Forstrom,R.J., Bjoras,M., and Alseth,I. (2012). AP endonuclease independent repair of abasic sites in Schizosaccharomyces pombe. Nucleic Acids Res. *40*, 2000-2009.

Pages,V., Johnson,R.E., Prakash,L., and Prakash,S. (2008). Mutational specificity and genetic control of replicative bypass of an abasic site in yeast. Proc. Natl. Acad. Sci. U. S. A *105*, 1170-1175.

Plo,I., Liao,Z.Y., Barcelo,J.M., Kohlhagen,G., Caldecott,K.W., Weinfeld,M., and Pommier,Y. (2003). Association of XRCC1 and tyrosyl DNA phosphodiesterase (Tdp1) for the repair of topoisomerase I-mediated DNA lesions. DNA Repair (Amst) *2*, 1087-1100.

Pommier,Y., Pourquier,P., Urasaki,Y., Wu,J., and Laco,G.S. (1999). Topoisomerase I inhibitors: selectivity and cellular resistance. Drug Resist. Updat. *2*, 307-318.

QIAGEN®. (2003). Handbook for High-Level Expression and Purification of 6xHis-Tagged Proteins.

Rosenthal,N. and Brown,S. (2007). The mouse ascending: perspectives for human-disease models. Nat. Cell Biol. *9*, 993-999.

Rossi,J.J. (2005). Receptor-targeted siRNAs. Nat. Biotechnol. *23*, 682-684.

Sambrook,J. and Russel,D.W. (2001). Molecular Cloning, A Laboratory Manual. Volume 3. 3rd Edtition. Cold Spring Harbor Laboratory Press. pp. 16.2-16.4. ISBN 0-87969-577-3

Santa Cruz®. (2012). *NTHL1*-siRNA. http://Datasheets.Scbt.Com/Sc-38134.Pdf.

Sarker,A.H., Ikeda,S., Nakano,H., Terato,H., Ide,H., Imai,K., Akiyama,K., Tsutsui,K., Bo,Z., Kubo,K., Yamamoto,K., Yasui,A., Yoshida,M.C., Seki,S. (1998). Cloning and characterization of a mouse homologue (mNthl1) of Escherichia coli endonuclease III. J. Mol. Biol. *282*, 761-774.

Slupphaug,G., Mol,C.D., Kavli,B., Arvai,A.S., Krokan,H.E., and Tainer,J.A. (1996). A nucleotide-flipping mechanism from the structure of human uracil-DNA glycosylase bound to DNA. Nature *384*, 87-92.

Sugo,N., Aratani,Y., Nagashima,Y., Kubota,Y., and Koyama,H. (2000). Neonatal lethality with abnormal neurogenesis in mice deficient in DNA polymerase beta. EMBO J. *19*, 1397-1404.

Sung,J.S. and Demple,B. (2006). Roles of base excision repair subpathways in correcting oxidized abasic sites in DNA. FEBS J. *273*, 1620-1629.

Svilar,D., Goellner,E.M., Almeida,K.H., and Sobol,R.W. (2011). Base excision repair and lesion-dependent subpathways for repair of oxidative DNA damage. Antioxid. Redox. Signal. *14*, 2491-2507.

Takao,M., Kanno,S., Kobayashi,K., Zhang,Q.M., Yonei,S., van der Horst,G.T., and Yasui,A. (2002). A back-up glycosylase in Nth1 knock-out mice is a functional Nei (endonuclease VIII) homologue. J. Biol. Chem. *277*, 42205-42213.

Takashima,H., Boerkoel,C.F., John,J., Saifi,G.M., Salih,M.A., Armstrong,D., Mao,Y., Quiocho,F.A., Roa,B.B., Nakagawa,M., Stockton,D.W., Lupski,J.R.(2002). Mutation of TDP1, encoding a topoisomerase I-dependent DNA damage repair enzyme, in spinocerebellar ataxia with axonal neuropathy. Nat. Genet. *32*, 267-272.

Tomkinson,A.E., Vijayakumar,S., Pascal,J.M., and Ellenberger,T. (2006). DNA ligases: structure, reaction mechanism, and function. Chem. Rev. *106*, 687-699.

Tu,C.P. and Cohen,S.N. (1980). 3'-end labeling of DNA with [alpha-32P]cordycepin-5'-triphosphate. Gene *10*, 177-183.

Valasek,M.A. and Repa,J.J. (2005). The power of real-time PCR. Adv. Physiol Educ. *29*, 151-159.

van Kuppeveld,F.J., Johansson,K.E., Galama,J.M., Kissing,J., Bolske,G., van der Logt,J.T., and Melchers,W.J. (1994). Detection of mycoplasma contamination in cell cultures by a mycoplasma group-specific PCR. Appl. Environ. Microbiol. *60*, 149-152.

Vidal,A.E., Hickson,I.D., Boiteux,S., and Radicella,J.P. (2001). Mechanism of stimulation of the DNA glycosylase activity of hOGG1 by the major human AP endonuclease: bypass of the AP lyase activity step. Nucleic Acids Res. *29*, 1285-1292.

Watson,J.D., Baker,T.A., Bell,S.P., Gann,A., Levine,M., and Losick,R. (2004). Molecular Biology of the Gene. Cold Spring Harbor Laboratory Press. Benjamin Cummings. pp. 568, 675, 676. ISBN 0-321-22368-3.

Wiederhold,L., Leppard,J.B., Kedar,P., Karimi-Busheri,F., Rasouli-Nia,A., Weinfeld,M., Tomkinson,A.E., Izumi,T., Prasad,R., Wilson,S.H., Mitra,S., Hazra,T.K. (2004). AP endonuclease-independent DNA base excision repair in human cells. Mol. Cell *15*, 209-220.

Wilson,D.M. and Bohr,V.A. (2007). The mechanics of base excision repair, and its relationship to aging and disease. DNA Repair (Amst) *6*, 544-559.

Xu,Y.J., DeMott,M.S., Hwang,J.T., Greenberg,M.M., and Demple,B. (2003). Action of human apurinic endonuclease (Ape1) on C1'-oxidized deoxyribose damage in DNA. DNA Repair (Amst) *2*, 175-185.

Yang,S.W., Burgin,A.B., Jr., Huizenga,B.N., Robertson,C.A., Yao,K.C., and Nash,H.A. (1996). A eukaryotic enzyme that can disjoin dead-end covalent complexes between DNA and type I topoisomerases. Proc. Natl. Acad. Sci. U. S. A *93*, 11534-11539.

Yndestad,A., Neurauter,C.G., Oie,E., Forstrom,R.J., Vinge,L.E., Eide,L., Luna,L., Aukrust,P., and Bjoras,M. (2009). Up-regulation of myocardial DNA base excision repair activities in experimental heart failure. Mutat. Res. *666*, 32-38.

Zharkov,D.O. (2008). Base excision DNA repair. Cell Mol. Life Sci. *65*, 1544-1565.

Zou,G.M., Luo,M.H., Reed,A., Kelley,M.R., and Yoder,M.C. (2007). Ape1 regulates hematopoietic differentiation of embryonic stem cells through its redox functional domain. Blood *109*, 1917-1922.

Appendix A: Recipes of buffers and solutions

Solutions needed for purification of enzymes	
LB-medium	25 g Difco LB Broth, Miller in 1l MQ
LB-kanamycin	25 g/l Difco LB Broth, 50 mg/l kanamycin
LB-sorbitol medium	25 g/l Difco LB Broth, 91 g/l sorbitol, 0.4 g/l betain
LB-kanamycin medium plates	25 g/l Difco LB Broth, 20 g/l agar, 50 mg/l kanamycin
Buffer A/B/C	50 mM Na_2HPO_4, pH 8.0, 300 mM NaCl, 10 mM β-mercaptoethanol, 10/50/300 mM imidazole
Solutions needed for SDS PAGE	
Comassie Blue staining solution	40 % methanol, 10 % acetic acid, 0.1 % Coomassie Blue
Destaining solution	40 % methanol, 10 % acetic acid, 4 % glycerol
Solutions needed during transfection and harvesting cells	
Cryo-medium	50% FBS, 10% DMSO in DMEM
Culture medium	10% FBS, 2% 100x GlutaMAX™, 2% Pen-Strep, 2g/l glucose in DMEM .
Protein-cracking buffer	2x NuPAGE® LDS Sample Buffer, 200 mM DTT
Lysis buffer	150 mM NaCl, 1% IPEGAL® CA-630, 0.5% DOC, 0.1% SDS, 1 mM PMSF, 1 mM protease inhibitor cocktail
1 mM Protease inhibitor cocktail	1.5 mM Benzamidine, 2 mg/l pepstatin A (stock made in DMF) and 2 mg/l leupeptin.
Solutions needed for Western blot	
PBS-Tween buffer	1xPBS, 0.05% Tween®20
Drymilk –blocking buffer	5% or 3% Skim Milk Powder in 1xPBS
Stripping buffer	20 ml 10% SDS,12.5 ml 0.5 M Tris-HCl pH 6.8, 0.8 ml β-mercaptoethanol , 67.5 ml MQ
Solutions needed during activity assay	
MOPS buffer	50 mM MOPS pH 7.4, 1 mM EDTA, 100 mM KCl, 1 mM DTT
Dilution buffer	20 mM Hepes pH 7.4, 100 mM KCl, 1 mM EDTA, 2 mM DTT, 0.1 µg/µl BSA, 20% glycerol
5xTDP1 buffer	750 mM KCl, 50 mM Tris-HCl pH 7.5, 5 mM EDTA, 5 mM DTT
Tris-sucrose buffer	84% sucrose, 40 mM Tris pH 8, 10 mM EDTA
5xReaction buffer	350 mM MOPS pH 7.5, 5 mM EDTA, 25% glycerol, 5 mM DTT
Tris-sucrose/MOPS buffer	20% Tris-sucrose buffer, 80% MOPS buffer
20% denaturing gel (For one 10x8 cm gel)	7 M urea (2.1 g), 0.25 ml 20xTaurin buffer, 2 ml Long Ranger™ Gel Solution, 1 ml MQ, 25 µl 10% APS, 2.5 µl TEMED
20 % denaturing sequencing gel	7 M Urea (26 g), 3 ml 20xTaurin buffer or 6 ml 10xTBE buffer, 24 ml Long Ranger™ Gel Solution, 14 or 11 ml MQ, 400 µl 10% APS, 40 µl TEMED
Formamide loading dye	5% Bromophenol Blue, 5% Xylene Cyanol, 10 mM EDTA in formamide
1xTBE	90 mM Tris Base, 90 mM Boric acid, 2 mM EDTA (pH 8.0)
Solutions needed for mycoplasma detection	
10x DNA Loading Buffer	30 % Glycerol, 20 mM EDTA, 0.01 % Bromophenol Blue
1 % Agarose	0.5 g Agarose, 50 ml 0.5 x TBE, 1.5 µl SYBR Safe

Appendix B: Protocol, PCR Mycoplasma Test Kit II

Derived from: http://www.promocell.com/fileadmin/promocell/PDF/PK-CA20-700-20.pdf

Ready-to-use PCR Mix PK-CA20-700-10

Protocol:

A. Test sample preparation:

Transfer 0.5-1.0 ml cell culture supernatant into a 2 ml centrifuge tube. To pellet cellular debris, centrifuge the sample at 250 x g briefly. Transfer the supernatant into a fresh sterile tube and centrifuge at 15,000-20,000 x g for 10 minutes to sediment mycoplasma. Carefully decant the supernatant and keep the pellet (the pellet will not always be visible). Re-suspend the pellet with 50 µl of the Buffer Solution and mix thoroughly with a micropipet. Heat at 95 ˚C for 3 minutes. The test sample can be stored at this stage at -20°C for later use.

B. PCR amplification:

1. Prepare the reaction mixture in a PCR tube by combining the reagents shown below:

Reagents	**Volume**
H_2O	35 µl
Reaction Mix	10 µl
Test sample	5 µl

2. If not using a thermal cycler having a heated lid, overlay mixture with mineral oil (approximately 40 µl) to avoid evaporation of the reaction mixture.

3. Place all tubes in a PCR thermal cycler. Set the parameters for the following conditions and perform the PCR.

94°C 30 seconds
94°C 30 seconds ┐
60°C 120 seconds ├ 35 cycles
72°C 60 seconds ┘
94°C 30 seconds
60°C 120 seconds
72°C 5 min

C. Analysis of amplified products by gel electrophoresis:

1. Apply 20 µl of the PCR product onto an agarose gel for electrophoresis. Do not add loading buffer to the samples. Use a 2% agarose gel.
2. Perform agarose gel electrophoresis with the PCR-amplified samples to verify the amplified product and its size. The size of DNA fragments amplified using the specific primers in this kit is around 270 bp (± 270 bp; depending on the mycoplasma species).

D. Control Template:

To check PCR efficiency use 1 µl of the "Positive Template Control" as a test sample. The size of the PCR product obtained using the positive template with primer pairs is 270 bp. *If desired, you may add 4 µl 1X Gel Loading Buffer containing a marker dye (e.g. bromophenol blue) to the samples.

Appendix C: Protocol, Forward Transfection

Derived from:
http://www.invitrogen.com/etc/medialib/en/filelibrary/pdf.Par.34731.File.dat/Transfecting_Stealth_using_Lipofectamine_RNAiMAX.pdf

Forward transfection

Use this procedure to forward transfect Stealth™ RNAi or siRNA into mammalian cells in a 24-well format (for other formats, see Scaling Up or Down Transfections). In forward transfections, cells are plated in the wells, and the transfection mix is generally prepared and added the next day. Optimize transfections as described in Optimizing Transfections, especially if transfecting a mammalian cell line for the first time. All amounts and volumes are given on a per well basis.
Note: For some cell lines, we recommend reverse transfections.

1. One day before transfection, plate cells in 500 µl of growth medium without antibiotics such that they will be 50-70% confluent at the time of transfection.

2. For each well to be transfected, prepare RNAi duplex-Lipofectamine™ RNAiMAX complexes as follows:
a. Dilute 6 pmol RNAi duplex in 50 µl Opti-MEM® I Reduced Serum Medium without serum. Mix gently.
b. Mix Lipofectamine™ RNAiMAX gently before use, then dilute 1 µl in 50 µl Opti-MEM® I Reduced Serum Medium. Mix gently.
c. Combine the diluted RNAi duplex with the diluted Lipofectamine™ RNAiMAX. Mix gently and incubate for 10-20 minutes at room temperature.

3. Add the RNAi duplex-Lipofectamine™ RNAiMAX complexes to each well containing cells. This gives a final volume of 600 µl and a final RNA concentration of 10 nM. Mix gently by rocking the plate back and forth.

4. Incubate the cells 24-48 hours at 37°C in a CO_2 incubator until you are ready to assay for gene knockdown. Medium may be changed after 4-6 hours.

Optimizing Transfections

To obtain the highest transfection efficiency and low non-specific effects, optimize transfection conditions by varying RNAi duplex and Lipofectamine™ RNAiMAX concentrations. Test 0.6-30 pmol RNAi duplex (final concentration 1-50 nM) and 0.5-1.5 µl Lipofectamine™ RNAiMAX for 24-well format. For extended time course experiments (> 72 hours), consider a cell density that is 10-20% confluent 24 hours after plating.
Note: The concentration of RNAi duplex required will vary depending on the efficacy of the duplex.

Scaling Up or Down Transfections

To transfect cells in different tissue culture formats, vary the amounts of Lipofectamine™ RNAiMAX, RNAi duplex, cells, and medium used in proportion to the relative surface area, as shown in the table.

Culture vessel	Rel. surf. area[1]	Vol. of plating medium	Dilution medium reverse transfection	Dilution medium forward transfection	RNAi (pmol)	RNAi (nM)	Lipofectamine™ RNAiMAX[2]
96-well	0.2	100 µl	20 µl	2 x 10 µl	0.12-6	1-50	0.1-0.3 µl
48-well	0.4	200 µl	40 µl	2 x 20 µl	0.24-12	1-50	0.2-0.6 µl
24-well	1	500 µl	100 µl	2 x 50 µl	0.6-30	1-50	0.5-1.5 µl
6-well	5	2.5 ml	500 µl	2 x 250 µl	3-150	1-50	2.5-7.5 µl
60 mm	10	5 ml	1 ml	2 x 500 µl	6-300	1-50	5-15 µl
100 mm	30	10 ml	2 ml	2 x 1 ml	12-600	1-50	15-35 µl

Continues on the next page

Useful Numbers for Cell Culture

There are various sizes of dishes and flasks used for cell culture. Some useful numbers such as surface area and volumes of dissociation solutions are given below for various size culture vessels.

	Surface Area (mm^2)	Seeding Density	Cells at Confluency[1]	Versene (ml of 0.53 mM EDTA)	Trypsin (ml of 0.05% trypsin, 0.53 mM EDTA)	Growth Medium (ml)
Dishes						
35 mm	962	0.3×10^6	1.2×10^6	1	1	2
60 mm	2,827	0.8×10^6	3.2×10^6	3	2	3
100 mm	7,854	2.2×10^6	8.8×10^6	5	3	10
150 mm	17,671	5.0×10^6	20.0×10^6	10	8	20
Cluster Plates						
6-well	962	0.3×10^6	1.2×10^6	2	2	3–5
12-well	401	0.1×10^6	0.4×10^6	1	1	1–2
24-well	200	0.05×10^6	0.2×10^6	0.5	0.5	0.5–1.0
Flasks						
T-25	2,500	0.7×10^6	2.8×10^6	3	3	3–5
T-75	7,500	2.1×10^6	8.4×10^6	5	5	8–15
T-160	16,000	4.6×10^6	18.4×10^6	10	10	15–30

[1] The number of cells on a confluent plate, dish, or flask will vary with cell type. For this table, HeLa cells were used.

Figure C.1. Useful numbers used in passaging and transfection of the cells.

Appendix D: Protocol, Novex® Semi-Dry Blotting

Derived from: http://tools.invitrogen.com/content/sfs/manuals/novex_semidry_blotter_man.pdf

Equilibrating the Gel

Equilibrating the gel in transfer buffer removes salts that may increase conductivity and heat during transfer. Be careful to equilibrate for the recommended time, as longer equilibration can result in protein diffusion.

1. After electrophoresis, remove the gel from the cassette.
2. Place the gel in a shallow tray containing 100 ml (for Midi Gels and E-PAGE™ Gels) or 50 ml (for Mini Gels) of the appropriate 2x NuPAGE® Transfer Buffer. Equilibrate for 10 minutes on an orbital shaker.

PVDF

1. Use a pre-cut Invitrolon™/Filter Paper Sandwich or cut a PVDF membrane to the appropriate size for your gel.
2. Pre-wet the membrane for 30 seconds in methanol, ethanol, or isopropanol. Briefly rinse the membrane in deionized water.
3. Soak the membrane in the appropriate Transfer Buffer for a few minutes in a shallow tray.

Semi-Dry Blotting Protocol

Follow the instructions below to blot 1–2 Midi Gels or 1–4 Mini Gels using the Novex® Semi-Dry Blotter:

1. In a shallow tray, briefly soak 2 stacked pieces of 3-mm thick Blotting Filter Paper in the appropriate Transfer Buffer.
2. Remove any air bubbles trapped between the filter paper sheets by rolling the stack with a blotting roller while it is still submerged in buffer. **Note:** Removing air bubbles is essential, as they can block the transfer of biomolecules.
3. Place the stack of pre-soaked Blotting Filter Paper on the anode plate of the Novex® Semi-Dry Blotter. Remove any air bubbles between the paper and plate by rolling the stack with the blotting roller.
4. Place the pre-soaked blotting membrane on top of the Blotting Filter Paper stack and remove any air bubbles with the blotting roller.
5. Carefully remove the gel from the transfer buffer and place on top of the blotting membrane. (Gently remove any air bubbles with the blotting roller or a wet gloved finger. **Note:** Be careful not to disturb the gel after it has been placed on the membrane. Moving the gel can result in protein smearing on the membrane.
6. Briefly soak the remaining 2 stacked pieces of 2.5-mm thick Blotting Filter Paper in the appropriate Transfer Buffer. Remove any air bubbles with the blotting roller while the stack is still submerged in buffer.
7. Mini or Midi Gels: Transfer at 20 V for 30–60 minutes.

Appendix E: Protocol, High Capacity RNA-to-cDNA

Derived from: http://tools.invitrogen.com/content/sfs/manuals/cms_050470.pdf

Using the High Capacity RNA-to-cDNA Master Mix

Note: Use the same procedure for preparing No-RT control.

STEP	ACTION
1	Prepare the RT Reactions with High Capacity RNA-to-cDNA Master Mix a. Place the Master Mix components on ice, then mix and briefly centrifuge them. b. Calculate the total volume of components needed to prepare the required number of reactions. Use the table below. c. Include additional reactions in the calculations to provide excess volume for the loss that occurs during reagent transfers. **Note:** Prepare the reaction mix on ice.. d. Seal the plate or tubes. e. Briefly centrifuge the plate or tubes to spin down the contents and to eliminate any air bubbles. f. Place the plate or tubes on ice until you are ready to load the thermal cycler.
2	Perform Reverse Transcription withHigh Capacity RNA-to-cDNA Master Mix a. Program the thermal cycler conditions as shown below. **IMPORTANT!** These conditions are optimized for High Capacity RNA-to-cDNA Master Mix. •Step 1: 5 minutes at 25 °C •Step 2: 30 minutes at 42 °C •Step 3: 5 minutes at 85 °C •Step 4: Hold at 4 °C b. Set the reaction volume to 20 µL. c. Load the reaction plates or tubes into the thermal cycler. d. Start the reverse transcription run. **Note:** Perform PCR amplification with one-tenth of the first-strand reaction.

Component	Volume per Reaction	Final Concentration
High Capacity RNA-to-cDNA Master Mix (or No-RT control)	4.0 µL	1X
RNA template	up to 16 µL	1 pg - 1 µg
Nuclease-free H_2O	sufficient to 20 µL	–
Total	20.0 µL	–

Storage

Reactions prepared with High Capacity RNA-to-cDNA Master Mix can be stored for up to **24 hours at -20 °C** and up to **one year at -70 °C**. For prolonged storage at 2 to 8 °C, add EDTA to a final concentration of 1 mM to chelate cations and to prevent nucleic acid degradation.

Figure E.1. Protocol, High Capacity RNA-to-cDNA Master Mix.

Appendix F: Mycoplasma detection in HeLa S3 cells and HaCaT cells

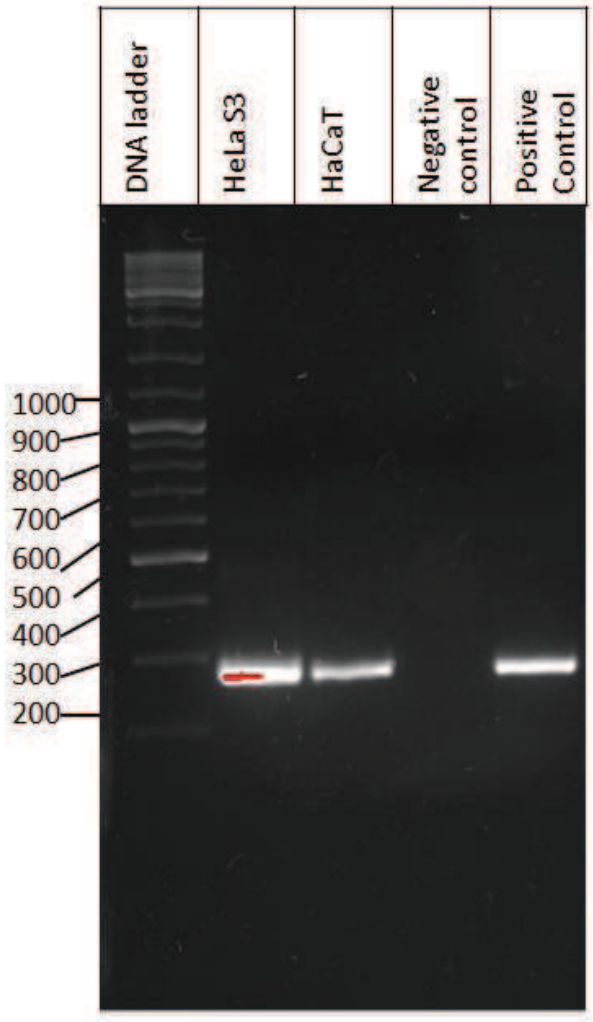

Figure F.1. Mycoplasma detection using PromoKine's PCR mycoplasma Test Kit II. 5 µl GeneRuler™ DNA ladder mix was used as DNA marker. The size of the PCR product detected is 270 basepairs.

Appendix G: Standard curves generated using *ACTB* and *NTHL1* primers

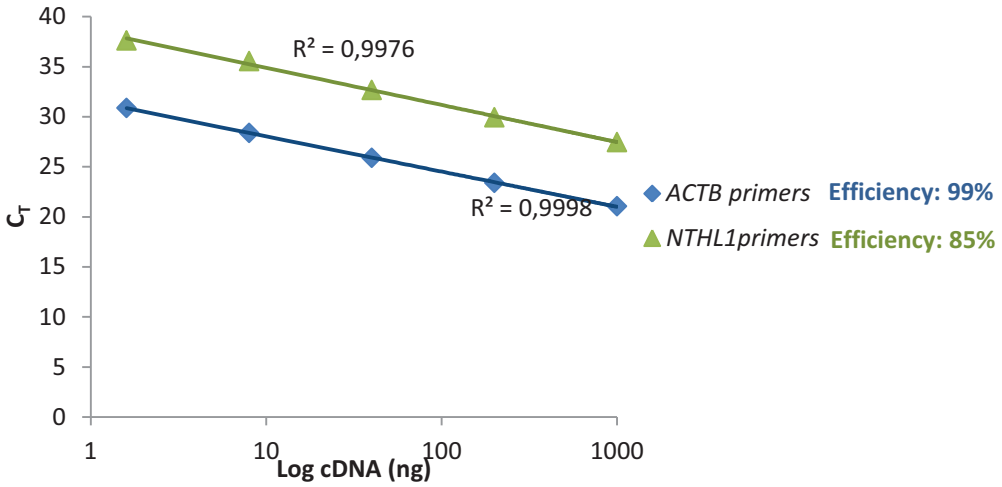

Figure G.1. HeLa S3 cells were transfected in triplicates with siRNA targeting *NTHL1* and non-targeting siRNA. After 48 h, cells were harvested, RNA was purified and RT-PCR was performed on cDNA samples prepared from non-targeting siRNA-transfected cells, using primers specific for the reference gene *ACTB* (blue) and NTHL1 (green). Standard curves were constructed by plotting C_T values of standard dilutions against the logarithm (log) of the amount of cDNA template.

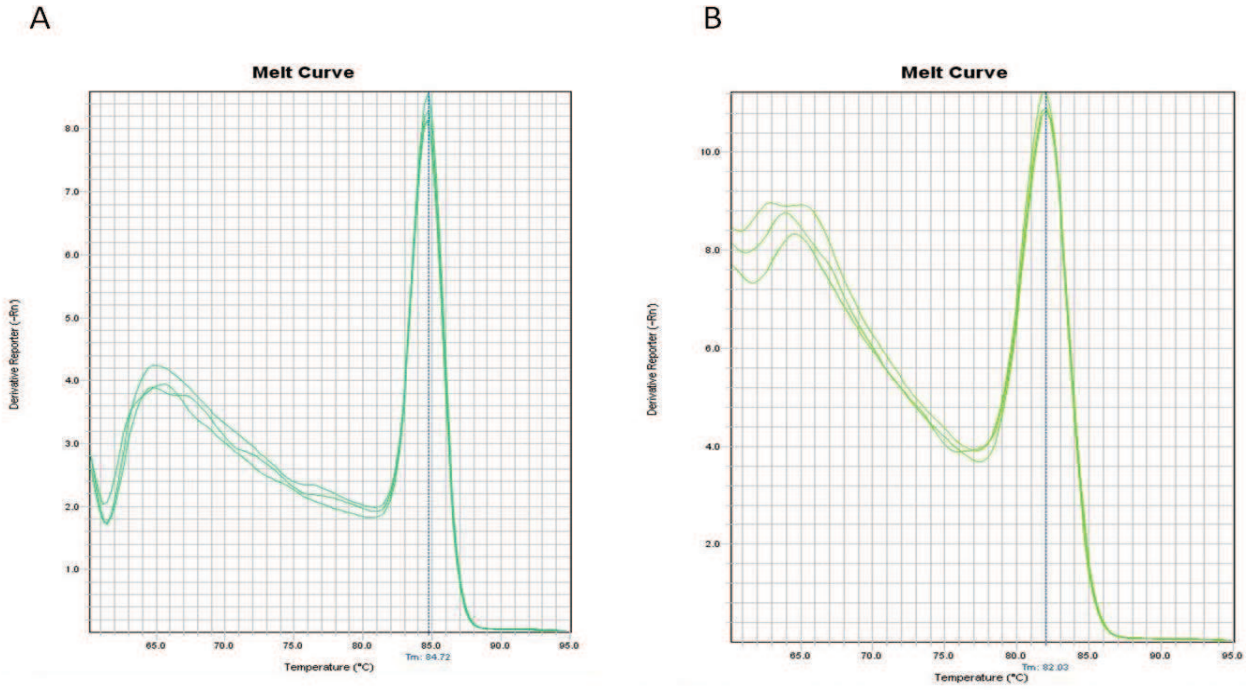

Figure G.2. Melting curve analysis was performed on RT-PCR products using (A) *NTHL1* primers and cDNA template prepared from cells transfected with *NTHL1*-siRNA or (B) *ACTB* primers and cDNA template prepared from cells transfected with non-targeting control siRNA. Analysis was performed in triplicates. All three replicates overlap in a single peak, showing the specificity of the PCR and the absence of primer-dimers.